ISAS - INTERNATIONAL SCHOOL
FOR ADVANCED STUDIES

Characterization of neuronal nicotinic receptors of rat chromaffin cells.

Thesis submitted for the degree of
"Doctor Philosophiae"

Biophysics sector

Candidate:
Dr. Silvia Di Angelantonio

Supervisor:
Prof. Andrea Nistri

SISSA - SCUOLA
INTERNAZIONALE
SUPERIORE
STUDI AVANZATI
TRIESTE
Via Beirut 2-4

TRIESTE

NOTE

Part of the data reported in the present thesis have been published in the article listed below. In all cases the candidate personally performed the experimental work and data analysis, and contributed to paper writing.

Giniatullin R, **Di Angelantonio S**, Marchetti C, Sokolova E, Khiroug L, Nistri A (1999) Calcitonin gene-related peptide rapidly downregulates nicotinic receptor function and slowly raises intracellular Ca2+ in rat chromaffin cells in vitro. J Neurosci 19: 2945-2953.

Di Angelantonio S, Nistri A, Moretti M, Clementi F, Gotti C (2000) Antagonism of nicotinic receptors of rat chromaffin cells by N,N, N-trimethyl-1-(4-trans-stilbenoxy)-2-propylammonium iodide: a patch clamp and ligand binding study. Br J Pharmacol 129: 1771-1779.

Giniatullin RA, Sokolova EM, **Di Angelantonio S**, Skorinkin A, Talantova MV, Nistri A (2000) Rapid relief of block by mecamylamine of neuronal nicotinic acetylcholine receptors of rat chromaffin cells in vitro: an electrophysiological and modelling study. Molecular Pharmacology 58: 778-787.

Di Angelantonio S, Nistri A (2001) Calibration of agonist concentrations applied by pressure pulses or via rapid solution exchanger. Journal of Neuroscience Methods 110: 155-161.

Di Angelantonio S., Costa V., Carloni P., Messori L. and Nistri A. 2002 A novel class of peptides with facilitating action on neuronal nicotinic receptors of rat chromaffin cells in vitro: functional and molecular dynamics studies. Molecular Pharmacology 61: 43-54.

Nistri A. and **Di Angelantonio S.** Enhancement of neuronal nicotinic receptor activity of rat chromaffin cells by a novel class of peptides. Will be published in "The chromaffin cell: transmitter, biosynthesis, storage, release, actions, and informatics". O' Connor D, Eiden L, eds. ANYAS.

ABSTRACT

The present study has investigated the functional properties of native neuronal nicotinic receptors (nAChRs) of rat chromaffin cells, using combined techniques of molecular biology, immunocytochemistry and electrophysiology. While the mRNA transcript for the α7 subunit was revealed by RT-PCR analysis, the protein was not expressed as indicated by lack of radio-ligand binding and of antagonism by selective blockers. Combining molecular biology, antibody staining and functional tests indicates the following subunit assemblies: α3β4, α3α5β4, α3β2 and α4β2 without excluding other combinations. The effect of the oxystilbene derivative F3 on nAChRs was tested using whole cell patch clamp recording or radioligand ^{125}I-epibatidine binding. Raceme F3 and its R isomer blocked nicotine evoked currents, shifting the dose-response curve to the right in a parallel fashion without changing the maximum response. Their action was voltage insensitive and not due to altered current reversal potential. ^{125}I-epibatidine binding was specifically displaced by cytisine or ACh. F3 specifically displayed ^{125}I-epibatidine binding although with lower affinity than in electrophysiological experiments. These results suggested F3 to behave as a relatively potent and apparently competitive antagonist of nAChRs in rat chromaffin cells.

Mecamylamine strongly depressed inward currents elicited by short pulses of nicotine, an effect slowly reversible on wash. The mecamylamine block was voltage-dependent and promptly relieved by a protocol combining membrane depolarization with a nicotine pulse. Either depolarization or nicotine pulses were per se insufficient to elicit block relief. Block relief was transient as response depression returned in a use-dependent manner. Exposure to mecamylamine failed to block nAChRs if they were not activated by nicotine or if they were activated at positive membrane potentials. Other nicotinic antagonists like DHβE

or tubocurarine did not share this action of mecamylamine while proadifen partly mimicked it. Mecamylamine is suggested to penetrate and block open nAChRs that would subsequently close and trap this antagonist. Only channel re-opening plus depolarization allowed mecamylamine escape and block relief.

The Calcitonin Gene Related Peptide (CGRP), which is physiologically present in adrenal medulla was tested on membrane currents and $[Ca^{2+}]_i$ transients elicited by nicotine. CGRP selectively and rapidly blocked nAChRs without affecting GABA receptors. The inhibitory effect of CGRP was independent of $[Ca^{2+}]_i$ or membrane potential and not accompanied by baseline current changes. Like F3, CGRP induced a rightward, parallel shift of the nicotine dose response curve; during coapplication of these blockers the nicotine dose ratio value was the sum of the ones obtained with each antagonist alone. The block by CGRP was insensitive to the receptor antagonist $hCGRP_{8-37}$ but mimicked by $CGRP_{1-7}$.

Looking for the minimal peptidic CGRP fragment which retained the ability to modulate nAChRs we tested peptides related to the CGRP N-terminal region. While $CGRP_{1-7}$ and $CGRP_{2-7}$ depressed responses mediated by nAChRs, $CGRP_{1-6}$, $CGRP_{1-5}$ or $CGRP_{1-4}$ rapidly and reversibly potentiated sub-maximal nicotine currents while sparing maximal currents. $CGRP_{1-3}$ was inactive. $CGRP_{1-5}$ or $CGRP_{1-4}$ were less effective than $CGRP_{1-6}$. Co-application of $CGRP_{1-6}$ and of the allosteric potentiator physostigmine gave additive effects on nicotine currents. $CGRP_{1-6}$ did not enhance responses generated by muscle type nicotinic or $GABA_A$ receptors.

We suggest that the ring structure imparted by the disulfide bridge between Cys_2 and Cys_7 to $CGRP_{1-7}$ and $CGRP_{2-7}$ was responsible for antagonism of nAChRs. In fact, replacing Cys_7 with Ala yielded $CGRP_{1-7A}$, a fragment with ability to enhance nicotine currents.

The present results demonstrated that nAChRs of rat chromaffin cells are a suitable model for testing nicotinic agonists and antagonists. In particular, this study has shown that short linear terminal fragments of CGRP represent a novel class of substances with selective, rapid and reversible potentiation of nAChRs.

INTRODUCTION

Ligand-gated ion channels mediate intercellular communication by converting the signal induced by the neurotransmitter released from the nerve ending into a transmembrane ion flux in the postsynaptic neuron or muscle fiber. According to the classical scheme of fast "wiring" transmission, the neurotransmitter is released into the synaptic cleft at high concentration (up to 3 mM) and for approximately 1 ms; (Katz and Miledi, 1977), whereas with the "volume transmission" or paracrine mode, lower concentrations of the neurotransmitter more slowly reach a distant target through intercellular space. Nicotinic receptors for acetylcholine (nAChRs) may contribute, like other ligand-gated ion channels, to both types of chemical communication depending on their topological distribution at pre- and/or postsynaptic level.

Acetylcholine (ACh) has long been recognised as a neurotransmitter active both in central and peripheral nervous system (for review see Gotti et al., 1997).

Two distinct categories of receptors are engaged in the biological effects of ACh: muscarinic and nicotinic receptors (for reviews see Caulfield, 1993; Dani, 2001). Muscarinic receptors belong to the super-family of G-protein coupled receptors; they consist of single integral proteins with seven transmembrane segments and interact, on their cytoplasmic face, with heterotrimeric G-proteins. Nicotinic acetylcholine receptors are a prototype of ligand-gated ion channels that mediate transmission in the central and peripheral nervous system.

Nicotinic receptors are key molecules for cholinergic transmission to the neuromuscular junction of striated muscles (muscle-type nicotinic receptors), peripheral ganglion synapses of the autonomic nervous system and in several brain areas (neuronal nicotinic receptors Gotti et al., 1997; Paterson and Nordberg, 2000).

Nicotinic receptor structure

Historically, the nicotinic acetylcholine receptors (nAChRs) expressed by vertebrate neuromuscular junction and Torpedo marmorata or electrical eel organs were the first ones to be characterised. Because these tissues contained a large density of such receptors, these biological sources became the model of nicotinic receptors.

During the 1970s the purification of the receptors from these tissues yielded a glycoprotein of 290 kDa. The protein was then divided into four different subunits named α, β, γ, δ according to their increasing molecular weight (reviewed in Changeux, 1990).

All nicotinic receptors are a pentameric sub-unit aggregate forming a structure (inserted within the cellular membrane) which contains a central channel (Itier and Bertrand, 2001). Various sub-unit combinations make up nicotinic receptors and, depending on such combinations, receptors show different functional and pharmacological properties.

The sub-units are named as below: α sub-units (α1-α9), i.e. sub-units which bind agonists and contain disulfide bridges between contiguous cysteine residues, exemplified by adjacent Cys 192-193 in the muscle α1 subunit. Non-α sub-units, which confer particular properties to the receptors, do not contain cysteine residues and, depending on their amino acid sequence, are named β1-β4, γ, ε, δ. All sub-units have a similar topographic structure including one extended extracellular domain (N-terminal), four trans-membrane domains (M1-M4), one intracellular domain (whose length depends on the sub-unit) which joins M3 and M4 domains and one small extracellular C-terminal domain (Changeux and Edelstein, 1998).

The amino acid sequence analysis of various sub-units shows that nicotinic receptors can be divided into three sub-classes. The first family includes muscle-type heteromeric receptors, typically found in skeletal muscle and fish electrical organs, with $(\alpha1)_2\beta1\gamma\delta$ and $(\alpha1)_2\beta1\gamma\varepsilon$

pentameric structures in fetal or adult form, respectively. These muscular receptors are selectively blocked by α-bungarotoxin.

The second family includes neuronal nicotinic receptor (nAChR) consisting of α-bungarotoxin-insensitive, heteromeric sub-units. Also these receptors have a pentameric structure resulting from various combinations of α2, α3, α4 and α6 with β2 or β4 and in some cases also with α5 or β3 sub-units.

The third family includes α-bungarotoxin-binding nicotinic neuronal homomeric receptors consisting of 5 identical sub-units (α7, α8 or α9).

The binding site of acetylcholine and other agonists is located on the N-terminal extracellular domain at the boundary between α and non-α sub-units. In heteromeric neuronal receptors the α and β sub-units contribute to the binding site.

While subunit composition at the neuromuscular junction was established rather early, less was known concerning the neuronal receptor composition. The small amount of biological material renders biochemical experiments difficult and putative stoichiometry must be derived from different converging information. First, like for muscle receptors, the molecular weight of purified nAChRs is always in the 300 kDa range (Lindstrom, 1997). Since nAChRs are expected to result from the assembly of 5 subunits, and all subunits so far identified are less than 600 aa in length, every subunit is expected to weight approximately 40-70 kDa.

Stoichiometry of neuronal nicotinic receptors

Immunoprecipitations, using antibodies directed against subunit specific epitopes, indicate that the ganglionic receptors probably result from the assembly of α3 and β4 subunits, while brain receptors seem to contain α4 and β2 subunits (Lindstrom, 1997). Expression and identification of small amount of α5 subunit suggest that this subunit may participate in

the formation of some ganglionic and central receptors (Balestra et al., 2000).

Heterologous expression systems have been used to determine the combination of nAChR subunits capable of forming functional ionic channels (McGehee and Role, 1995). Those studies indicated groupings of nAChRs that are easily formed in Xenopus oocyte expression system: α7 homomeric receptors; heterodimeric αβ nAChRs formed by a combination of α subunits (α2, α3 or α4) and β subunits (either β2 or β4); and complex receptors that include more than one type of α or β subunit (e.g. α3α5β4 or α4β2β4). This third group of complex combinations also includes nAChRs containing subunits such as α5 or β3 that do not form channels when they are expressed alone or in combination with any other single α or β subunit (Groot-Kormelink et al.; 1998; Yu and Role, 1998). α6 can rarely form an αβ receptor, and it also participates in more complex combinations (Olale et al., 1997; Le Novere et al., 1996). Evidence indicates that the α7 subunit can also form more complex combinations (Yu and Role, 1998; Zoli et al., 1998). The basic conclusion drawn from expression systems is that a limited number of subunit combinations are favoured but more rare combinations are possible. There is an enormous potential for nAChRs diversity within the CNS.

There are some general rules used to simplify the influence of a particular subunit. For example the homomeric α7 receptors possess high calcium permeability, rapid activation and desensitization kinetics, and they are specifically blocked by α-bungarotoxin and methyllycaconitine (Alkondon et al., 1998; Maggi et al., 2001; Sudweeks and Yakel, 2000).

In the central nervous system the majority of nAChRs contains α4β2 or α7 subunits. However, the agonist and antagonist profile of α4β2 receptors shows some differences for cells derived from different nuclei. For example, neurones from medial habenula and locus coeruleus express functional nAChRs with a pharmacological profile consistent

with the presence of α3 and β4 subunits (Mulle et al., 1991). Moreover, homomeric α7 has been considered the predominant nicotinic receptor in hippocampal neurons, but it seems more and more evident that also α4β2 and α3β4 containing receptors mediate nicotine response in that brain region (Sudweeks and Yakel, 2000).

Although one class of nAChRs often predominates within a region, more than one class (or subclass) of nAChRs is often present (Pidoplichko et al., 1997). In addition, individual neurons often express multiple classes of nicotinic receptors (Dani et al., 2000).

Binding site

The reconstitution of functional receptors isolated by biochemical purification of proteins from Torpedo electric organ constituted the first demonstration that these proteins contain both the ligand-binding site and the ionic pore (Reynolds and Karlin, 1978). From investigations in the 1980s on the kinetics of ionic currents through single channels, it has been accepted that nAChRs possess two agonist-binding sites. The occupancy of these two sites, in a positive cooperative way, stabilises the receptor channel in the open state (Colquhoun and Sakmann, 1985; Udgaonkar and Hess, 1987a; Udgaonkar and Hess, 1987b). Using the method of fluorescence resonance energy transfer, between a receptor-bound fluorescent agonist and two membrane-fluorescent probes, the ACh binding sites were estimated to be 25 A° below the extracellular apex of the nAChR (Unwin, 1996; Unwin, 1993). Later, high-resolution, electron microscopy data accorded with the proposed location for the ACh-binding sites in putative "pockets", on each of two α subunits in the pentameric receptor (Unwin, 1996; Unwin, 1993).

With the availability of specific chemical compounds and the amino acid sequences of the different nAChR subunits, important advances concerning our knowledge of the ACh binding site have been made. For instance, photo-affinity experiments carried out with the muscle-type

receptor have shown that the ligand binding site must be at the interface between the αs and their adjacent γ or δ subunits (Galzi et al., 1991; Changeux and Edelstein, 1998).

Six loops termed A-F have been identified in the formation of the ACh binding site. The α subunit, which harbours the principal component of the binding site, comprises the A, B and C loops, while the complementary component of the adjacent subunit (γ, δ or ε for the muscle and β for the neuronal) comprises the D, E and F loops. The important participation of tyrosine residues to the ACh binding pocket has been identified by combination of site-directed mutagenesis and electrophysiological investigation of the chick α7 receptor subtype (Galzi et al., 1991). Modelling the putative three-dimensional structure of the nAChRs (Le Novere et al., 1999) all confirmed that the ACh binding site must reside at the interface between two subunits and that the ligand must penetrate into a gorge to form appropriate chemical bridges and initiate the transduction. Modelling the extracellular domains with the known crystal structure of the copper-binding proteins was also attempted (Tsigelny et al., 1997). The very recent identification of Acetylcholine binding protein (AChBP), a molecule that efficiently binds ACh and that is secreted from glial cells of snails, allowed the first crystallisation of a protein that resembles the N-terminal domain of the nAChRs. X-ray diffraction analysis of this structure confirmed the predictions made from the various models and the existence of the A, B, C, D and E loops in the formation of the binding pocket (Smit et al., 2001). This crystal structure reveals two β sheet skeletons forming the gorge in which the ACh enters and binds to specific residues.

Function of nAChRs

Upon binding ACh, the nAChR ion channel is stabilised in the open conformation for several milliseconds. Then, the open pore of the

receptor/channel closes to a resting state or closes to a desensitized state unresponsive to ACh (or other agonists) for many milliseconds or more. While open, nAChRs conduct cations, which can cause local depolarization of the membrane and produce an intracellular ionic signal (Fig 1).

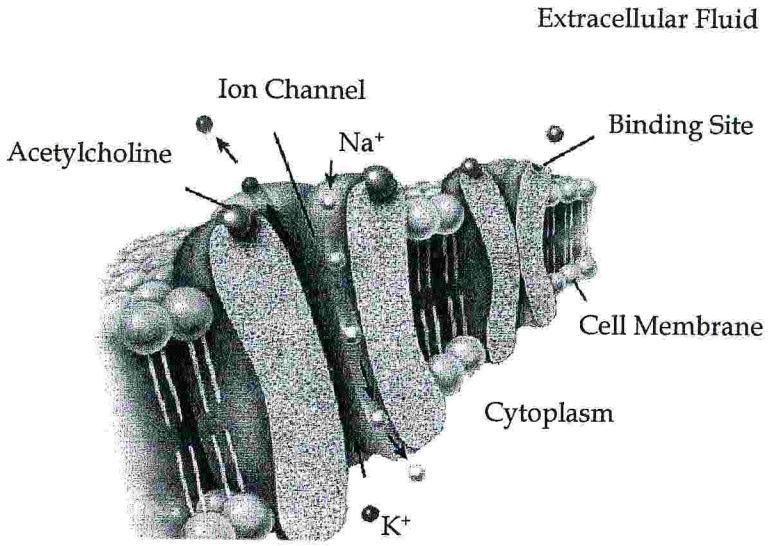

Fig. 1. Scheme of nicotinic receptor function. After binding of two ACh molecules the channel opens and cations pass through it.

Although sodium and potassium carry most of the nAChR current, calcium can also make a significant contribution (Castro and Albuquerque, 1995; Decker and Dani, 1990; Dani and Mayer, 1995; Vernino et al., 1994; Vernino et al., 1992). The biological relevance of calcium entrance through nAChRs seems to be different from that one mediated by voltage-gated calcium channels or by the N-methyl-D-aspartate (NMDA) subtype of glutamate receptors. In fact both voltage-gated calcium channels and NMDA receptors require membrane depolarization to pass current freely, because at hyperpolarized (negative) potentials, voltage-gated calcium channels generally do not open and NMDA receptors are blocked by extracellular magnesium ions. Nicotinic nAChRs open and pass current freely at negative potentials that provide strong driving force for cation entry into the cell. Thus, calcium influx mediated by nAChRs has different voltage

dependence from the one of other calcium-permeable ion channels. Also, calcium inflow has different spatial distribution that depends on the location of nAChRs on the cell surface.

The most basic conformational states of nAChRs are the closed state at rest, the open state, and the desensitized state. The rate at which the nicotinic receptor proceeds through these conformational states and the selectivity with which it conducts cations in the open state, depend on many factors, including its subunit composition. Therefore, the extensive nAChR diversity has the potential to produce many different responses to endogenous or exogenous agonists. The speed of activation, the intensity of the membrane depolarization, the size of the ionic signal, the rates of desensitization and recovery from desensitization, the pharmacology, and the regulatory controls of the ACh response will all depend on the subunit composition of nAChRs as well as other local factors. To add further complexity, the three basic conformational states (rest, open, and desensitized) do not account for the actual kinetic properties of nicotinic receptors. Rather, there are multiple conformations involved in gating. Desensitization, in particular, can encompass many time constants (Dani et al., 2000; Fenster et al., 1999a; Khiroug et al., 1997). Thus, there may be short- and long-lived states of desensitization. Long exposures to low concentrations of agonist will favour deeper levels of desensitization, and this situation is often found in smokers, who have low blood concentrations of nicotine throughout the day (Benowitz et al., 1989; Benwell et al., 1995; Wonnacott, 1990).

During the last 10 years, the view of the nAChR has grown from an on-off switch regulating cationic conductance to a sophisticated allosteric macro-molecule (Lena and Changeux, 1998; Lena and Changeux, 1993). Competitive antagonists and partial agonists can occupy the agonist binding sites. Open channel blockers, such as mecamylamine, can bind within the pore, and there are multiple sites for other non-competitive inhibitors and modulators such as physostigmine. In addition, nAChRs

are regulated by several other factors, including peptide transmitters, various protein kinases, the cytoskeleton, and calcium. Although calcium modulation can occur intracellularly (as it is usually the case, (Khiroug et al., 1997; Khiroug et al., 1998), nAChRs can also be allosterically modulated by extracellular calcium, leading to dramatic changes in the channel opening probability (Adams and Nutter, 1992; Amador and Dani, 1995; Mulle et al., 1992; Vernino et al., 1992). This modulation occurs over the physiological concentration range of external calcium. Therefore, high levels of neuronal activity that can diminish extracellular calcium (Heinemann et al., 1990; Wiest et al., 2000) could cause a negative feedback that lowers the opening probability of nAChRs. Calcium modulation is well documented, but there is potential for nAChR modulation by other allosteric effectors. This potential offers leads for new therapeutic drugs, such as those that can enhance nAChR activity to assist Alzheimer's disease (AD) patients. Presently, cholinergic activity can be enhanced in patients with AD by antiacetylcholinesterase, such as galantamine or physostigmine, drugs that prolong the life time of ACh. There is evidence, however, that some antiacetylcholinesterase drugs (such as physostigmine and galantamine) can allosterically potentiate nAChRs (Maelicke and Albuquerque, 2000).

Activation and desensitization of nAChRs

At a cholinergic synapse, approximately 3 mM ACh is rapidly released into the cleft, to activate nicotinic receptors. In a few milliseconds, ACh is then hydrolyzed by acetylcholinesterase and/or diffuses away. The delivery and removal of ACh is very rapid, and therefore desensitization is usually not thought to be important, even if the desensitization process is complex. As neuronal nicotinic receptors are diverse and neuronal synapses are anatomically and compositionally varied, the role of desensitization is not well understood. Repeatedly exposing a synapse to about 1 mM ACh might normally produce little

desensitization. If the synaptic stimulation is very high, however, even though the rates of recovery from desensitization are fast, they may not allow complete recovery (Dilger and Liu, 1992; Fenster et al., 1999a). Furthermore, the breakdown of ACh releases choline, which could reach locally high concentrations. High concentrations of choline could desensitize α7 containing nicotinic receptors (Alkondon et al., 1997a; Papke et al., 1996). The physiological role of desensitization may become especially important when considering the desensitizing levels of nicotine in the brain of smokers (Dani and Heinemann, 1996) or when considering the effects of drugs that inhibit acetylcholinesterase (e.g., to treat patients with AD). Under those two conditions, some nAChRs are likely to desensitize, but not in a uniform manner. At very active cholinergic synapses, nAChRs are more susceptible to the desensitizing influence of the endogenous agonist (ACh). When high rates of cholinergic activity are occurring in conjunction with antiacetylcholinesterase or long exposures to nicotine, then synaptic nAChRs are more susceptible to desensitization. Evidence indicates that longer exposures to agonist allow slow desensitization to come into play, such that some nicotinic receptors can enter longer lasting desensitization (Lester and Dani, 1994; Reitstetter et al., 1999).

Kinetic parameters including desensitization depend on the subunit composition, and modulatory processes, such as protein kinases, influence the nAChR subtypes differently and selectively (Fenster et al., 1999b; Paradiso and Brehm, 1998). Depending on dynamic modulatory influences, different nAChR subtypes might become particularly susceptible to desensitization, and the modulatory processes can vary from synapse to synapse. Thus, modulatory processes acting upon nAChRs could provide a varying computational mechanism for manipulating information processing at synapses.

Nicotinic receptors as allosteric membrane proteins

In the absence of structural information at atomic resolution, available data lead to the proposal of plausible but still hypothetical structural models for the ACh binding sites and the ion channel, ultimately accounting for their pharmacological and ionic selectivity, respectively.

Two mechanisms are currently used to fit nAChR data. On the one hand, the Monod-Wyman-Changeux (MWC) theory (Changeux and Rubin, 1968; Karlin, 1967) postulates that the protein spontaneously isomerizes between discrete allosteric states characterized by "all or none" symmetric changes. On the other hand, the sequential model (Del Castillo and Katz, 1957) postulates that the conformational transitions occur only after agonist binding, leading to agonist-induced multiple intermediate states. At this stage, it appears difficult to discriminate unambiguously between these theories.

"We still do not know in any detail how the function of a receptor relates to its structure, nor how exactly the agonist causes the structural rearrangement that is involved in opening and shutting." (Colquhoun and Sakmann, 1998).

Moreover, the subunit diversity of neuronal nAChRs is such that they may achieve a wide diversity of functions, such as fast wiring (phasic, α7 in CA1 interneurones of the hippocampus) and volume (tonic, α4β2 in CA1 interneurones of the hippocampus) transmission (Alkondon et al., 1999), according both to their intrinsic functional properties of activation and desensitization, and their anatomical localisation. Full understanding of these functions will require knowledge of the intimate biochemical and structural organisation of these receptors.

Acetylcholine-binding protein as a model for nAChRs

The recently reported crystal structure of the AChBP at 2.7 Å resolution can be used as an example of the N-terminal domain of an α-subunit of nAChRs. (Smit et al., 2001; Smit et al., 2001).

Acetylcholine-binding protein (AChBP) is a soluble protein found in the snail Lymnaea stagnalis (Smith et al., 2001). It is produced and stored in glial cells, and released in an ACh-dependent manner into the synaptic cleft, where it modulates synaptic transmission. Mature AChBP is 210 residues long and forms a stable homopentamer. It aligns with the N-terminal domains of pentameric ligand gated ion channels (LGICs) and lacks the transmembrane and intracellular domains present in the superfamily. AChBP is most closely related to the α-subunits of the nAChRs. Nearly all residues conserved within the nAChR family are present in AChBP, including those that are relevant for ligand binding. Moreover, AChBP binds known nAChR agonists and competitive antagonists such as acetylcholine, nicotine, d-tubocurarine and α-bungarotoxin (Smith et al., 2001). This crystal structure shows that molluscan AChBP is a homologue of the pentameric ligand gated ion channel superfamily ligand-binding domains. It confirms the predicted topology with the location of the binding site at the subunit interface.

This structure (Fig. 2) will be highly relevant for drug-design studies that are targeting the pentameric ligand gated ion channel superfamily. The general structural knowledge about its folding will be applicable to GABA, serotonin (5-HT3) and glycine receptors. It will help us to understand their ligand-binding characteristics and hence could have an impact on the development of, for example, anti-emetics aimed at the 5-HT3 receptor or the psychotropic drugs targeted to GABA receptors. The availability of a three-dimensional description of the nicotinic ligand-binding site will be especially relevant for the design of new drugs against, for example, Alzheimer's disease, epilepsy and addiction to smoking.

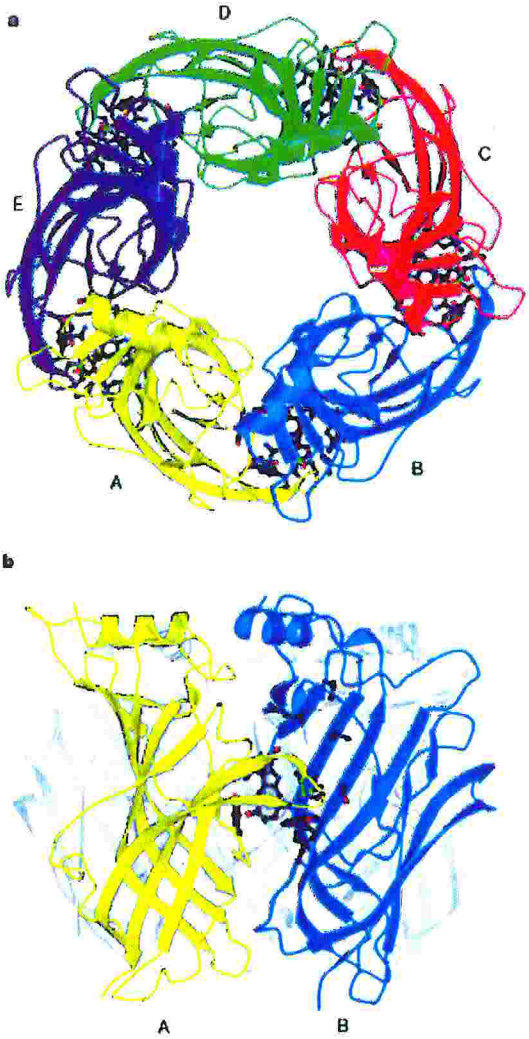

Fig. 2. The pentameric structure of AChBP. **a**, In this representation each protomer has a different colour. Subunits are labelled anti-clockwise, with A–B, B–C, C–D, D–E and E–A forming the plus and minus interface side, with the principal and complementary ligand-binding sites, respectively (ball-and-stick representation). **b**, Viewing the AChBP pentamer perpendicular to the five-fold axis. The equatorially located ligand-binding site (ball-and-stick representation) is highlighted only in the A (yellow)–B (blue) interface(From Smit et al., 2001).

Localization of nAChRs

Mapping of nAChRs in the brain yielded surprising results. Although it was observed that receptors are widely distributed, they seem principally localized to terminal boutons (for review see Dani, 2001b). The emerging pattern of nAChRs localization indicates that receptors are present in postsynaptic (Fig. 3 a), presynaptic(Fig. 3 b) or even axonic

areas (Fig. 3 c). Since nAChRs are highly Ca^{2+} permeable and receptor activation can cause a significant calcium influx, different effects were predicted depending on sub-cellular receptor localization. For instance, when presynaptic nicotinic receptors are activated, increased calcium in the presynaptic bouton modulates neurotransmitter release (Dani, 2001). It has been shown that nicotinic receptor activation influences release of dopamine, glutamate, GABA and serotonin. For example, it is supposed that nicotine addiction is mediated by nAChRs activation that modulates dopamine release by the mesolymbic pathway. Experiments carried out with β2 knock-out mice have shown that these animals display lower addiction to nicotine with respect to their wild type (Picciotto et al., 1998).

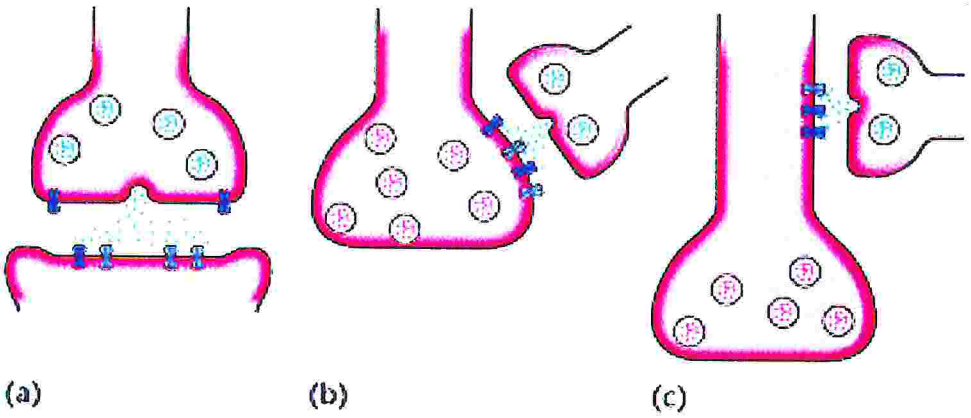

Fig. 3. Schematic representation of nAChRs localization. a) postsynaptic, b)presynaptic and c) axonic neuronal nicotinic receptor.

The cholinergic system in CNS

Before looking further into the roles of nAChRs, we need to consider some of the basic properties of cholinergic innervations. Although cholinergic systems provide diffuse innervations to practically all brain areas, only a relatively small number of cholinergic neurons innervate each region (Kasa, 1986; Woolf, 1991). Despite the sparse innervations,

cholinergic activity drives or modulates a wide variety of behaviours. By acting on nAChRs, nicotine or endogenous ACh can increase arousal, heighten attention, influence rapid eye movement sleep, produce states of euphoria, decrease fatigue, decrease anxiety, act centrally as an analgesic, transiently normalize sensory gating in schizophrenic patients, and influence a number of cognitive functions (Everitt and Robbins, 1997; Levin et al., 1991; Marubio et al., 1999; Levin and Rose, 1991). It is thought that cholinergic systems particularly affect discriminatory processes by increasing the signal-to-noise ratio and by helping to evaluate the significance and relevance of stimuli.

Although cholinergic neurons are distributed from the spinal cord to the basal telencephalon, there are two major cholinergic projections. One cholinergic system arises from neurons in the pedunculopontine tegmentum and the laterodorsal pontine tegmentum, providing widespread innervations mainly to the thalamus and midbrain areas, and also descending innervations that reaches to the brain stem (Fig. 4). The second major cholinergic system arises from the basal forebrain and projects mainly throughout the cortex and hippocampus (Fig. 4). Thus, the activity of a rather small number of cholinergic neurons can influence relatively large neuronal structures.

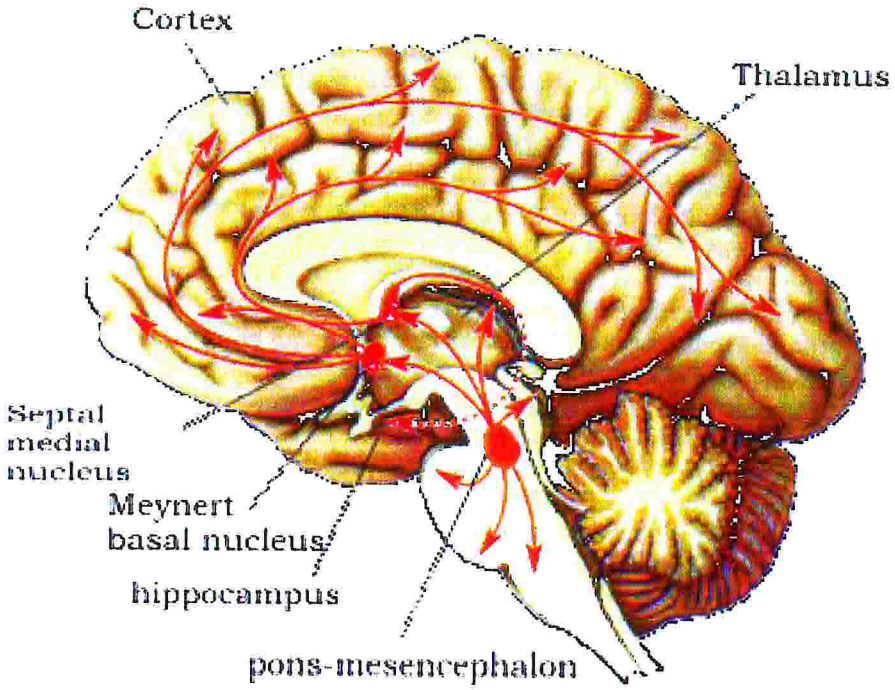

Fig. 4. Cholinergic innervations in the Central Nervous System.

Nicotinic Mechanisms in the CNS

The most widely observed synaptic role of nAChRs in the CNS is to influence neurotransmitter release. Presynaptic nAChRs (see Fig. 3 b), have been found to increase the release of nearly every neurotransmitter examined (Alkondon et al., 1997b; Albuquerque et al., 1997; Gray et al., 1996; Quiram et al., 1999; McGehee et al., 1995; McGehee and Role, 1995;

Radcliffe and Dani, 1998; Radcliffe et al., 1999; Role and Berg, 1996; Sullivan et al., 1997). Exogenous application of nicotinic agonists can enhance (and nicotinic antagonists can often diminish) the release of ACh, dopamine, norepinephrine, serotonin, glutamate, GABA and glycine. In many cases, the α7 containing nAChRs, which are highly calcium permeable, mediate increased release of neurotransmitter, but in other cases different nAChR subtypes are involved. In rat hippocampal slices and cultures, presynaptic α7 containing nAChRs have been shown to initiate calcium influx that, consequently, enhances glutamate release from presynaptic terminals (Albuquerque et al., 1997; Gray et al., 1996). Intense nicotinic stimulation enhances glutamate release and GABA release on multiple time scales (Radcliffe and Dani, 1998; Radcliffe et al., 1999). Enhancement lasting several minutes or more suggests that the influx of calcium may act as a second messenger to modify glutamatergic synaptic transmission indirectly.

At GABAergic synapses, activation of preterminal nAChRs has been found to depolarize the membrane locally, leading to activation of voltage-dependent channels that directly mediate synaptic calcium influx underlying enhanced GABA release (Alkondon et al., 1997b; Lena et al., 1993). The effect mediated by preterminal nAChRs is inhibited by tetrodotoxin, which blocks sodium channels and, thereby, prevents the regenerative voltage activation of calcium channels in the presynaptic terminal. Axonal nAChRs (Fig. 3 c) may also modulate transmitter release and local excitability. Strategically located nAChRs might enable an action potential to invade only a portion of the axonal arbour. By directly exciting or by shunting the progress of an action potential at a bifurcation, axonal nAChRs could initiate or alter the spread of neuronal excitation.

Fast nicotinic transmission has been detected as a small excitatory input at several neuronal areas. In the hippocampus, fast nicotinic transmission onto GABAergic interneurones has been reported

(Alkondon et al., 1998; Frazier et al., 1998; Hefft et al., 1999). In developing visual cortex, nicotinic transmission can be evoked onto both glutamatergic pyramidal cells and GABAergic interneurons (Roerig et al., 1997). Because nicotinic synapses have low density, they are difficult to detect experimentally in brain slice preparations. Where it has been reported, fast nicotinic transmission is a minor component of the excitatory input, which is overwhelmingly glutamatergic. Although direct nicotinic excitation of a neuron is a minor form of synaptic transmission, it could influence the excitability of groups of neurons owing to the broad cholinergic projections. An example of nicotinic modulation of circuit excitability is seen in the hippocampal slice (Ji and Dani, 2000). Local application of nicotinic agonists onto interneurons causes both inhibition and disinhibition of CA1 pyramidal neurons. In fact, activating nAChRs on interneurons that directly innervate pyramidal neurons causes inhibition of such pyramidal neurons, while nicotinic activation of interneurons that innervated other inhibitory interneurons causes pyramidal cell disinhibition (Alkondon et al., 1999).

Nicotinic receptor function in the CNS

Nicotine is a potent modulator of CNS function. It enhances ion flux and neurotransmitter release, augments or gates a number of neuronal systems and elicits a variety of behavioural states. Nicotine administration produces a number of physiological effects including increased heart rate and blood pressure, and dose dependent increase in the secretion of prolactin and ACTH, resulting in a subsequent increase in corticosterone secretion (Benowitz et al., 1989). In humans, nicotine increases arousal, visual attention and perception, but it also decreases reaction time, prevents a decline in efficiency over time and improves the ability to suppress inappropriate responses (Jones et al., 1992; Wesnes and Warburton, 1983). Despite these important effects elicited by nicotine, the exact role of brain nAChRs remains unclear. A

significant body of evidence suggests that presynaptic nAChRs exist on several cell populations in cortical, hippocampal and cerebellar brain regions (Sullivan et al., 1997). Nicotine interacts with a variety of presynaptic nAChRs to facilitate the release of a number of neurotransmitters which have been implicated in mediating/modulating a number of behavioral tasks (Wonnacott and Thorne, 1990; McGehee et al., 1995). Therefore, it has been proposed that the role of nAChRs in the brain is to modify the excitability of neurons, that is to produce the optimal performance of neurons by adjusting their excitability, an action which is likely to be important for a number of behavioral responses and, particularly, for cognitive processes (McGehee et al., 1995). The most obvious behavioral action mediated by nAChRs is addiction to nicotine smoking. The mesolimbic DA pathway is thought to mediate the addictive effects of nicotine and other substances of abuse, as nicotine is known to stimulate release of DA in this pathway (Pich et al., 1997).

Nicotinic AChRs also have a role in development and neuronal plasticity (Broide and Leslie, 1999; Role and Berg, 1996). The density of nAChRs varies during the course of development, and nAChRs can contribute to activity-dependent calcium signals. For example, presynaptic $\alpha 7$ containing nAChRs increases the release of glutamate preferentially onto postsynaptic NMDA receptors in the developing rat auditory cortex, but not in the mature cortex (Aramakis and Metherate, 1998). By enhancing glutamate release particularly at the location of NMDA receptors, nAChRs might help to modulate activity-dependent synaptic plasticity that is often initiated by postsynaptic NMDA receptors (Nicoll and Malenka, 1999).

In summary, the tremendous diversity of nAChRs provides the flexibility necessary for multiple functional roles. Broad, sparse cholinergic projections ensure that nicotinic mechanisms modulate neuronal excitability of relatively wide circuits. Although fast nicotinic

transmission is not the predominant driving force, it can contribute excitatory input to many synapses at one time.

During the progression of Alzheimer's Disease (AD), cholinergic inputs degenerate and the number of nAChRs in some areas decreases (Nordberg, 1994; Perry and Perry, 1995). Loss of nicotinic mechanisms, which modulate the gain and fidelity of synapses and modulate the excitability of circuits, are likely to contribute to the overall cognitive deficits associated with AD.

However, further work is necessary to determine which nAChR subtypes are involved in cognitive processes and to elucidate the interactions of these receptors with other neurotransmitter systems that are critical in cognitive function.

Pathology of neuronal nicotinic receptors

Some of the pathologies resulting from dysfunction of neuronal nicotinic receptors are, for example, Alzheimer's disease (AD), Parkinson's disease, epilepsy, and other mental diseases such as schizophrenia, Tourette's syndrome, anxiety and depression.

a. Alzheimer's disease

AD is a progressive neurodegenerative condition affecting 1/10 of the over 65 y old individuals. It determines more than 50 % of senile dementias (and the majority of the pre-senile dementias) and is characterized by a gradual deterioration of higher cognitive functions, including memory. The brains of AD patients, inspected post-mortem, show two neuropathological characteristics representing the two principal indicators for the AD diagnosis: intracellular deposits of neurofilaments and extracellular plaques.

AD brains show severe loss of cholinergic innervation within the cerebral cortex and hippocampus (Coyle et al., 1983). This results in the hypothesis that the cognitive deterioration is strictly related to

degeneration of the cholinergic pathways (cholinergic hypothesis; (Bartus et al., 1982).

Furthermore, in AD brains, nicotinic agonist binding is remarkably reduced with respect to controls. In these brains, however, α-bungarotoxin binding is not reduced, indicating that apparently no loss of homomeric α7 receptors occurs. Studies carried out on AD affected brains have shown the α4β2 to be the most damaged receptor class (Marutle et al., 1999).

The commonest treatment for AD aims at restoring decreased cholinergic transmission. Usually such an approach relies on cholinesterase inhibitors, such as tacrine, donezepil and rivastigmine, which avoid degradation of acetylcholine released from cholinergic neurons, and therefore increase the acetylcholine concentration available for interaction with nAChRs. This class of drugs provides only a palliative effect on AD symptoms while it is questionable their ability to slow down the neurodegeneration (Amberla et al., 1993; Maltby et al., 1994; Hellstrom-Lindahl et al., 1998; Nordberg and Svensson, 1998). It is likely that any potential benefit of these drugs originates from nAChRs activation both via increased neurotransmitter extracellular concentration and via allosteric nAChR modulation carried out by tacrine or galantamine (Maelicke et al., 1997; Maelicke et al., 2000; Nordberg and Svensson, 1998).

Several studies suggest activation of nAChRs to be important for AD therapy:

1. nAChR activation by nicotine increases memory function. In animal models it was observed that β2 sub-unit lacking mice show learning memory deficits (Picciotto et al., 1995) and that healthy animals, chronically treated with nicotine, show better memory (Levin et al., 1991). Nicotine increases memory in AD patients as well (Rusted et al., 1994).

2. Nicotinic receptor activation facilitates release of many brain neurotransmitters like acetylcholine, dopamine, GABA and glutamate (Sullivan et al., 1997).

3. nAChR activation partially protects against β-amyloid toxicity. In fact, nicotine prevents β-amyloid induced cell death of cultured neurons, an effect blocked by dihydro-β-erythroidine, which is an α4β2 receptor antagonist. Also cytisine, another nicotinic agonist, inhibits β-amyloid toxicity (Kihara et al., 1998).

Hence, nicotinic neuronal receptor activation is an important therapeutic object but, up to now, it is hardly achievable and not fully understood with respect to its implications for long-term receptor function (Perry et al., 2000).

b. Parkinson's disease

In analogy with AD, Parkinson's disease (PD) also shows loss of cholinergic neurons in the basal ganglia, together with strong reduction in high affinity nicotine-binding sites (Whitehouse et al., 1988; Lange et al., 1993). In addition to motor dysfunction, PD patients often show cognitive deficits associated with nAChR loss (Perry et al., 1995). The most important environmental factor in PD patients is that this pathology is less frequent in smokers (Morens et al., 1996). Although tobacco contains numerous substances in addition to nicotine, the latter is the most probable candidate for such an effect. For example, in rodents chronic treatment with nicotine prevents degeneration of dopaminergic neurons, a pathophysiological hallmark of PD (Janson and Moller, 1993). In mice nicotine is partially neuroprotective against the basal ganglia lesions experimentally induced by the drug MPTP. Furthermore, the new, specific α4β2 receptor agonist, SIB-1508Y, when administered in combination with L-DOPA, increases the cognitive capacities in monkeys with experimental PD (Schneider et al., 1998; Schneider et al., 1999).

c. Epilepsy

Epilepsy includes a heterogeneous group of central nervous system disorders. Among these, autosomal frontal lobe epilepsy (ADNFLE) is a partial epilepsy causing short lasting convulsions during sleep. It was recently demonstrated that one form of ADNFLE results from a mutation of the gene encoding for the nAChR α4 sub-unit. This mutation consists of the replacement of a phenylalanine for serine (Ser247) in the M2 transmembrane domain (Steinlein et al., 1995). This mutation modifies the properties of the α4β2 channels expressed in frog oocytes. A second mutation, again at the level the α4 sub-unit, was found in another family affected by the same epilepsy syndrome. This mutation consists of the insertion of a leucine into the C-terminal at position 259 (extracellular) in the M2 domain (Steinlein et al., 1995). Although the latter mutations is better tolerated clinically, both mutations reduce the calcium permeability of the α4β2 receptors (Weiland et al., 1996).

Furthermore the serine 247 mutated receptors show an ACh affinity 7 times smaller than normal receptors and desensitize more readily (Bertrand et al., 1998).

Since epilepsy is thought to originate from excessive activation of brain neurons, it seems contradictory that reduced function of nicotinic receptors can produce convulsions. The explanation possibly stems from the fact that α4β2 receptors possess a pre-synaptic action to modulate release of inhibiting neurotransmitters such as GABA and glycine (Sullivan et al., 1997). Higher release of GABA and glycine from inhibitory neurons, or activation of these same neurons mediated by α4β2 receptors, could prevent epileptic seizures.

For these reasons, drugs which can enhance directly this class of nicotinic receptors could be useful for the treatment of this form of epilepsy.

d. Other mental disorders

In addition to these neuropathologies, schizophrenia has also been suggested to be related to abnormal nAChR activation because in schizophrenics there is a significant reduction in α7 receptors in the hippocampal CA3 region and in the frontal cortex (Freedman et al., 1997; Freedman et al., 2000). Likewise, for the therapy of the Tourette's syndrome, the aim is to develop nAChR targeting drugs (Olale et al., 1997). Nicotinic receptors are also apparently involved in the physiopathology of anxiety and depression (Decker et al., 1994; Maggio et al., 1998).

In view of above considerations, it is therefore apparent the need to identify and provide chemical substances for the therapy of diseases resulting from nAChR dysfunction. Ideally these substances should be able to enhance rapidly and persistently the responses mediated by the nAChR activation without desensitizating them. If these substances could act directly on the agonist binding sites (for acetylcholine or nicotine), there would be the additional advantage of highly specific action without affecting other receptor systems.

Up to date there are problems to study nAChRs in native systems because nAChRs are widely localized at post-synaptic as well at pre-synaptic level, within the main cholinergic pathways of central and peripheral nervous systems (Lindstrom, 1997).

Looking for a model to study native nAChRs: the chromaffin cell

Many studies have been carried out on heterologous expression systems, consisting of cells constitutively lacking nicotinic receptors and made to express nAChRs with various sub-unit combination. Different biophysical and pharmacological properties of numerous subunit aggregates can then be investigated.

Often, the first step is the use of Xenopus oocytes as expression system. This approach may be, however, unsuitable to understand many aspects concerning the role and function of native receptors, probably because in amphibian cells, with half gene complement, produce post-translational modifications of nAChRs to alter their activity.

For example it has been shown (Sivilotti et al., 1997) that heterologous expression in Xenopus oocytes of the cloned rat α3 and β4 subunits which might be expected to be expressed in Superior Cervical Ganglia (SCG) generates receptors that differ in single-channel conductance or kinetics from native SCG receptors (Sivilotti et al., 1997), and which also differ from SCG in relative agonist potencies (Covernton et al., 1994). This fact can suggest that the oocyte assembles neuronal nAChRs incorrectly (Sivilotti et al., 1997). It has been also shown that atropine and ivermectine, which modulate oocyte-expressed nAChRs, do not have a similar effect on native receptors (Krause et al., 1998). However the use of oocyte as expression system is useful to investigate the molecular properties of nAChRs, because it allows to use a reporter mutation strategy (Groot-Kormelink et al., 2001).

The use of mammalian cells, e.g. HEK cells, as expression systems, presents also considerable limitations because these are not neuronal cells and they may lack the intracellular receptor modulation mechanisms typical of neurons. In fact Lewis and colleagues, that constructed a stable mammalian cell line (L-α3β4) which expresses the cloned rat neuronal nicotinic acetylcholine receptor (nAChR) subunits α3 and β4, demonstrated that the ion channel properties of nAChRs expressed in L-α3β4 do not mimic exactly those expressed in rat SCG and also differ considerably from the same subunit combination expressed in oocytes (Lewis et al., 1997).

Thus, native receptor-expressing cells remain indispensable for biophysical and pharmacological studies of nAChRs, particularly for the

development of drugs active on central and peripheral neurons for the diagnosis and treatment of various neuropsychiatric disorders.

A suitable experimental model, used in the present project, is represented by rat chromaffin cells which are found in the medullary portion of adrenal glands.

Chromaffin cells

The adrenal medulla is an endocrine gland that affects other tissues and organs by discharging hormones into the bloodstream. Adrenal medulla are part of the sympathetic nervous system, and help to regulate such involuntary functions as heart rate, intestinal movements and pupil dilation. Like the neurons of the sympathetic system, the activity of adrenal medulla is controlled by nerves originating in the spinal cord, in particular the splanchnic nerve that release ACh. The primary chromaffin cell hormone, adrenaline, is closely related to noradrenaline, the characteristic neurotransmitter of the sympathetic nerves. Moreover, the adrenal medulla itself secretes some noradrenaline, and it also releases various neuropeptides.

Chromaffin cell function is relevant under conditions of fear or stress, in which they release the hormone adrenaline into blood vessels to mobilize the body for peak physical response. Flooding the bloodstream at up to 300 times the normal concentration, the adrenaline interacts with receptors on cells in various organs, increasing the heart rate and blood pressure and prompting the release from the liver of extra sugar to fuel muscular work. Taken together, these reactions constitute a "fight or flight" response that prepares one to combat an enemy or flee from danger.

When chromaffin cells, which have the same embryological origin as postganglionic sympathetic neurons (Anderson, 1993), are grown in culture, they extend axon-like processes, which indicates their close kinship with neurons. Adrenal chromaffin cells are readily collected as a

monotypic cell group and they are therefore accessible to biochemical analysis. As a result, they have served as a laboratory model of neurons, and much of what is known about the production and secretion of neurotransmitters was established through studies of the chromaffin cell. Since these are exposed to acetylcholine released by the splanchnic nerve and possess high nAChR density, they have been widely used for pharmacological and physiological studies aiming at characterizing nAChRs (Giniatullin et al., 1999; Khiroug et al., 1998; Khiroug et al., 1997).

The α3, α5, α7 and β4 subunits have been reported to be expressed in bovine chromaffin cells (Criado et al., 1992; Campos-Caro et al., 1997). In rat chromaffin cells the homomeric α7 receptor is not expressed; in fact, α-bungarotoxin is not bound by rat chromaffin cell membranes and does not depress nicotine evoked currents (Di Angelantonio et al., 2000). Bovine chromaffin cells express α-bungarotoxin sensitive receptors (Campos-Caro et al., 1997; Lopez et al., 1998) but they appear to be not relevant to secretion mechanisms probably because of their fast desensitization (Tachikawa et al., 2001).

On chromaffin cells it was observed that nAChRs activation mediate a sustained rise in intracellular calcium concentration (Khiroug et al., 1997; Khiroug et al., 1998; Amador and Dani, 1995; Vernino et al., 1994); the fraction of current carried by Ca^{2+} has been shown to be about 4% of the nicotine induced current. This Ca^{2+} flux through neuronal nAChRs of rat adrenal chromaffin cells is also insensitive to α-bungarotoxin (Vernino et al., 1994).

AIMS OF THE PRESENT STUDY

The aims of the present study are:

1. Molecular biology investigation into the nAChR subunits present in rat chromaffin cells.

2. Immunocytochemical demonstration of the receptor subunits expressed by the same cell type.

3. Electrophysiological characterization of the antagonists actin on such receptors using as prototypes the F3 compound and mecamylamine.

4. Demonstration of the modulatory role of the locally occurring neuropeptide CGRP on nAChRs activity.

5. Identification and characterization of a novel class of peptides endowed with the ability of enhance nAChRs function.

METHODS

Cell Preparation

Rat chromaffin medullary cells were cultured according to the method of Brand et al (1976). Adrenal glands were removed from 25-35 d old rats (anaesthetized with slowly raising levels of CO_2), and were rinsed in a medium (pH 7.2) containing (mM): NaCl 137, KCl 3, Na_2HPO_4 0.7, HEPES 25, glucose 10 and 350 units ml-1 of penicillin and streptomycin. Cells were dissociated by treating adrenal tissue fragments at 37°C for about 60 min with collagenase A and DNAse I (0.5 units ml^{-1} and 10 μgml^{-1}, respectively; both from Sigma) and drawing them gently up and down inside a Pasteur pipette every 15 min. The cell containing suspension was centrifuged at 750 g for 5 min, and rinsed twice with the HEPES-buffered medium. Finally, cells were suspended in Dulbecco's modified Eagle's medium supplemented with 10% foetal calf serum, plated on poly-Lysine (5 mg/ml; Sigma)-coated Petri dishes, and cultured at 37°C for 1-2 days under a 5 % CO_2 containing atmosphere (Khiroug et al., 1998; Giniatullin et al., 2000; Di Angelantonio et al., 2000).

I28 cells in culture were prepared as descript by Irintchev et al. (1997). HEK 293 cells were transfected with $\alpha1\beta2\gamma2$ $GABA_A$ receptors as previously reported (Granja et al., 1998).

Electrophysiology

Patch-clamp recording and confocal imaging

Cell-containing culture dishes (used at 0-3 days from plating) were mounted on the stage of an inverted Nikon Diaphot microscope and superfused (5-10 ml/min) with control saline solution containing (mM): NaCl 135, KCl 3.5, $MgCl_2$ 1, $CaCl_2$ 2, glucose 15, HEPES 10 (pH adjusted to 7.4 with NaOH, osmolarity 285 mOsm). Patch pipettes pulled from

thin glass had 5-6 MΩ resistance when filled with (mM) CsCl 120; HEPES 20; $MgCl_2$ 1; Mg_2ATP_3 3, BAPTA 10 (240 mOSM). The pH of the pipette solution was always adjusted to 7.2 with CsOH.

Cells were voltage-clamped at -70 mV (unless otherwise indicated) in the whole-cell configuration after obtaining GΩ seals (usually not less than 2 GΩ). Series resistance was compensated by 60 %. In the whole cell configuration the cell resistance was usually 100-200 MΩ after compensation. After obtaining whole-cell configuration, a 10 min period of stabilization normally elapsed before membrane currents were recorded, filtered at 1 kHz and acquired on the hard disk of a PC by means of pCLAMP 6.04 software (Axon Instruments Inc., Foster City, California).

When experiments involved confocal $[Ca^{2+}]_i$ imaging the Ca^{2+}-sensitive dye fluo-3 was added to this pipette solution. The pH of the pipette solution was always adjusted to 7.2 with CsOH. Unless otherwise indicated, cells were voltage clamped at -70 mV.

For $[Ca^{2+}]_i$ imaging in the visible light range the Ca^{2+}-sensitive dye fluo-3 (Minta et al., 1989) was applied via the patch pipette (25 μM) or by preincubation (5 μM; cell permeant AM compound). BAPTA was omitted from the patch pipette. Emission of fluo-3 was induced by an Ar-Kr laser (488 nm) and detected by the photomultiplier tube of a MultiProbe 2001 confocal laser scanning microscope (Molecular Dynamics, Sunnyvale, CA) using a combination of 510 nm high-pass and 530±30 nm band-pass filters. Fluorescence signals were digitized over the whole central optical section as 64 x 32 pixel images in the 32-line rapid scan mode (temporal resolution 320 ms per scan; pixel size 0.6 μm; confocal aperture 200 μm), thus yielding a 38 x 19 μm image. $[Ca^{2+}]_i$ transients were analyzed in terms of fractional amplitude ($\Delta F/F_0$; where F_0 is the baseline fluorescence level, and ΔF is the rise over the baseline).

Drug application methods and theoretical calculations

Puffer and fast superfusion

For pressure application, glass micropipettes (thin glass of 1.5 mm o.d. from Hilgenberg, Malsfeld, Germany) were pulled with a PP830 Narashige puller (Narashige International Limited, London, UK) to obtain a resistance of 4 MΩ when filled with patch electrode solution (tip diameter was about 3 µm). For standard use, the pressure pipette was filled with nicotine diluted in external solution and connected to the Picospritzer II instrument (General Valve Co. Fairfields, New Jersey, USA). The pipette was positioned at about 20 µm from each single chromaffin cell under microscopic control. We also performed some preliminary test to monitor the distribution of the solution released by pressure application. For this purpose we filled the puffer pipette with phenol red or methylene blue (0.1 % dilution in extracellular solution) and observed under the microscope how the dye distributed at cell level. With standard puffer pulses (see results) and the pipette positioned in the usual way, the dye solution immediately engulfed the entire chromaffin cell, indicating rapid and homogeneous distribution of the material released by the puffer pipette.

When using the rapid solution exchanger (BioLogic, Strasbourg, France) we filled a number (up to six) of glass barrels (from Clark Electromedical, Pangbourne, UK; type GC100 F15, 1 mm o.d., 0.58 mm i.d.) with various concentrations of nicotine diluted in extracellular solution and we positioned the capillary array as close to the recorded cell (about 1 mm) as possible to avoid mechanical artefacts. Empirically we observed that closer positioning of the perfusion system led to significant pressure artefacts when switching from one solution to another one. This was probably exacerbated by the use of rather small (about 15 µm diameter), dissociated cells without dendritic arbor. In addition, if the perfusion system was too close to the cell, it tended to

mechanically disturb the puffer pipette and to distort responses produced by the latter. Applications via the fast perfusion system were controlled by a PC which commanded the prompt opening of electromagnetic valves and solution flow. With this arrangement the recorded cell was exposed to the rapid flow from one barrel only as the others were kept off stream. Preliminary experiments indicated that there was substantial backfilling (by capillarity) of the glass barrels immersed in the bathing medium with consequent dilution of the nicotine concentration at the tip. This could give the impression of "run up" of cell responses for repeated applications, because successive application blew away the diluted solution and finally delivered nicotine concentrations near or equal the initial one. We found empirically that, to eliminate backfilling dilution, a given barrel had to be activated for 1 s immediately prior to use when its flow stream was still out of line of the cell. Furthermore, the 1 s application included adequate time for rotation of the perfusion multiarray. This procedure ensured reliable responses as long as the barrel nicotine concentration was up to 500 μM. Higher concentrations had to be placed in the farthest away barrel to avoid nAChR activation by a certain amount of nicotine released during the pre-application phase. We also estimated the time required for solution exchange by monitoring the changes in liquid junction potential with a pipette filled with extracellular solution and exposed to rapid superfusion with 3 M KCl applied from various barrels. Switching the flow to the barrels closest to the central one gave a peak of junction potential change at approximately 50 ms. The most remote barrels induced the peak change in junction potential at about 100 ms.

To calculate drug concentration profiles after their delivery by pressure application or rapid superfusion we employed the equations used by Jaeger (1965) to describe the diffusion properties of drugs flowing out of a constricted tube considered either as a point source (puffer pipette) or a source with a certain radius (rapid solution exchanger). Calculations

were performed with the aid of Maple V Release 4 (Waterloo Maple Inc., Waterloo, Ontario, Canada) in Unix version.

Comparing pressure application versus rapid superfusion of agonist

On each single chromaffin cell we recorded inward currents induced by incrementing the pulse duration from the puffer pipette (at constant pressure) containing 100 μM nicotine. One example of raw data is provided in Fig. 5 A when pulse duration varied from 20 ms to 1 s. The peak current amplitude increased with increasing pulse duration, and decayed monoexponentially for pulses up to 100 ms (119 ms time constant for receptor deactivation which is, of course, a distinct process from receptor desensitization). For 1 s pressure delivery, during nicotine application, there was a very large decline (fading) of the current from its peak amplitude, representing desensitization with time constant of 127 ms. This observation accords with our previous report that the fastest time constant of desensitization of rat adrenal chromaffin nAChRs is 110±20 ms (Khiroug et al 1998). After the end of application of a large amount of nicotine 40 % cells displayed an inward current rebound ("off response") with eventual, slow recovery to baseline. The rebound is likely caused by transient reactivation of desensitized nAChRs as previously reported (Maconochie and Knight 1992); (Khiroug et al., 1997).

Note, however, that in general a similar behaviour might have been due to rapid recovery from agonist induced channel block. It has been shown that this kind of block is produced by ACh, that in high concentration (> 1 mM) is known to plug its own open receptor (Sine and Steinbach, 1984; Ogden and Colquhoun, 1985), and by GABA (Bianchi and Macdonald, 2001). Single channel analysis should help to distinguish between desensitization and agonist channel block, because during receptor desensitization, channel opening is characterized by bursts not present when channels are blocked (Grosman and Auerbach, 2001). However, in

the present case it seems unlikely that nicotine itself was blocking the channel for a number of reasons: 1) while at pH=7.4 ACh is positively charged and can sense the electric field across the membrane, at the same pH value nicotine is practically neutral. Hence, it seems difficult that at non saturating concentration (0.1 mM) nicotine could block open channels. 2) If nicotine had been trapped inside the receptor, the fading of the current response should have been voltage dependent, contrary to what was experimentally observed. 3) When an agonist is blocking the open channel, the current deactivation time differs in the absence or the presence of competitive antagonists (Bianchi and Macdonald, 2001).In the present study when the apparently competitive antagonist F3 was bath applied, the current deactivation time was left unchanged.

Note that all nicotine current responses occurred very rapidly (mean time to peak=73 ± 9 ms for the four responses illustrated in Fig. 5 A) with monophasic time course, suggesting that desensitization was not limiting the onset of the current response. Nevertheless, very fast desensitization could also develop during the current onset, thus reducing the peak of the current response (Feltz and Trautmann, 1982). To mimimize this possibility we used a drug delivery protocol that relied on short pulses of non saturating concentration of the agonist.

As long as nicotine applications were spaced at intervals of 1 min, observed responses were closely reproducible (see also Khiroug et al., 1998).

With the rapid solution system (application time was 1 s), Fig. 5 B shows that, on the same cell illustrated in Fig. 5 A, increasing barrel nicotine concentration (50, 100, 500 μM and 1 mM) elicited larger inward currents. Note also the delay between the valve opening (indicated by the small artefact on the left of each trace) and the actual onset of the membrane response. With 50 or 100 μM nicotine (Fig. 5 B), responses reached an apparent steady level, probably reflecting non-desensitized receptor activation because of lack of current fading and high

reproducibility of inward currents. As shown in Fig. 5 B, the on/off response kinetics were slower than those observed with the puffer application because of the different drug delivery system: in fact, the current onset was 269±37 ms (n=20 responses), while the current decay time constant values ranged from 840±104 ms (when desensitization was apparently absent; 50-100 μM nicotine), to 200±10 ms (500-1000 μM nicotine).

The peak elicited by 500 μM superfused nicotine (Fig. 5 B, third from left) showed fading and current rebound after stopping agonist superfusion. The response peak to 1 mM fast superfused nicotine showed even stronger fading and complex decay (Fig. 5 B, right).

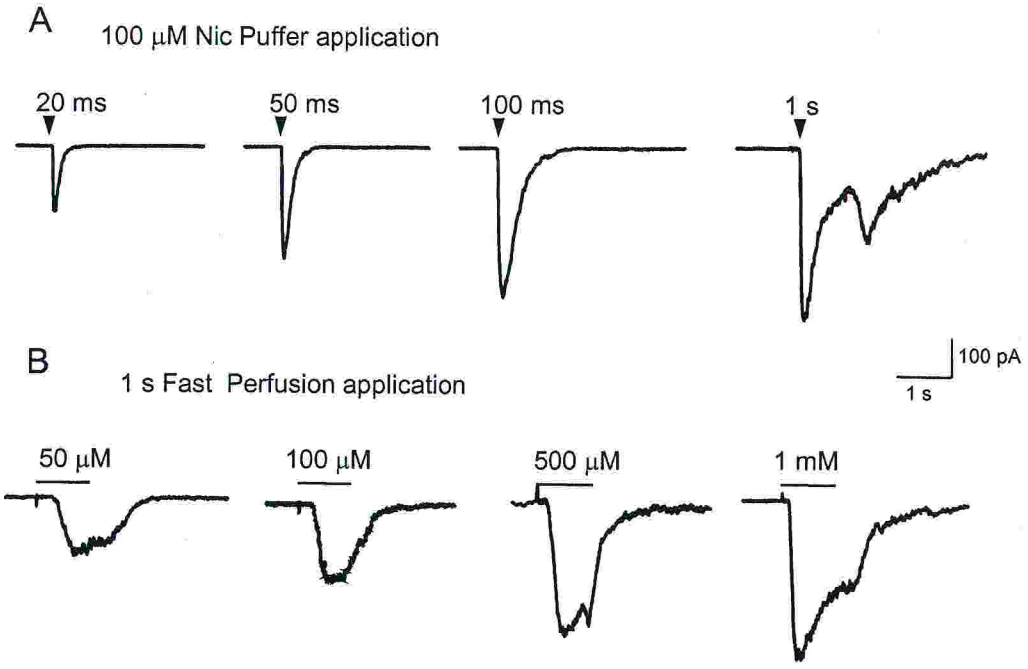

Fig. 5. Examples of responses evoked by nicotine applied by pressure or rapid superfusion. A, inward currents induced by puffer pipette application of various duration. Arrows show time of application. Note large fade of response to 1 s pulse with subsequent rebound. B, comparable responses induced by various concentrations of nicotine applied via rapid solution exchanger. Application times are indicated by horizontal bars. Small vertical deflections are mechanical artefacts due to switching on of superfusion system. All data are from the same cell.

Calibration of pressure applied agonist

Fig. 6 shows plots of peak currents (normalized with respect to the response induced by 20 ms pulses for each cell, n=8 cells) versus log pulse duration (A) or log barrel nicotine concentration (B). Assuming that peak currents, in both types of experiment, reflected the fraction of open nAChRs over those either desensitized or closed, and implying that such peak currents were not limited by desensitization whenever fading was absent, plots in Fig. 6 A, B could be compared to calibrate pressure responses. Thus, the peak responses generated, for instance, by a typical 20 ms pressure application of nicotine should be equivalent to those induced when the concentration of nicotine in the fast superfusion barrel was 43 μM (obtained by extrapolation from Fig. 6 B). The approximately linear portion of these semi-log plots (between 10 and 50 ms in Fig. 6 A or between 20 and 100 μM in Fig. 6 B) allowed direct comparison of the effects induced by various pulse durations and different nicotine concentrations.

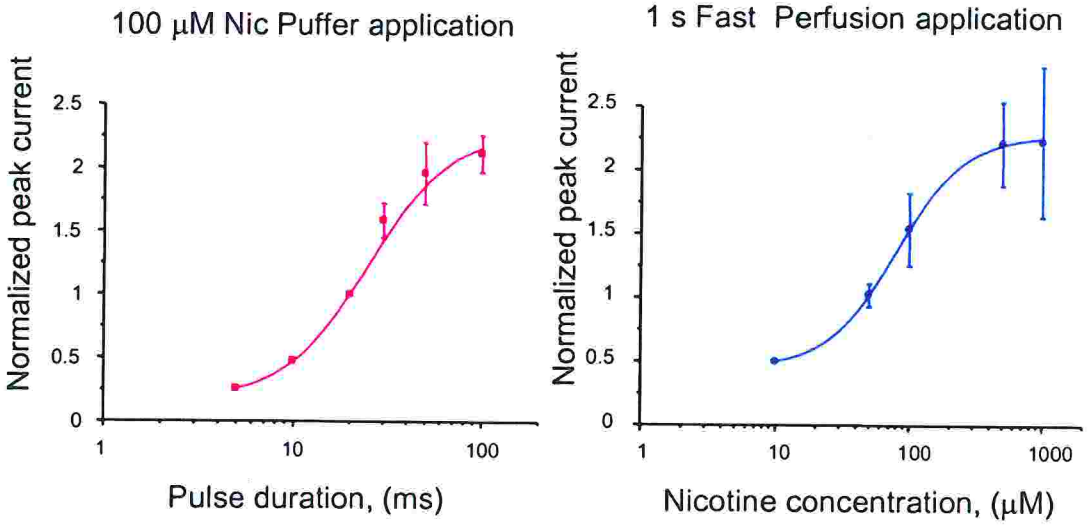

Fig. 6. Log nicotine dose response plots obtained with two methods of application. A, for puffer applications "dose" is expressed as pulse duration (ms) and responses are normalized with respect to the one generated by 20 ms pulses on each cells. B, for rapid superfusion the nicotine concentration is expressed as the amount present in the barrels of the exchanger system. Data are from 8 cells.

Of course, this calibration procedure is not readily applicable to large, near maximal responses like those induced by doses of nicotine higher than 100 μM because desensitization became the prominent phenomenon.

Estimate of nicotine dilution near the cell membrane

It should be noted that the present calibration method relied on the cell responses to the effective concentration of nicotine reaching the cell membrane and not on the initial concentration of nicotine in the pressure pipette or perfusion tubes. As both application methods were based on dynamic delivery under non equilibrium conditions, significant drug dilution was expected to take place depending on various factors like distance from the cell, diffusion coefficient, etc. It is however possible to identify the concentration profile of the agonist at a given distance and time on the basis of the physical properties shown by drugs diffusing out of a constricted tube (Jaeger, 1965).

For pressure applications we assumed that at rest the pneumatically closed circuit did not allow significant passive flow out of the tip of the micropipette and that the amount of drug delivered by pressure was linearly related to ejection pressure as experimentally validated by Obata (Obata et al., 1970). Because we initially estimated the drug concentration at a time much larger (5 fold) than the puffer application time, the physical condition could be approximated by an instantaneous point source (because the pipette tip was very small) as given by Jaeger (1965), thus allowing the use of the following equation (taken from Jaeger, 1965):

$$C_{max} = \frac{M}{8r^3}\sqrt[3]{\frac{6}{\pi}}e^{-3/2} = 0.0736\frac{M}{r^3} \qquad \text{eq (1)}$$

where C_{max} is the maximum value of agonist at cell level and M is the amount of the same agonist delivered at time zero and distance zero. The fluid volume liberated by the puffer pipette with standard pulses

was found to be 0.1 μl, as determined by precision weighting (with a micro-balance) the amount of phenol red dyed solution delivered by pressure pulses. In the case of 100 μM nicotine in the puffer pipette, the effective amount of nicotine during sustained release at a distance r=20 μm was therefore calculated (with eq 1) to be 92 μM. Thus, with the pressure application technique the cell membrane was exposed to a relatively undiluted solution of nicotine if applied continuously.

The following equation (from Jaeger, 1965)

$$t_{max} = \frac{r^2}{6D} \qquad \text{eq (2)}$$

in which the coefficient of diffusion (D) of nicotine in Ringer solution is 5.7 x 10^{-6} ($cm^2\ s^{-1}$; Peper et al 1975), could then be used to estimate the time (t_{max}) required to reach C_{max}. In this case the calculated value was 117 ms from the start of application. In practice, this value indicates that applying pressure pulses >100 ms corresponded to maximal drug delivery and would not lead to further increases in response to nicotine, as confirmed experimentally (see Fig. 6 A).

A different case is estimating the amount of nicotine present at membrane level at a certain time following a short (for example 20 ms) pulse. The time point used for the calculation should be relatively close to the pulse duration otherwise the condition of eq (1) would apply. As the peak of the nicotine inward current developed at 54 ms (Fig. 5 A), we consider this as the time to calculate the nicotine effective concentration (C). The equation (from Jaeger 1965) is:

$$C = \frac{m}{4\pi Dr}\left\{erfc\left(\frac{r}{2\sqrt{Dt}}\right) - erfc\left(\frac{r}{2\sqrt{D(t-t_1)}}\right)\right\} \qquad \text{eq (3)}$$

where

$$erfc\,(z) = 1 - \int_0^z e^{-u^2}\,du$$

t_1=20 ms, t=50 ms, *D* and *r* have the usual values and *m* is the rate of delivery, experimentally measured as the volume of fluid released by puffer pipette in the unit of time (0.1 µl/s). Solution of eq (3) gave 41.9 µM, that is nearly 42 % dilution of original agonist concentration is found 50 ms after a short pulse.

It seemed also useful to examine the concentration profile of agonist concentration applied via fast superfusion. Due to the relatively large orifice (the internal diameter was 0.58 mm) of the perfusion tubes, this case can be equated to diffusion across a small area into a large volume. This can be expressed by the following equation (Jaeger 1965):

$$C = \frac{8aDC_0\sqrt{t}}{\pi a^2\sqrt{D}}\left\{ierfc\left(\frac{z}{2\sqrt{Dt}}\right) - ierfc\left(\frac{\sqrt{z^2+a^2}}{2\sqrt{Dt}}\right)\right\} \qquad \text{eq (4)}$$

where

$$ierfc\,(z) = \int_z^\infty erfc(u)du = \int_z^\infty\left(1 - \frac{2}{\sqrt{\pi}}\int_0^u e^{-x^2}dx\right)du$$

C is the concentration at membrane level at time t=1 s and distance z=1 mm from the orifice of the perfusion barrel, *a* is the radius of the barrel (0.29 mm), D is the coefficient of diffusion and C_0 is the concentration in the barrel.

Solving this equation provided

$$C = 0.46C_0$$

which corresponds to approximately 50% dilution of the initial nicotine concentration once it had reached the cell.

The correspondence between experimentally derived concentration values and calculated concentrations was reasonably good considering that calculations were based on several assumptions and disregarded the fact that cells were continuously superfused rather than in a stationary medium. Thus, assuming that the dilution from the solution exchanger was effectively 46 % according to the diffusion equation, the

calibration of pressure concentrations for 20 ms pulses obtained from Fig. 6 B should be corrected to 21 μM while the Jaeger equation predicted 42 μM for such a short pulse application. This is a relatively small difference probably due to local factors (tip diameter, distance etc) which cannot be standardized.

In conclusion, pressure application of agonists appears to be a simple method to deliver drugs at concentrations which can be estimated with reasonable accuracy through the procedure described in the present report. With short pressure applications receptor desensitization is minimized and the agonist can be delivered quickly to mimic the natural course of action of the endogenous transmitters. Dilution of agonist concentration was relatively limited when the present experimental conditions were applied.

In the present study agonists were usually delivered by short pressure pulses via a puffer pipette. Antagonists were applied by the rapid solution exchanger or in earlier experiments (those with F3 and CGRP) by a second puffer filled with the antagonist solution and positioned at about 100 μm from a single chromaffin cell under microscopic control. The antagonist was puffed continuously for at least 60 s. After 15 s of antagonist preapplication, nicotine was then applied to the cell in the continuous presence of the antagonist. Tests were run to check for the possibility of drug washout by the stream of solution applied through the second puffer: for this purpose we filled the two puffer pipettes with phenol red or methylene blue (0.1 % dilution in extracellular solution) and observed under the microscope how the two dyes distributed at cell level. With puffer pulses ranging from a few millisecond to minutes (to examine the all spectrum of puffer delivery times) both solutions were seen to immediately engulf the entire cell, indicating homogeneous distribution of the solutions released by the puffer pipettes without apparent dilution of the two compounds when co-applied.

Electrophysiological data analysis

Data are presented as mean±sem (n=number of cells) with statistical significance assessed with Wilcoxon test (for non parametric data) or paired *t*-test (for normally distributed data). A value of $P \leq 0.05$ was accepted as indicative of statistically significant difference. Agonists dose/response curves were fitted with a standard logistic equation:

$$I = I_{max} \frac{x^n}{k^n + x^n} \qquad \text{eq(5)}$$

where I and I_{max} were the test and maximal nicotine currents, respectively, and x was the nicotine dose (expressed as pulse duration if the puffer pipette was used) and k was a constant, n was the Hill coefficient.

At various holding potentials (-120 to -30 mV range) the IC_{50} values (concentration producing 50 % reduction in nicotine current amplitude) for mecamylamine block were calculated with the following equation:

$$I_c - I_b = \frac{I_c}{1 + \left[\frac{IC_{50}}{[B]}\right]^{n_H}} \qquad \text{eq (6)}$$

where I_b and I_c are amplitudes of blocked and control currents, [B] the mecamylamine concentration and n_H the Hill coefficient. These values were plotted against membrane potentials to estimate the IC_{50} value at 0 mV. The latter value was used for the Woodhull's standard equation (1973)

$$I_b = \frac{I_c}{1 + \frac{[B]}{K_d(0) \cdot e^{\delta z FV / RT}}} \qquad \text{eq (7)}$$

by assuming that the mecamylamine IC_{50} value could be used instead of its K_d value (equilibrium dissociation constant).

The Woodhull's equation enabled us to estimate the portion of membrane electric field sensed by the mecamylamine binding site

(expressed as δ) inside the nAChR. For this we considered that at pH 7.4 this agent is almost fully charged (pK_a=11.2; Goldstein et al., 1979).

Note that using the IC_{50} value instead of the K_d value may introduce an error when calculating the δ value. It is possible to work out the extent of deviation of δ from its correct value resulting from this simplification. It is therefore useful to relate K_d to IC_{50} as indicated by the Cheng-Prusoff equation (Lazareno and Birdsall, 1993) :

$$K_d = \frac{IC_{50}}{\frac{[A]}{EC_{50}} + 1} \qquad \text{eq (8)}$$

where [A] is the agonist concentration and EC_{50} is the agonist concentration causing 50% of its maximal effect.

We can then relate $\delta(K_d)$ (the correct δ value) to $\delta(IC_{50})$ (the δ value obtained when IC_{50} was employed):

$$\delta(K_d) = \delta(IC_{50}) + \frac{zRT}{FV}\ln\left(\frac{[A]}{EC_{50}} + 1\right) \qquad \text{eq (9)}$$

Since we are usually working at agonist concentration near the nicotine EC_{50}, at room temperature and clamping the cell at V=-70 mV, eq(9) gives:

$$\delta(K_d) = \delta(IC_{50}) - 0.25$$

Therefore our method for calculating δ would overestimate it by approximately 25%.

RT-PCR

RNA Extraction

The total RNA content of chromaffin cells cultures was isolated with TRIzol ™ (Gibco) method. Briefly cells were lysed directly in the culture dish by adding 1 ml TRIzol ™ Reagent, then passed several times through a pipette and incubated 5 minutes at room temperature (RT) to

allow the complete dissociation of nucleoprotein complexes. To perform phase separation, after shaking for 15 s and incubating at room temperature (RT) for 2-3 min, samples were centrifuged at 12.000 *g for 10 min at 4° C. The aqueous phase, containing RNA, was then collected in a fresh tube to precipitate RNA by mixing it with isopropyl alcohol (0.5 ml per 1 ml TRIzol™ used). Samples were then incubated at RT for 10 min and centrifuged at 12.000 *g for 10 min at 4° C. The gel-like pellet on the side and bottom of the tube contained the precipitated RNA. The supernatant was removed and the RNA pellet was washed with 75% ethanol (1 ml per 1 ml TRIzol™ used). The sample was then mixed by vortexing and centrifuged at 7.500 *g for 5 min at 4° C. At the end of the procedure RNA pellet was air-dried for 5-10 min and dissolved in RNase-free water by passing the solution a few times through a pipette tip, and incubating for 10 min at 60° C. RNA was then stored at -20°C.

Reverse Transcription reaction (RT)

The RT mix consisted of (in mM unless otherwise stated): 50 KCl, 10 Tris-HCl (pH 8.3), 5 $MgCl_2$, 1 DTT, 1 each dNTP, 2.5 μM random hexamers, 0.33 U/μl RNase inhibitor, 10 U/μl Reverse transcriptase, in DEPC treated water (all reagents from ROCHE), and 20 μl RNA. RT had total volume of 100 μl.

Reactions were run at 25° C for 10 min, 42°C for 60 min and 95°C for 5 min in a thermal Cycler. Reaction products were stored at 4°C until running PCR.

Polymerase Chain Reaction (PCR)

The first round of multiplex PCR was performed by adding the following to 10 μl of the RT reaction (in mM unless otherwise stated): 50 KCl, 10 Tris-HCl (pH 8.3), 2.5 $MgCl_2$,0.25 each dNTP, 0.2 μl each upstream and downstream primers for the nAChR subunits and β-actin

primer, and 0.05 U/μl DNA Taq polymerase in DEPC treated water to a final volume of about 30 μl.

PCR was held at 94°C for 30 s, then cycled 25 times. Each cycle consisted of: 92°C for 15 s, 55°C for 20 s, and 72°C for 30 s. 2μl samples of the initial multiplex PCR were used as substrate for the second round of specific PCR. A 25 μl reaction was prepared for each specific sequence analysed.

These reaction consisted of (in mM unless otherwise stated): 50 KCl, 10 Tris-HCl (pH 8.3), 1.5-3 $MgCl_2$,0.25 each dNTP, 1 μl each upstream and downstream general primers for the nAChR subunits and β-actin primer, and 0.025 U/μl DNA Taq polymerase in DEPC treated water. The second round product specific used the same primers listed in Table1.

Reactions were held at 92°C for 30 s and then cycled 40 times as follows: 92°C for 15 s, annealing temperature (55-63°C) for 20 s, and 72°C for 30 s. 7 μl samples were analysed on 2% agarose gels using ethidium bromide and U.V. illumination.

RT-PCT control

Solutions were tested periodically to insure they had no inherent RNase activity. Gloves were worn during all experiments and all tubes and tips were handed to be RNAse free. Beta-actin detection was used as positive control for RNA extraction.

Primer design

The first consideration for primer design is the sequence region to amplify. The second consideration is that the upstream and downstream primers should bind to exon regions. On the basis of these two requirements primers were designed to amplify mRNAs for different nAChR subunits while recognizing their non homologous sequences. This was a difficult task because of the large homology between

different subunits; for instance α3 and α6 subunits share 98% of their sequence (Le Novere et al., 1996).

Candidate primers were examined with the PCRPLAN module of the PC/GENE™ software package (kindly provided by Dr. Jerry Yakel, NIH). This program examines primer pairs for a number of parameters. In particular, primer self-complementarity, stem-loop formation, complemantarity between primers, complemetarity to other regions of the template, and compatible calculated annealing temperature (calculated annealing temperatures within 5° C of each other). Primers that have self-complementarity (that is, they bind to another primer molecule of the same sequence) leading to stem-loops (primer folds over and bind to itself), or that are complementary to the other primer sequence, can remove a large fraction of the primer pool available for PCR. Primers that have significant complementary to other regions of the same template (or other unknown templates) can generate multiple PCR products.

Candidate PCR primer sequences were screened against the GenBank DNA sequence database using the BLASTN computer program. Primers that showed possible binding to other known sequences were rejected. Finally, primers were compared with those used by other research groups (Le Novere et al., 1996; Sheffield et al., 2000; Sudweeks and Yakel, 2000)).

Primers used for the present investigation are listed in Table1.

Alpha2FOR	GAT CTG GAT CCC AGA CAT TG
Alpha2REV	CGC CGA TGA GTG GGA TGA CC
Alpha3FOR	GGA GAA GTG ACT TGG ATC C
Alpha3REV	CAA GTG GGC ATG GTG TGT G
Alpha4FOR	CCA GAT GAT GAC AAC CAA CG
Alpha4REV	CCA CAC GGC TAT GAA TGC TC
Alpha5FOR	CGA ACG TCT GGT TGA AGC
Alpha5REV	CAC CAT AAT GGA TAG GG
Alpha6FOR	TCT TAA GTA CGA TGG GGT GAT AAC
Alpha6REV	AAC ATG GTC TTC ACC CAC TTG
Alpha7FOR	TTG CCA GTA TCT CCC TCC AG
Alpha7REV	CTT CTC ATT CCT TTT GCC AG
Beta2FOR	CCG GGA CCG GCA AGA AGC CG
Beta2REV	ACT AGC CGC TCC TCT GTG TC
Beta4FOR	GGT TGC CTG ACA TCG TGT TG
Beta4REV	GCC AAT GAG CGG TAT GTC
ActinFOR	AAG ATC CTG ACC GAG CGT GG
ActinREV	CAG CAC TGT GTT GGC ATA GAG G

Table1. List of primer sequences

Protein detection

Antibody staining of cultured chromaffin cells

For double staining of cultured chromaffin cells with antibodies against nAChR subunits, cells were fixed for 10 min at room temperature (RT) in 4% paraformaldeyde in phosphate buffer saline (PBS), washed in PBS and permeabilised in 100% ethanol for 15 min at -20°C. Cells were permeabilized because some of the antibodies recognized intracellular portions of the epitopes.

After rehydratation with decreasing ethanol concentrations in PBS at RT, cells were incubated overnight at 4°C with polyclonal antibodies against different nAChRs subunits at different dilutions (as indicated in the results) diluted in 10% FCS in PBS plus 0.01% Tween 20 detergent (PBST). After washes in PBST, cells were incubated 2 hour at r.t. with fluorescence conjugated secondary IgG antibodies, diluted 1:100 in 10% FCS in PBS. Cells were then washed in PBS twice and mounted in Vectashield (Vector). Fluorescence was analysed with fluorescein and rhodamine filter under dark field, on a Zeiss Axiophot microscope.

As control, some cover-slips were incubated with the secondary antibody only.

Western Blot of adrenal glands homogenates

Whole extracts from rat adrenal glands were analyzed by Western blots. Tissues were homogenized in five volumes of boiling lysis buffer (1% SDS, 10 mM Tris-HCl, pH 7.4) and centrifuged at 550 × g for 10 min. Supernatant was collected, aliquoted, and frozen at -80°C until use.

Fifty microgram aliquots of either sample were separated by SDS-PAGE (10% gels). Proteins were transferred to nitrocellulose membranes, blocked overnight with 5% non-fat dry milk in TBST buffer (10 mM Tris-HCl, pH 7.5, 100 mM NaCl, and 0.1% Tween 20) at 4°C and then

incubated at room temperature with antibodies against nAChR subunits at different dilutions (as indicated in the results) in the same blocking buffer for 1 hr, washed with TBST, and incubated with a peroxidase-conjugated secondary antibody (diluted 1:5000) for 1 hr, after which membranes were washed again. Bound peroxidase was detected using enhanced chemiluminescence.

RESULTS

While neuronal nicotinic receptors (nAChRs) are key molecules for synaptic transmission, the role and function of most of their subtypes are difficult to establish because they may be co-expressed by the same individual neurons. For this reason, tools to improve their pharmacological dissection would be very useful to elucidate the relative contribution by nAChR subtypes to normal synaptic transmission and, potentially, to the pathophysiology of neurological disorders like AD, PD, epilepsy, schizophrenia, and Tourette's syndrome (Lena and Changeux, 1997; Lindstrom, 1997).

Starting from this consideration we investigated the action of different chemicals capable of modulating nicotinic receptor function by different mechanisms of action.

1. Functional and molecular characterization of the subunit composition of nAChRs in rat chromaffin cells

Neuronal type of nicotinic acetylcholine receptors are expressed by chromaffin cells that receive ACh from splanchnic nerve endings. While bovine chromaffin cells are known to posses both homomeric α7 receptor and heteromeric α3β4 ore α3α5β4 receptors (Campos-Caro et al., 1997; Lopez et al., 1998) the subunit composition of nAChRs expressed by rat chromaffin cells is still unknown.

We then examined with different techniques the properties of nAChRs of rat chromaffin cells in order to know their subunit composition.

1.1 RT-PCR analysis of native nAChRs

We used RT-PCR to investigate the presence of mRNA for the various nAChR subunit in cultured chromaffin cells. We used primers specific

for the α2, α3, α4, α5, α6, α7, β2, β3, and β4 nAChR subunits and for β-actin. The β-actin primers served as positive controls.

Fig. 7 reports the result of representative experiments for the detection of nAChR α subunit transcripts from cultured chromaffin cells. The primers for the α2 (A), α3 (B), α4 (C middle line), α5 (C right line) and α7 (D right line) subunits always yielded products of the expected size, whereas the α6 (D middle line) did not.

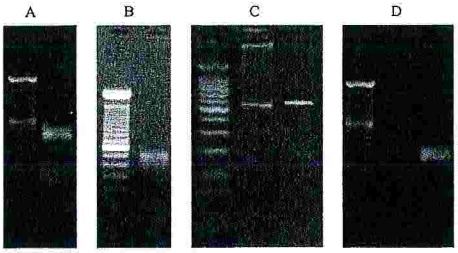

Fig. 7. Detection of nAChR α subunit transcripts in cultured rat chromaffin cells. In each panel A-D the right hand side lane shows the nicotinic transcript while the left hand side shows the markers which are 100 bp compounds. The α2 (A), α3 (B), α4 (C, middle lane), α5 (C right lane), α7(D right lane), subunit primers yielded products of the expected size, the α6(D middle lane) subunit was not detected.

This pattern of expression was the same in most of the experiments. Fig. 8 shows the results of experiments for the detection of nAChR β subunits and of the positive control β-actin. The primers for the β2 (A), β4 (C), subunits and those for β-actin always yielded products of the expected size, whereas the β3 (B) was not detected.

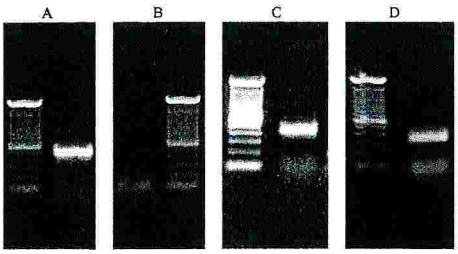

Fig. 8. Detection of nAChR β subunit transcripts in cultured rat chromaffin cells. In panels A, C and D the marker lane is on the left while it is on the right in panel B. The β2 (A) and β4 (C) subunit primers yielded products of the expected size, as well as the β-actin (D) used as positive control; the β3 (B) subunit was not detected.

Since the presence of mRNA for different subunits does not allow extrapolating the exact receptor composition (mRNA might not be transduced into a functional protein), we then moved to a method for protein detection (immunocytochemical staining and immunoblotting).

1.2 Immunofluorescence detection of proteins recognized by specific antibodies for the nAChR subunits.

In order to detect the protein expression of nAChR subunits we tested the commercially available antibodies against different subunits. After determining the most suitable antibody dilution, we performed single and double-immunofluorescence tests using antibodies against α2, α3, α4, α5, α7, β2, and β3 subunits. Unfortunately, the antibody against β4 subunit was not commercially available.

No chromaffin cell was immunoreactive for the α7 or the β3 subunits, when used at different concentrations (from 1:3000 to 1:500 for the monoclonal α7, RBI; and from 1:200 to 1:50 for the polyclonal β3, Santa Cruz).

We determined the expression of α3 protein in chromaffin cells by examining the binding to cultured cells of a polyclonal rabbit IgG specific for the human α3 sequence (Santa Cruz Biotechnology) used at 1:100 dilution. Binding was detected with a fluorescein conjugated chicken anti-rabbit secondary antibody (used 1:100, Chemicon). We found antibody staining in 36 over 40 cells examined. Fig. 9 A reports the results of three representative immunofluorescence labelling experiments for α3. On the same cells the goat polyclonal anti α5 antibody (1:100, Santa Cruz), detected with a Cy3 conjugated rabbit anti secondary antibody (1:100, Sigma) stained 12 over 20 cells (Fig. 9 B). Fig. 9 C shows the double staining of sample cells when visualized with the triple filter. No staining was detected if we omitted the primary antibodies.

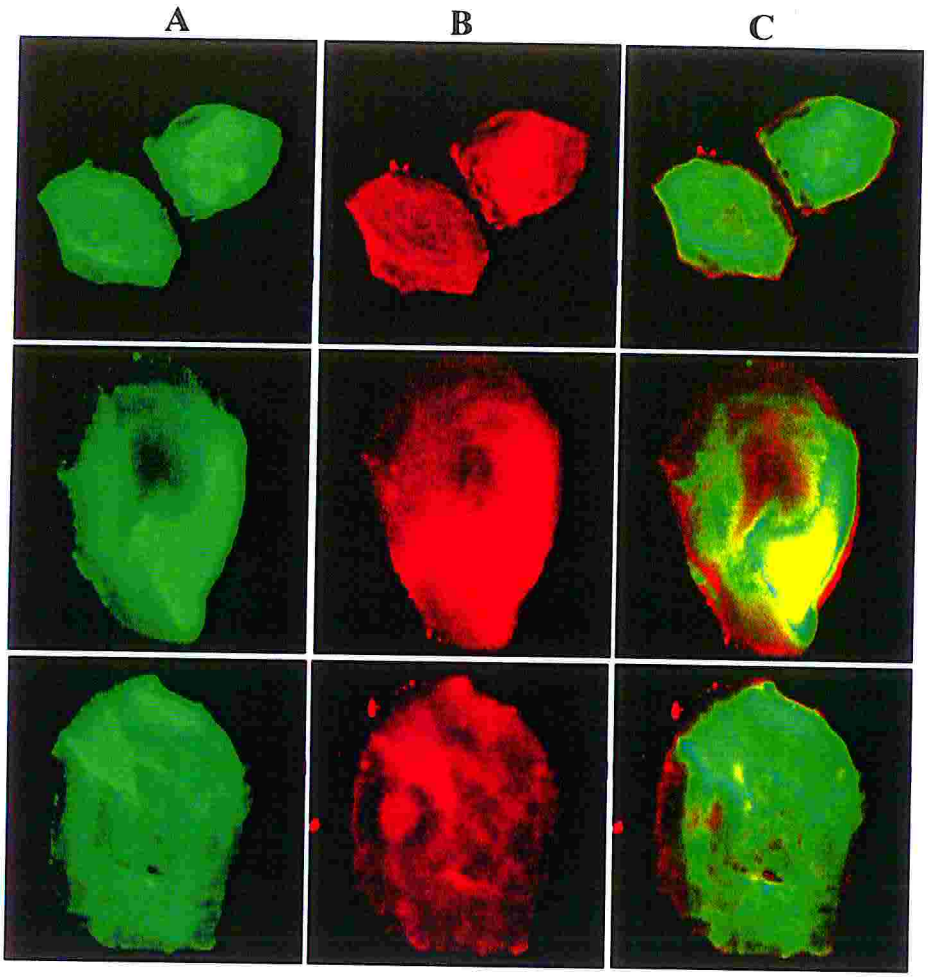

Fig. 9. Staining for α3 and α5 antibodies. Examples of chromaffin cells from three experiments stained with anti-α3 nAChRs subunit antibody (green, Column A), anti α5 nAChRs subunit antibody (red, Column B). The presence of both subunit antibodies bound to the cells is revealed the superimposed signals as shown with triple filter (Column C).

We determined also the expression of α2 subunits in chromaffin cells by examining the binding of a polyclonal goat antibody for the human α2 sequence (Santa Cruz Biotechnology) used at 1:100 dilution. Binding was detected with a Cy3 conjugated rabbit anti goat secondary antibody (used 1:100, Sigma). We found antibody staining in 8 over 30 cells examined. Fig. 10 B reports the results of three representative immunofluorescence labelling experiments for α2, while Fig. 10 A shows the same cells labelled with the anti α3 antibody. Fig. 10 C shows the

double staining of some sample cells when visualized with the triple filter. No staining was detected if we omitted the primary antibodies.

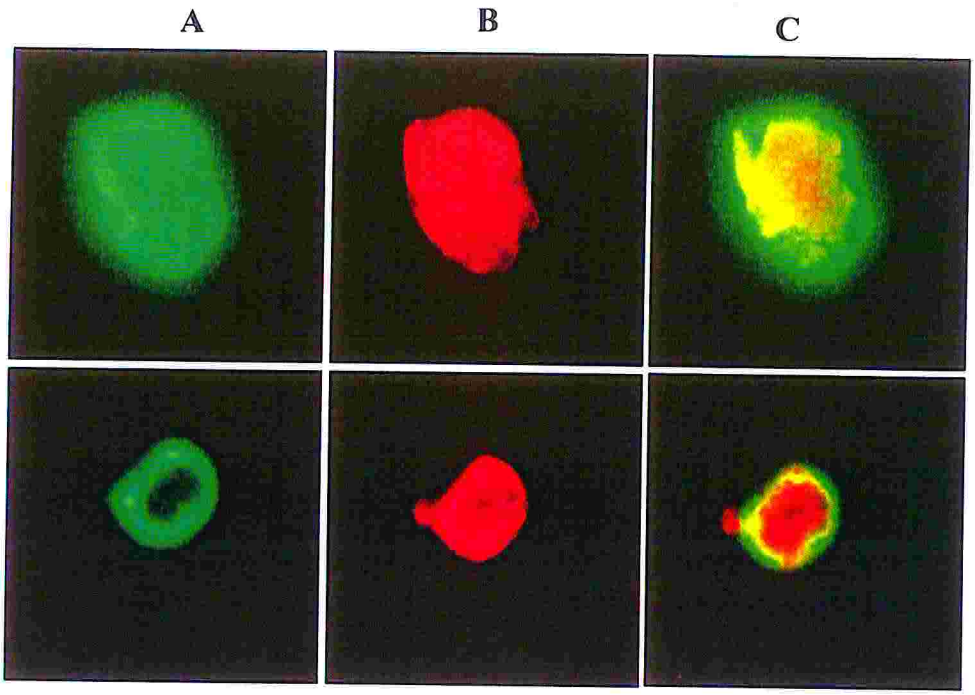

Fig. 10. Staining for α3 and α2 antibodies. Examples of chromaffin cells from three experiments stained with anti-α3 nAChRs subunit antibody (green, Column A), anti α2 nAChRs subunit antibody (red, Column B). The presence of both subunit antibodies bound to the cells is revealed the superimposed signals as revealed with triple filter (Column C).

Fig. 11 A shows the expression of α4 subunits in chromaffin cells by examining the binding of a polyclonal goat antibody for the human α4 sequence (Santa Cruz Biotechnology) used at 1:100 dilution. Binding was detected with a Cy3 conjugated rabbit anti goat secondary antibody (used 1:100, Sigma). We found antibody staining in 4 over 32 cells examined. Fig. 11 B shows the same cells labelled with the anti α3 antibody used as before. Fig. 11 C shows the double staining of some sample cells when visualized with the triple filter. No staining was detected if we omitted the primary antibodies.

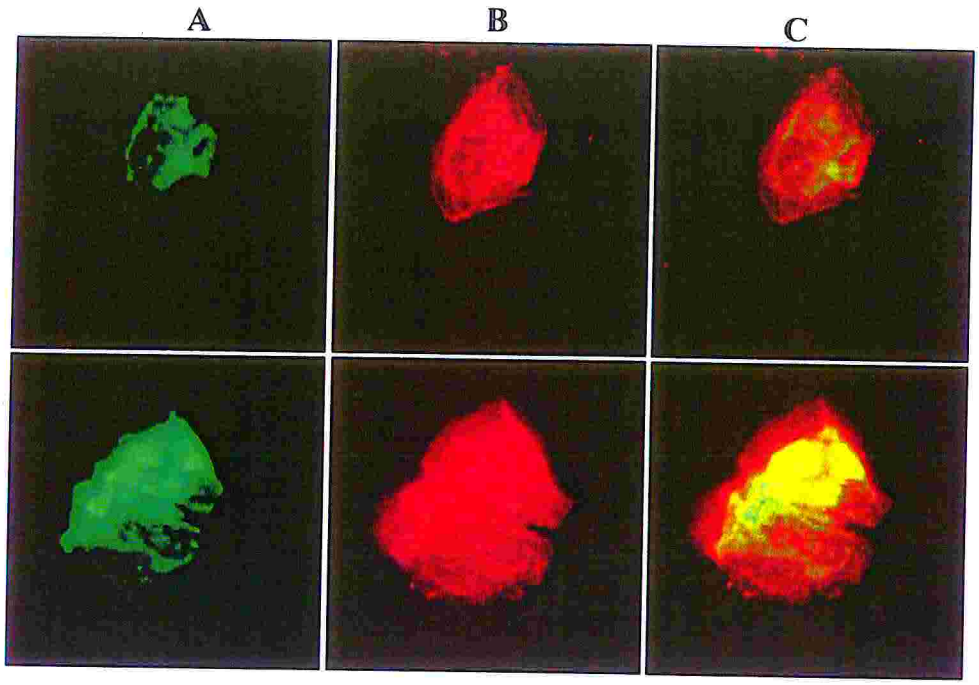

Fig. 11. Staining for α4 and α3 antibodies. Examples of chromaffin cells from three experiments stained with anti-α4 nAChRs subunit antibody (green, Column A), anti α3 nAChRs subunit antibody (red, Column B). The presence of both subunit antibodies bound to the cells is revealed the superimposed signals as revealed with triple filter (Column C).

Fig. 12 A shows the expression of α3 and β2 proteins in chromaffin cells by examining binding of the same polyclonal rabbit anti-α3 antibody (Santa Cruz Biotechnology) and a monoclonal rat anti-β2 antibody used at 1:700 dilution.

The α3 labelling was detected with a fluorescein conjugated chicken anti-rabbit secondary antibody, while the β2 labelling (Fig. 12 B) with a rhodamine conjugated goat anti-rat antibody. Binding was detected with a Cy3 conjugated rabbit anti goat secondary antibody (used 1:100, Sigma) which was pre-adsorbed by incubation overnight with rat adrenal glands slices to avoid non-specific binding to rat tissue. We found β2 staining in 30 over 35 cells examined. Fig. 12 C shows the double staining of some sample cells when visualized with the triple filter. No staining was detected if we omitted the primary antibodies.

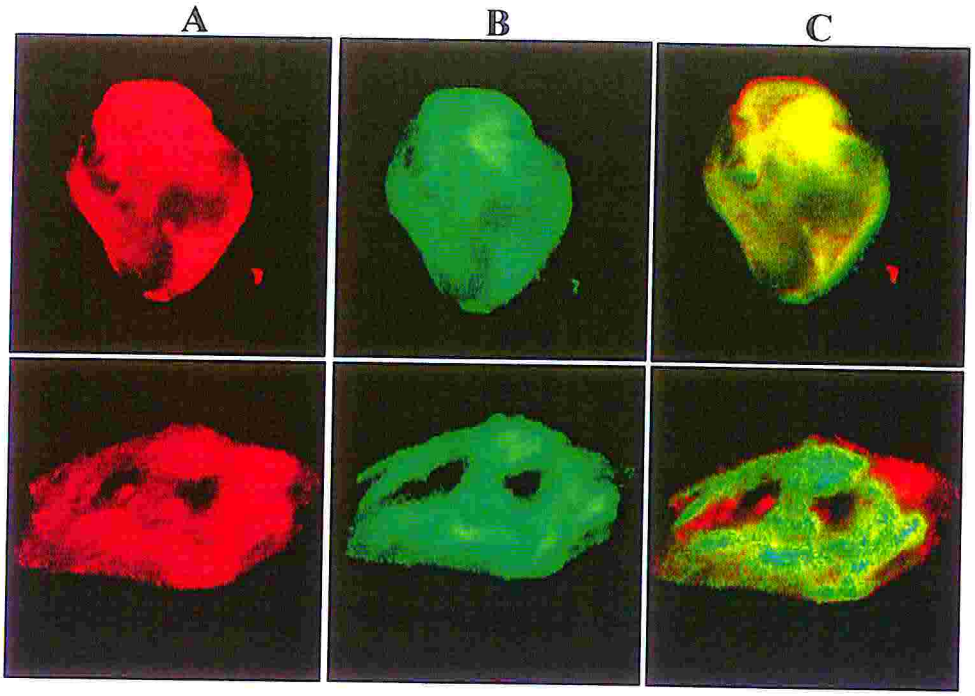

Fig. 12. Staining for α3 and β2 antibodies. Examples of chromaffin cells from three experiments stained with anti-α3 nAChRs subunit antibody (green, Column A), anti β2 nAChRs subunit antibody (red, Column B). The presence of both subunit antibodies bound to the cells is revealed the superimposed signals as revealed with triple filter (Column C).

1.3 Western blot analysis of rat adrenal glands homogenates.

The rabbit anti-α3 and β2 antibodies are suitable also for detection of α3 and β2 subunits in Western blots. Goat polyclonal antibodies for α2, α4 and α5 subunits (Santa Cruz Biotechnology) did not work properly in Western blot analysis because of non selective binding by the secondary antibody. We used the rabbit antibodies to test (by Western blotting) several independent preparations of adrenal glands homogenates. Fig. 13 reports the results of representative experiments in which subunits of the correct molecular weight of α3 and β2 were detected.

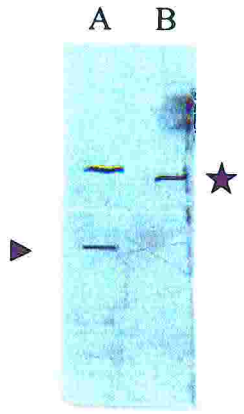

Fig. 13. Western blot detection of subunit bands recognized by antibodies specific for β2 (A) and α3 (B) subunits. Triangle and star indicate the position of bands of molecular mass of ~45 and 70 kDa that were consistently present in the adrenal gland extracts.

1.4 Functional characterization of native nAChRs using selective blockers

The presence of mRNA, detected with RT-PCR analysis, together with the expression of the protein, detected with immunostaining and immunoblotting, did not allow to speculate about the real stoichiometry of various heteromeric receptors since more than one composition of subunits is possible.

In order to characterize the functional properties of nAChRs expressed by rat chromaffin cells we then tested pharmacological tools to discriminate between different receptor compositions.

Starting from the α7 homomeric receptor, that we revealed as mRNA content but not as protein expression (although αBgtx binding sites have been reported in bovine adrenal medullary tissue; Garcia-Guzman et al., 1995), we tested α-bungarotoxin and methyllycaconitine (MLA) at various concentrations.

α-Bungarotoxin (in addition to blocking muscle nicotinic receptors) potently blocks the α7 homomeric receptor (Seguela et al., 1993). MLA, an alkaloid toxin from *Delphinium brownii* , is a specific α7 receptor

blocker when used at nanomolar concentrations (Alkondon et al., 1997a; Couturier et al., 1990).

We tested if α-bungarotoxin could interfere with nicotine-evoked currents of rat chromaffin cells. Application of αBgtx in concentrations up to 5 μM for 30 min failed to change nicotine-induced currents. Preliminary experiments using an imaging technique to assess changes in intracellular Ca^{2+} levels (Giniatullin et al., 1999; Khiroug et al., 1997) did not detect any variations in nicotine-evoked rises in internal Ca^{2+} in the continuous presence of 1-5 μM αBgtx (data not shown).

Fig. 14 A shows that, when MLA was used at nanomolar concentration as specific blocker for α7 containing receptors, nicotine evoked currents (20 ms, 0.1 mM) were left unchanged. Increasing the MLA concentration lost receptor specificity and at concentration of 1 μM MLA reduced nicotine evoked currents by 44±3% (n=8, $p<0.05$; see Fig. 14 B as representative traces). Complete current block was obtained with 10 μM MLA.

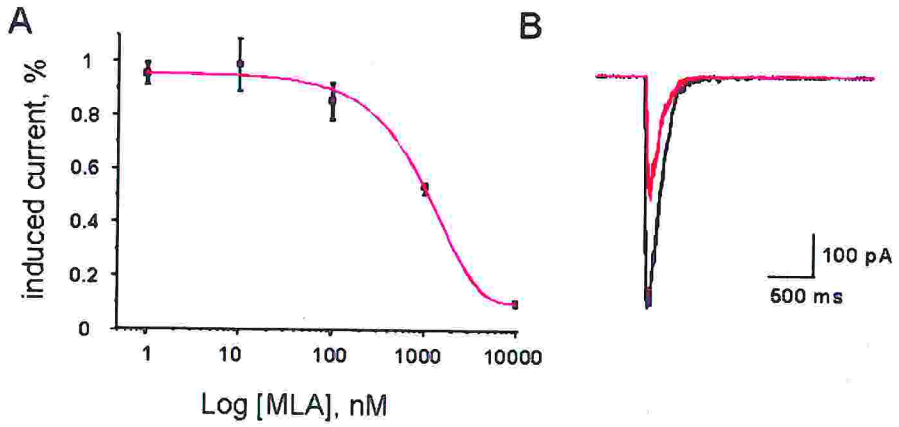

Fig. 14. MLA antagonism on nicotine evoked currents. A: Plot of the fractional reduction in current amplitude against different log concentrations of MLA (ranging from 1 nM to 10 μM). The test pulse (20 ms, 100 μM) of nicotine was the same for all concentration of MLA (n=8 cells). The IC_{50} value for MLA was 1 μM. B: superimposed traces of nicotine evoked currents in control and in the presence of 1 μM MLA.

Other available pharmacological tools for distinguish between different nAChR subunits have been isolated from the venom of carnivorous marine snail *Conus* by John McIntosh's group in Salt Lake City, Utah. This lab kindly provided samples of MII α-conotoxin that targets α3β2 nAChRs (Cartier et al., 1996), as well as samples of AuIB α-conotoxin that selectively blocks α3β4 nAChRs (Luo et al., 1998).

Fig 15 shows the effect of MII conotoxin on nicotine evoked currents (0.1 mM, 20 ms pressure application). The current, in the presence of 1 nM MII, was depressed by 13±3 % (n=12, $p<0.05$), indicating a small presence of α3β2 receptors. However, the IC_{50} value was about 1μM, that is very distant from the one reported for pure α3β2 receptors expressed in *Xenopus* oocytes (0.5-8 nM, ACh 0.3 mM; Cartier et al., 1996; Harvey et al., 1997; Kaiser et al., 1998)

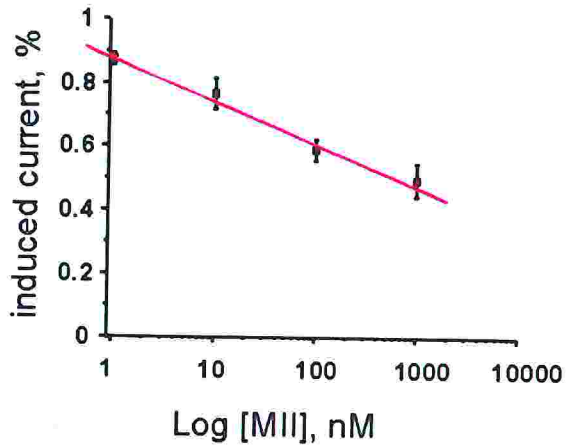

Fig. 15. Dose-response curve for MII toxin antagonism on nicotine evoked currents. Plot of the fractional reduction in current amplitude against different log concentrations of MII (ranging from 1 nM to 1 μM). The test pulse (20 ms, 100 μM) of nicotine was the same for all concentration of MII (n=12 cells). The calculated IC_{50} value for MII was 1 μM.

Since the dose-response curve for MII toxin antagonism stretched over four concentration log-units, this observation indicates heterogeneity of chromaffin nAChRs and that such a toxin was blocking a fraction of them only.

Similar considerations may be applied to the findings concerning the AuIB toxin. In fact, the dose response curve for this antagonist was very shallow, indicating that it was blocking a limited subgroup of nAChRs contributing to the overall current response amplitude.

The blocking action of AuIB α-conotoxin is shown in Fig. 16: nicotine evoked currents were partially blocked when the toxin was used at nanomolar concentrations (16±3 % at 10nM AuIB, n=9, $p<0.05$), but, also in this case, the extrapolated IC_{50} (70 μM) was very different from that one reported for pure α3β4 receptors when they are expressed in *Xenopus* oocytes (750 nM, ACh 0.3 mM; Luo et al., 1998). At 1 μM concentration, in fact, we only obtained a current reduction of 35±5 % (n=9, $p<0.05$), respect to the control.

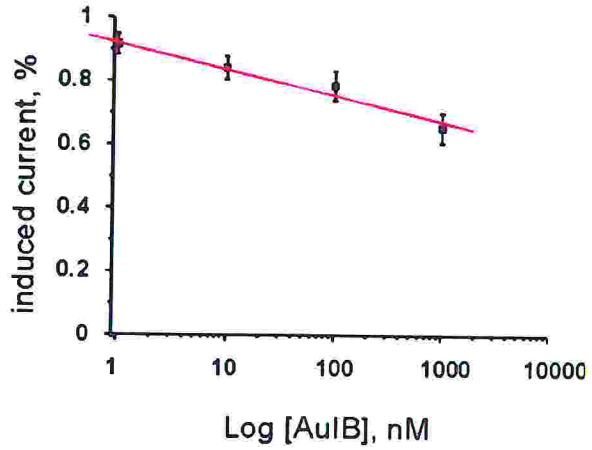

Fig. 16. Dose-response curve for AuIB toxin antagonism on nicotine evoked currents. Plot of the fractional reduction in current amplitude against different log concentrations of AuIB (ranging from 1 nM to 1 μM). The test pulse (20 ms, 100 μM) of nicotine was the same for all concentration of AuIB (n=9 cells). The extrapolated IC_{50} value for AuIB was 70μM.

Note that it is difficult to compare our data with those based on IC_{50} values obtained by different laboratories under different experimental conditions (cultured cells versus expression systems; patch versus two electrode voltage clemp; different drug delivery etc.).However, the very considerable discrepancy (orders of magnitude) between the sensitivity

of nAChRs to the conotoxins suggests that the receptor assemblies for which they are selective made a limited contribution to the overall nAChR population.

Table2 summarizes the subunit composition observed for nAChRs of chromaffin cells: α3, β2 and β4 although the potential role of α5 subunits remains to be established owing to lack of blockers selective against it.

Subunit	mRNA	Protein (IHC)	Protein(WB)	Pharmacology
α2	+	+		
α3	+	+	+	+
α4	+	+		+
α5	+	+		
α6	-			
α7	+	-		-
β2	+	+	+	+
β3	-	-		
β4	+			+

Table2. Results of detection of different subunit by different methods. + indicates the presence of the subunit; - indicates data contrary to the presence of the subunit. Empty boxes indicate not tested due to lack of available tools.

2. Antagonism of nicotinic receptors of rat chromaffin cells by N,N,N-trimethyl-1-(4-*trans*-stilbenoxy)-2-propylammonium iodide (F3).

While searching for new compounds active on nAChRs, two oxystilbene derivatives (MG624 and its more recently synthesized derivative F3) were shown to be selective ligands for chick nAChRs sensitive to αBgtx (Gotti et al., 1998; Maggi et al., 1999). Nevertheless, since MG624 has been originally developed as a ganglioplegic drug and found to produce potent ganglion blocking activity measured as strong hypotension (Cavallini *et al.*, 1953; Mantegazza and Tommasini, 1955), we investigated whether in mammals oxystilbene derivatives could also affect the α3(α5)β4 receptor subtype which is reported as the principal nAChR class on autonomic ganglia as demonstrated by immunocytochemical and molecular biology techniques (Role and Berg, 1996; Campos-Caro et al., 1997) . To this end we studied the action of F3 (Fig. 17) as this compound was apparently more active than MG624 itself in binding to the β4 receptors (Gotti et al., 1998).

To characterize the action of the F3 compound on the native nAChRs present on rat chromaffin cells we performed electrophysiological recordings and binding studies. All binding experiments were performed by Dr. Cecilia Gotti group (CNR, Milano, Italy), for binding methods see (Di Angelantonio et al., 2000).

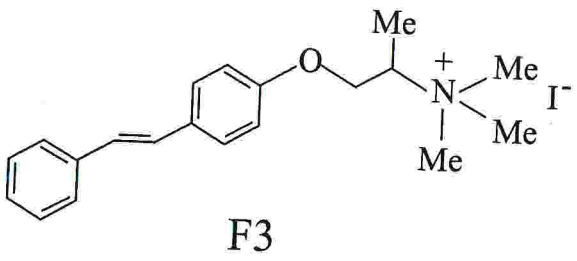

F3

Fig. 17. Chemical structure of N,N,N-trimethyl-1-(4-*trans*-stilbenoxy)-2-propylammonium iodide (F3) molecule.

2.1 Effect of racemic F3 on nAChR evoked currents

Fig. 18 describes the principal features of the action of racemic F3 on nicotine induced currents of rat chromaffin cells. Nicotine was applied with brief pressure pulses (5-100 ms) which elicited reproducible responses without apparent desensitization (Khiroug et al., 1997). As exemplified in Fig. 18 A, the fast inward current induced by a pressure application of nicotine (50 μM pipette concentration) was reduced by 30% after a 15 s application of F3 (30 nM pipette concentration), which was continuously ejected from a second puffer during the agonist delivery. This block had thus a relatively rapid onset with full recovery after 45 s washout. F3 *per se* did not elicit changes in baseline current or input resistance of the cell. Fig. 18 B shows the average time course of the F3 depressant action for 6 cells. The extent of the depression did not progressively change during F3 application and recovery was achieved 90 s later.

Further tests were performed to characterize the mechanism underlying this depression of nAChRs. Fig. 18 C shows that increasing the duration (5-100 ms) of nicotine pulses (50 μM pipette concentration) caused a progressive increment in current amplitude with apparent saturation at 50 ms pulse. When the same protocol was repeated in the presence of 30 nM F3 (15 s puffer pipette preapplication), evoked currents induced by 5-30 ms application of nicotine were depressed while those induced by 50-100 ms pulses were unaffected (8-30 cells). Thus, the plot was shifted to the right without changes in the maximal response. This pattern of action is suggestive of an apparently competitive type of nAChR antagonism. At midpoint of this curve (20 ms pulse) the average value of this depression was 44 ± 3 % (n=30). By applying different concentrations of this antagonist and using the same test pulses of nicotine (20 ms from 50 μM pipette solution) the current depression was 61 ± 1 % for 250 nM F3 (n= 5) and 81 ± 3 % for 500 nM F3 (n = 4). All

nicotine induced currents generated with 50 μM agonist pipette concentration were fully abolished by 10 μM F3.

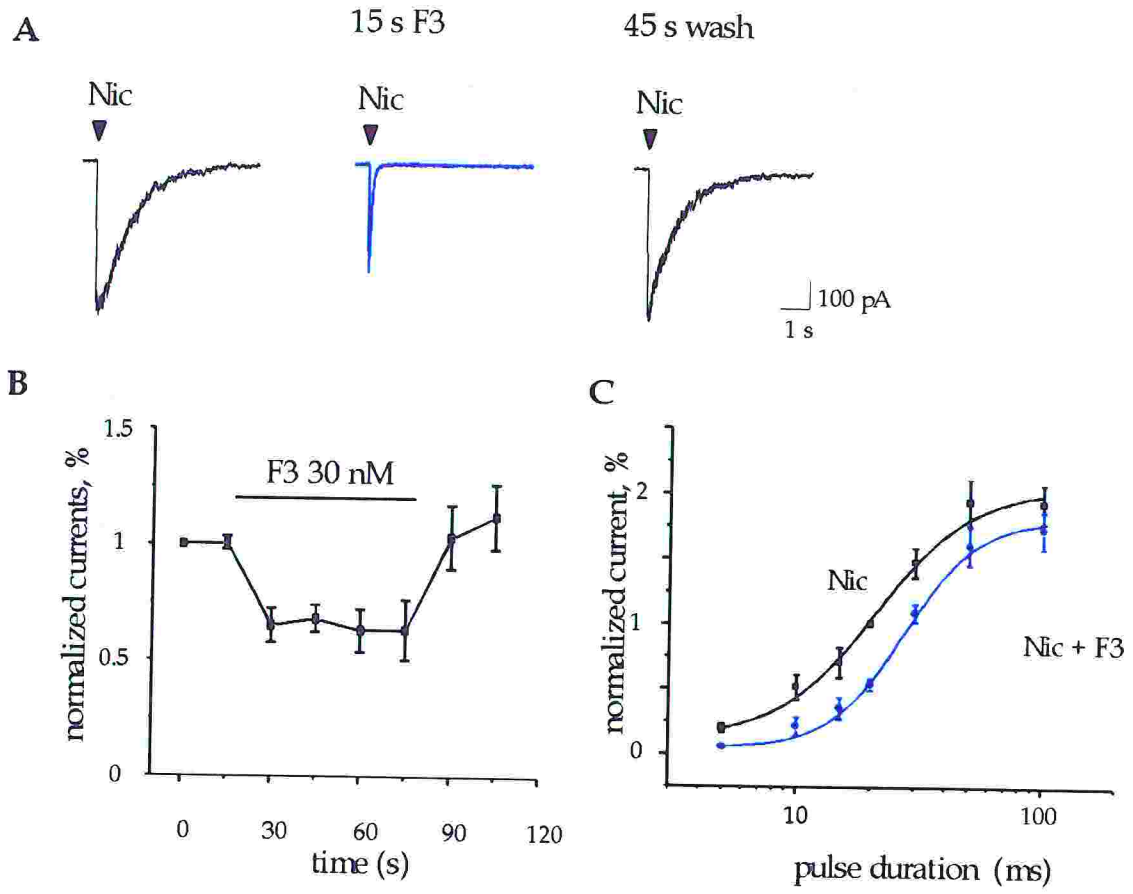

Fig. 18. Rapid block of nicotine induced responses by racemic F3. *A* Current records obtained with 20 ms nicotine (50 μM pipette concentration; left), 15 s after starting pressure application of F3 (30 nM pipette concentration; middle) and 45 s after washout of F3. Note reversible reduction in nicotine current amplitude. *B*, Time course of depression of nicotine currents (50 μM pipette concentration, 20 ms application) after pressure application of F3 (30 nM pipette concentration) to six cells. *C* Plot of nicotine current amplitude *vs* increasing duration of nicotine pressure pulses in control solution and in the presence of F3. *Ordinate*, current amplitude normalized with respect to the response evoked by 20 ms in control solution for each cell. *Abscissa*, pulse duration of nicotine (50 μM) applications. F3 (30 nM pipette concentration) was applied for ~15 s before each nicotine response (8-30 cells). Note rightward shift of the plot without decrease in maximal response.

2.2 F3 blocking action did not depend on membrane potential

We next explored if the action of F3 on nAChRs was voltage dependent as this property might provide clues to its mechanism of action.

The example in Fig. 19 shows that, on the same cell held at -70, -100 or -40 mV, F3 elicited a similar reduction in nicotine induced currents. On average the depression at -110 mV was 49 ± 6 % (n = 4), and 42 ± 5 % (n = 4) at -40 mV. The reversal potential (about 0 mV) of nicotine currents was left unchanged. These data thus indicated that the block exerted by F3 was voltage independent and not caused by a negative shift in current reversal.

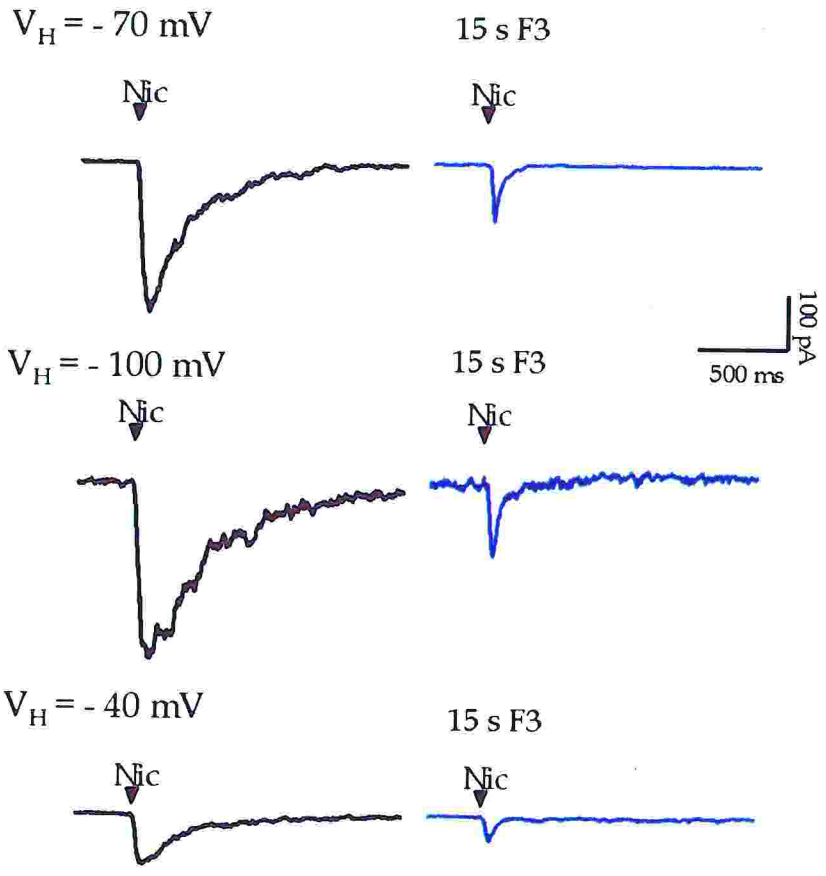

Fig. 19. F3-induced depression of nicotine currents is voltage independent. Comparison of currents induced by 20 ms nicotine (50 µM pipette concentration) in control solution and in the presence of F3 (30 nM pipette concentration; continuously applied before and during nicotine delivery) at -70 mV (*top*), -120 mV (*middle*) and -40 mV (*bottom*) holding potential (V_H). Note that fractional peak current depression was similar for all holding potentials. Traces are from the same cell.

2.3 Blocking potency of the optical stereoisomers of F3

To investigate any stereo-selectivity in the action of F3, we tested its two optically resolved isomers to isolate the most potent one. The *R*-isomer was found more potent than the corresponding *S*-form enantiomer: in fact, 100 nM *R*-F3 (applied via rapid solution exchanger) depressed by 45 ± 3 % responses induced by 20 ms nicotine pulses (100 μM pipette concentration; n=15). Conversely, the same concentration of *S*-F3 reduced such current by 5 ± 4 % only (n=5). Fig. 20 A shows an example of the action of *R*-F3 on nicotine induced currents: like in the case of the racemic compound the block displayed a fast onset and a full recovery after a few min washout.

Fig. 20 B shows a plot of the fractional reduction in current amplitude against different log concentrations of *R*-F3. *R*-F3 concentrations (ranging from 100 nM to 3 μM) were tested on responses evoked by the same pulse duration of nicotine (20 ms, 100 μM; n=4-15). From these data the calculated IC_{50} value for *R*-F3 was 350±30 nM. The same protocol was applied to calculate the IC_{50} value for *S*-F3 (n=5) which was 1.5±0.3 μM.

It should be noted that these experiments provided only an approximate estimate of the affinity by R-F3 for nAChRs and did not provide strong evidence concerning its mechanism of action. These issues should be examined by performing agonist dose-response curves in the absence and in the presence of the antagonist under equilibrium conditions. With this approach it should then be possible to construct a Shild plot to characterize the mode of action of the antagonist. Nevertheless the present study could not meet those requirements in view of the strong desensitization of nAChRs and the limited availability of the antagonist.

In analogy with the observation with the racemic F3 (*cf* data in Fig. 18 C), application of *R*-F3 on responses evoked by different pulse durations of nicotine also elicited a rightward shift of the curve obtained with

nicotine alone (plot in Fig. 20 C), thus confirming a similar profile of action consistent with competitive antagonism. Taking the average value at midpoint of the curve (corresponding to a 20 ms pulse of nicotine), the depression was 45±3 % (n=15). No voltage dependence in the *R*-F3 block was observed.

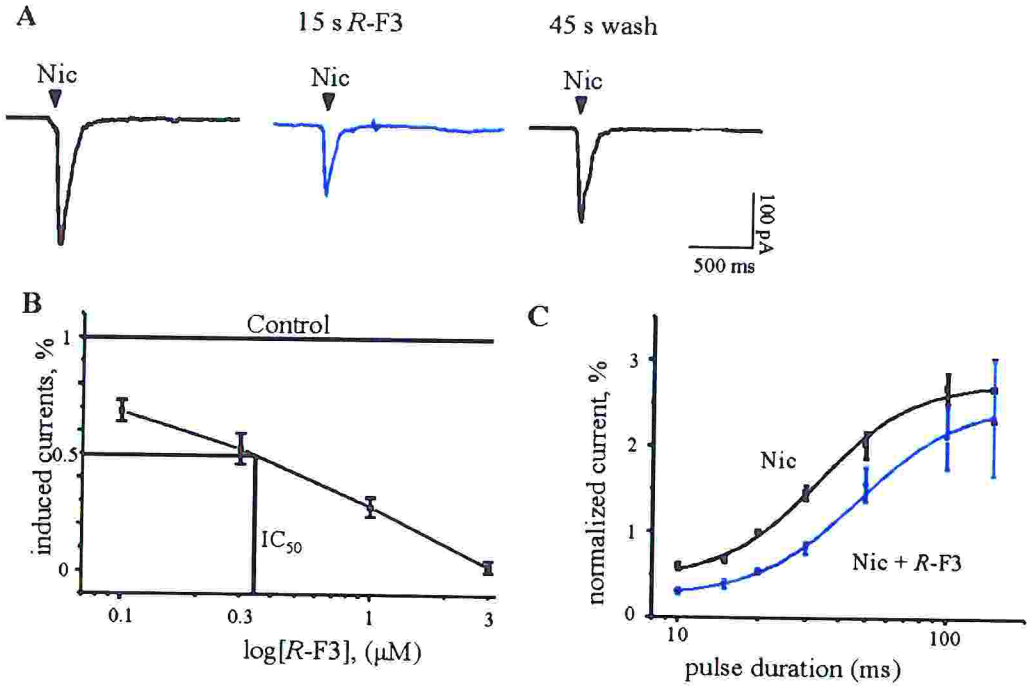

Fig. 20. Stereo-selectivity of the two isomers of F3. *A* Inward currents evoked by 20 ms nicotine (0.1 mM pipette concentration) in control solution (left), in the presence of *R*-F3 (100 nM applied via rapid solution exchanger, middle) and 45 s after washout of *R*-F3 (right). Note reduction in nicotine current amplitude, fast onset and full recovery. *B* Plot of the fractional reduction in current amplitude against different log concentrations of *R*-F3 (ranging from 100 nM to 3 μM). The test pulse (20 ms, 100 μM) of nicotine was the same for all concentration of *R*-F3 (n=4-15 cells). The calculated IC_{50} value for *R*-F3 was 350±30 nM. *C* Plot of nicotine current *vs* increasing duration of nicotine pressure pulses in control solution and in the presence of *R*-F3. *Ordinate*, current amplitude normalized with respect to the response evoked by 20 ms in control solution for each cell. *Abscissa*, pulse duration of nicotine (0.1 mM) applications. *R*-F3 (100 nM via the rapid solution exchanger) was applied for ~15 s before each nicotine response (5-15 cells). Note rightward shift of the plot without decrease in maximal response.

2.4 Action of F3 on nicotine and epibatidine

Amongst nAChR agonists epibatidine is considered to be very potent and for this reason it is the most commonly used radio-labelled agonist for binding assays (Gotti et al., 1997). To investigate if there was any differential block by F3 of responses induced by nicotine and epibatidine, these agonists were applied by two separate puffer pipettes to the same cell while *R*-F3 was continuously superfused via the bathing solution.

To elicit inward currents of the same amplitude, i.e. to activate approximately the same number of nAChRs, nicotine was used at 100 μM and epibatidine at 100 nM concentrations (test pulses were 20 ms in all cases). As shown in the example of Fig. 21 (left) the epibatidine induced current decayed much slower than the nicotine one (Gerzanich et al., 1995; Zhang et al., 1999). The slow time course of epibatidine currents and their strong tendency to desensitize made it difficult to obtain reliable responses over a sustained period of recording. Nevertheless, the block exerted by *R*-F3 was comparatively the same (right panels) as against nicotine. On a sample of 4 cells we observed 52 ± 1 % depression for nicotine and 55 ± 4 % for epibatidine. Note that the extent of nicotine depression was virtually identical to the one found with the fast perfusion system. This finding allowed us to compare patch clamp data routinely obtained with nicotine with binding experiments in which epibatidine was the ligand.

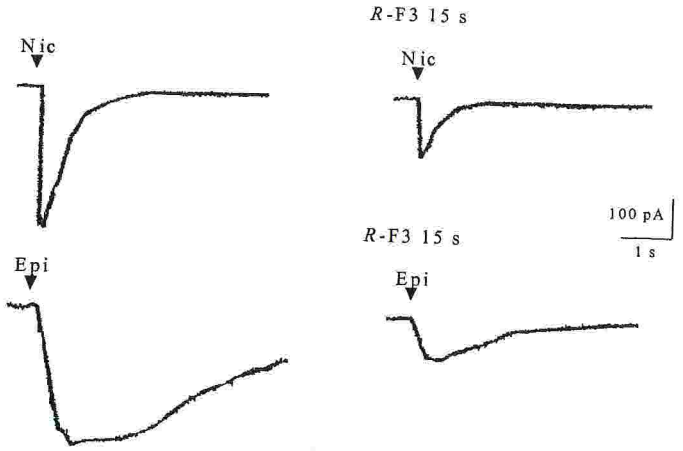

Fig. 21. Action of F3 on different nicotinic agonists. Similar amplitude currents induced by 20 ms nicotine (0.1 mM pipette concentration, top left) or 20 ms epibatidine (0.1 μM pipette concentration, bottom left) before and during bath application of *R*-F3. Note similar depression of either response.

2.5 Binding assays

Initial experiments using ^{3}H-epibatidine to test for nAChR binding gave a very low signal from adrenal gland homogenates because of the small number of these receptors (see also Davila-Garcia et al., 1997). We therefore decided to use ^{125}I-epibatidine and compared its binding activity with that of ^{3}H-epibatine in preliminary experiments on rat SCG homogenates (in the presence of αBgtx to saturate possible αBgtx binding sites).^{125}I-epibatidine binding had 140 pM (coefficient of variation, CV, = 20%) K_d value and 210 ± 20 fmol/mg protein B_{max} value. Corresponding data for ^{3}H-epibatine were 127 pM (CV=20%) and 230 ± 25 fmol/mg protein. Hence, the two ligands had similar K_d and B_{max} values. Since the radioactivity signal was much stronger with ^{125}I-epibatidine, we decided to use this substance for binding studies of adrenal gland homogenates.

Fig. 22 A shows a representative experiment, in which ^{125}I-epibatidine bound adrenal gland membranes in a specific and saturable manner. These data were fitted with a linear Scatchard plot, thus demonstrating the presence of a single class of high affinity sites (see Fig. 22 B). The apparent K_d value of ^{125}I-epibatidine calculated from five separate experiments performed in duplicate was 159 pM (CV=37%) while B_{max} was 6.5±1.3 fmol /mg protein. Non-specific binding was determined in parallel by incubating samples in the presence of 100 nM unlabelled epibatidine, and it averaged 5-40% of total binding. Pilot tests with membranes isolated from rat adrenal medulla showed that in these samples ^{125}I-epibatidine K_d value was similar to that measured with whole gland tissue, although the number of receptors was almost double. Nevertheless, in view of the very small amount of tissue provided by isolated adrenal medulla, we decided to perform all binding experiments with whole gland tissue.

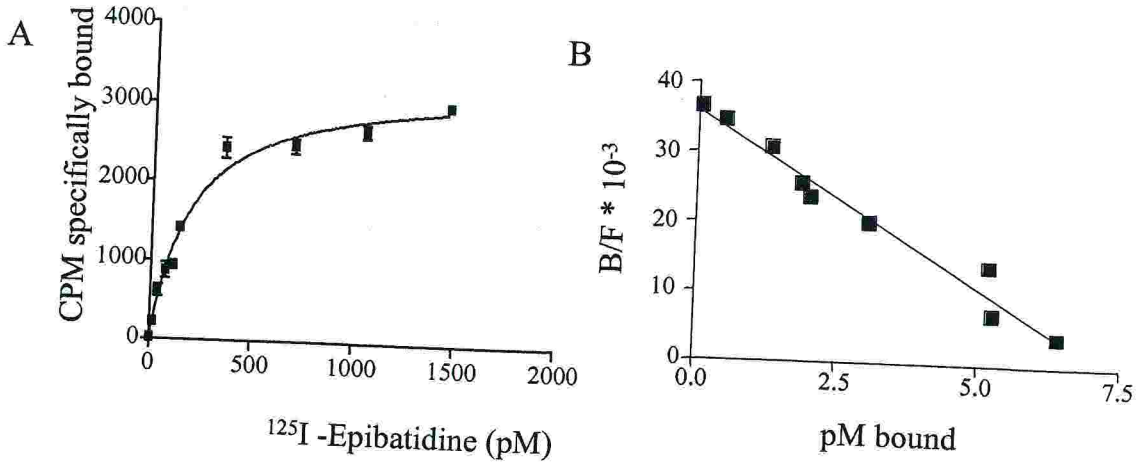

Fig. 22. Saturation of specific ^{125}I-epibatidine binding to adrenal gland homogenates. A: plot of bound radioactivity against concentration of ^{125}I-epibatidine. The homogenates were incubated overnight with ^{125}I-epibatidine (5 to 1500 nM) at 4°C. Non specific binding was determined in the presence of 100-250 nM cold epibatidine. The data shown are the mean values±sem of one representative experiment performed in triplicate. B: Scatchard plot of data from experiments shown in A.

Some of the basic pharmacological characteristics of rat adrenal gland nAChRs were examined in binding competition experiments against 150-200 pM ^{125}I-epibatidine (see Fig. 23). Cytisine was more potent than ACh in inhibiting binding with cytisine K_i=68 nM (CV 13%) *vs* ACh K_i=348 nM (39%). F3 was much less potent with K_i =29.6 μM. Almost no difference in potency was found between the two stereoisomers of F3, *S*-F3 and *R*-F3, which had K_i values of respectively 17.2 (CV 29%) and 25.7 (30%) μM.

Note that in order to obtain true physical binding constants, displacement of a radioactive competitive antagonist by a cold antagonist should be investigated. However, the present data obtained from saturation and competition agonist binding were analyzed using the LIGAND software (Munson and Rodbard, 1980). By fitting homologous (^{125}I-epibatidine binding) as well as heterologous (displacement of ^{125}I-epibatidine binding performed at the K_d concentration by increasing F3 concentration) binding data the software provides the K_d value of the hot ligand and the K_i value of the competitive drug, regardless of agonist or antagonist activity. This approach allows calculating K_i values when no radioactive hot pure competitive antagonists are commercially available, like in the case of nAChRs. Note also that values obtained using this non-linear fitting method are close to the ones obtained from displacement curves with the Cheng-Prusoff correction.

Bovine chromaffin cells are known to express high affinity αBgtx binding sites containing the α7 subunit (Garcia-Guzman et al., 1995). In order to find out if rat adrenal glands also possess α7 receptors that bind αBgtx, we performed saturation binding experiments on rat adrenal homogenates using ^{125}I-αBgtx: no specific ^{125}I-αBgtx binding was detected.

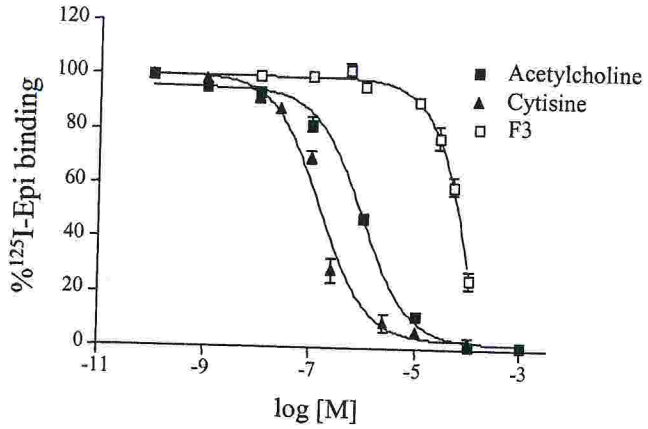

Fig. 23. Displacement of bound ^{125}I-epibatidine by ACh, cytisine or F3. Homogenates were preincubated for 30 min with the indicated drug concentrations and then incubated with 0.2 nM ^{125}I-epibatidine overnight at 4°C. The data are the mean±sem of three experiments for F3 and of two experiments each for ACh and cytisine. Data were analyzed by means of a non-linear least square procedure using the LIGAND programme. The calculated binding parameters were obtained by simultaneously fitting three independent experiments. An "extra sum of squares" F-test was performed by the LIGAND programme to evaluate the different binding models statistically (i.e. one site versus two sites models, comparison of the binding parameters, etc.)(Munson and Rodbard, 1980)

3. Mecamylamine of block of neuronal nicotinic acetylcholine receptors.

Mecamylamine is a secondary amine acting as an antagonist on nAChRs (Ascher et al., 1979; Fiebers and Adams, 1991; Nooney et al., 1992). The blocking action of mecamylamine is exerted on all native subtypes of nAChRs despite their different subunit composition (Connolly et al., 1992). *In vivo* mecamylamine lowers blood pressure and can prevent experimental seizures induced by nicotine (Gyermek, 1980). In view of this widespread action which remains, however, highly selective against nAChRs, mecamylamine is commonly used to probe the role of such receptors in central and peripheral synaptic transmission processes.
On the basis of measurements of ACh-evoked currents, mecamylamine has been suggested to be a competitive antagonist on submandibular ganglion cells (Ascher et al., 1979; Gurney and Rang, 1984). Biochemical work on recombinant $\alpha_3\beta_4$ nAChRs (the predominant type expressed in chromaffin cells; Campos-Caro et al., 1997) has shown mecamylamine to block them in a non-surmontable fashion (Xiao et al., 1998). This type of action might indicate "un-competitive" antagonism, a term which has been recently used to define the block by memantidine and amantadine of NMDA receptors (Blanpied et al., 1997; Chen and Lipton, 1997). Un-competitive antagonism may be due to two distinct mechanisms, namely simple open channel block or trapping of the blocker inside the closed channel (for a review see Dingledine et al., 1999). The trapping mechanism was first proposed by (Lingle, 1983) on the basis of experiments on ACh receptors of lobster muscle. On submandibular ganglion neurons hexamethonium and some closely related derivatives could be trapped by nAChRs and subsequently released by combining depolarization with agonist application (Gurney and Rang, 1984). Nevertheless, mecamylamine did not share this effect on such ganglion cells. Conversely, Nooney et al. (Nooney et al., 1992) briefly reported

that on bovine chromaffin cells the antagonism by mecamylamine was voltage dependent. The antagonism by mecamylamine of native nAChRs of autonomic ganglia (Shen and Horn, 1998) and of recombinant $\alpha_3\beta_4$ nAChRs (Nelson and Lindstrom, 1999) was suggested to be due to simple block of open channels.

We tried to provide a quantitative description of the blocking properties of mecamylamine on nAChRs of rat chromaffin cells and its rapid relief when the membrane potential was depolarized in the presence of nicotine.

3.1 Characteristics of the depression of nicotinic currents by mecamylamine

Records in Fig. 24 A, taken from a chromaffin cell held at -70 mV, are submaximal inward currents (-320 pA) induced by brief (30 ms) pressure applications of nicotine (0.1 mM pipette concentration). These responses were very reproducible as long as nicotine was applied at intervals of at least 15 s. In the presence of 1 μM mecamylamine (applied via the fast superfusion system) the first response to nicotine (about 5 s exposure to mecamylamine) was only slightly reduced; the extent of the current block was however increased with successive applications until it reached steady state (-78 pA current amplitude) approximately 2 min later. On a random sample of 12 cells the steady state depression was 80±6%. Once the block was at steady state, its extent was relatively insensitive to the rate of nicotine application within the 0.3 to 0.016 Hz range. Further tests were mainly carried out with 30 ms pressure application of nicotine (0.1 mM) at 0.066 Hz while mecamylamine was administered by fast superfusion. Fig. 24 B shows average data (n=12 cells) for the time course of the mecamylamine induced block of nicotine current amplitude with slow onset (τ=40±5 s) and minimal recovery on washout. After 10 min response recovery was 32±9% of control amplitude (n=4). The reduction in current peak amplitude by

mecamylamine was also accompanied by shortening of the monoexponential nicotine current decay from 89±14 to 68±8 ms (n=9; P<0.05).

When 1 μM mecamylamine was bath-applied (n=3), the depression (81±2%) of nicotine current amplitude had also slow onset and recovery. Likewise, when mecamylamine was applied for 1-3 min via a separate pressure pipette (1 μM pipette concentration; n=5), current depression at steady state level was 76±5%.

Fig. 24 C shows that, on chromaffin cells held at -70 mV, mecamylamine was a rather potent nAChR blocker as, under steady state conditions, the IC_{50} value was 0.34 μM. The Hill coefficient (n_H) value was 1.08, indicating that the stoichiometry for nAChR block apparently required one mecamylamine molecule only.

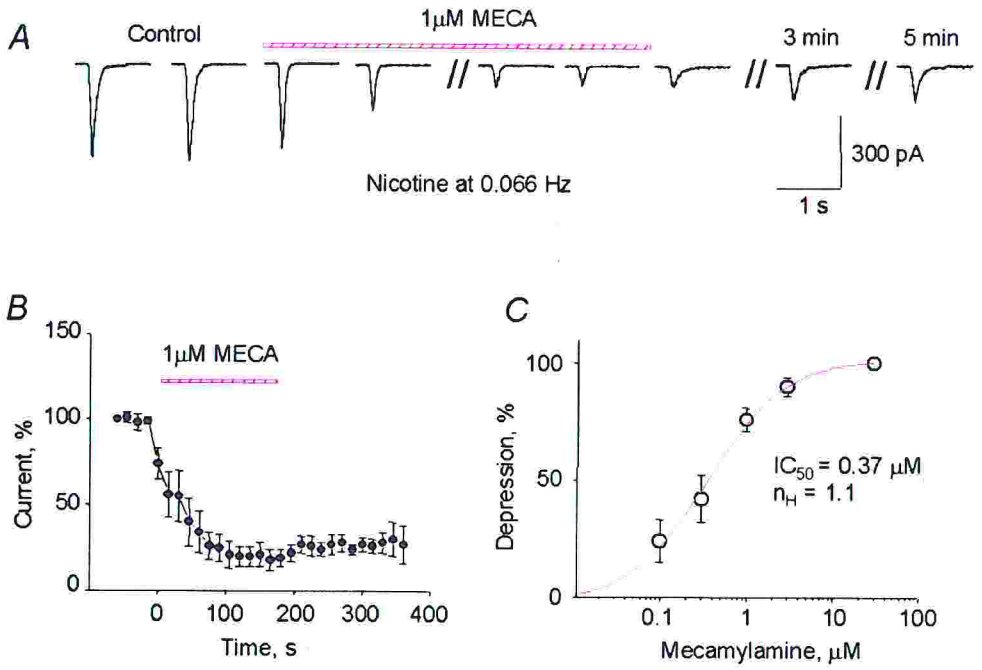

Fig. 24. Effect of mecamylamine on membrane currents evoked by pressure-applied 0.1 mM nicotine. A, control currents elicited by pulsing nicotine at 0.066 Hz are depressed by mecamylamine with steady state block attained at 2 min. Washout is associated with minimal recovery in current amplitude. B, plot of nicotine current amplitude (%) *versus* elapsed time from start of mecamylamine superfusion. Data are from 12 cells. C, plot of log concentration of mecamylamine against % depression in nicotine current amplitude. The concentration producing 50 % reduction was taken as IC_{50} (0.34 μM). The curve had a Hill coefficient (n_H) of 1.1. Data points are from 5-12 cells.

3.2 Voltage sensitivity of mecamylamine block.

Several nAChR blockers are known to display a variable degree of voltage dependence (Ascher et al., 1979; Gurney and Rang, 1984; Colquhoun et al., 1987; Buisson and Bertrand, 1998)). The present experiments were performed to examine if the effect of mecamylamine on chromaffin cells was also voltage dependent. Fig. 25 A (filled circles) shows that the extent and time-course of mecamylamine block for two holding potentials. If mecamylamine was tested on cells held at -30 mV, the depression of nicotine (30 ms) currents was relatively weak and readily reversible. Conversely, a much stronger (and longer) block was observed when cells were held at -120 mV (Fig. 25 A, open circles). Fig. 25 B shows the plot of % depression in nicotine current by various concentrations of mecamylamine (at two different holding potentials). This plot enabled us to calculate *H* (coefficient for *e*-fold variation in % current depression with membrane potential) which was 50 mV. From the experimentally obtained IC_{50} values of mecamylamine (see Fig. 24 C and 25 B) it was possible to estimate the IC_{50} value (1.6 μM) at 0 mV. This value was used for the Woodhull's equation (Woodhull, 1973) to infer the portion of membrane electric field (expressed as δ) which was sensed by the mecamylamine binding site. As the calculated δ was 0.72, it is suggested that mecamylamine reached a relatively deep site inside the nAChR channels.

Note that this δ value has been calculated using the IC_{50} value instead of the K_d one. As detailed in the Methods section, this may have overestimated δ. The expected δ value should be 0.47, that it is still compatible with the notion that the mecamylamine binding site sensed a considerable portion of membrane electric field inside the nAChR.

The voltage dependence of the block was also explored by constructing full I/V curves after clamping cells at several membrane potentials within the -120 to +30 mV range as indicated in Fig. 25 C. Mecamylamine reduced membrane currents at all test potentials with no

change in the apparent reversal potential or in the strong rectifying properties of nAChRs (which allow minimal current flow at positive potentials; Nooney et al., 1992).

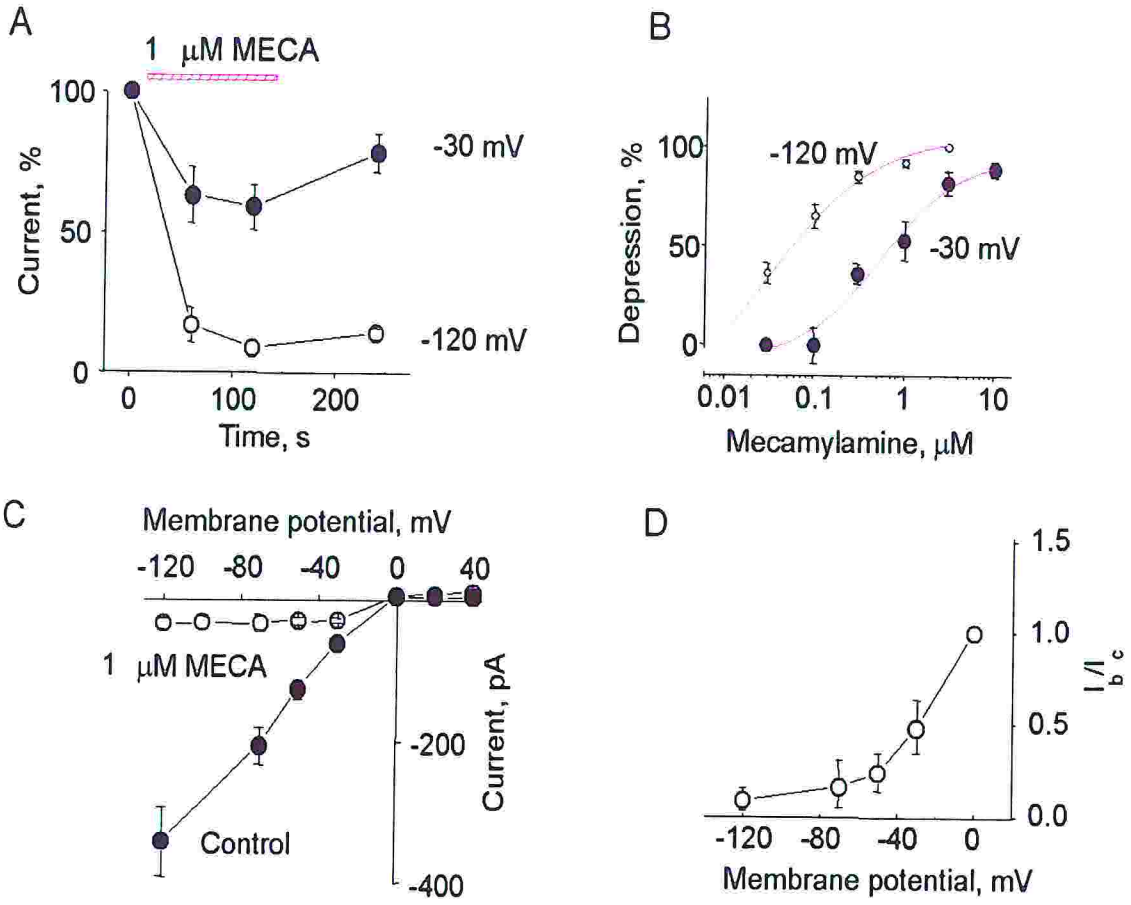

Fig. 25. Voltage dependence of mecamylamine block. A, time course of changes in nicotine current amplitude (%) in the presence of 1 μM mecamylamine (applied as indicated by the horizontal bar) at -30 or -120 mV holding potential. Compare stronger block at -120 mV with less recovery after washout. Data are from 5-8 cells. B, plot of the depression of nicotine induced currents by increasing log concentrations of mecamylamine at -120 or -30 mV holding potential. Data are from 5 cells. C, I/V curve obtained by clamping cells (n=5) at various holding potentials in control solution (filled circles) or in mecamylamine solution (open circles). D, plot of nicotine current block (expressed as I_b/I_c, that is the ratio of blocked current over control) versus different membrane potentials (n=5). Note stronger block at more negative membrane potentials.

The mecamylamine-induced depression was proportionally much larger at negative values as shown in Fig. 25 D in which the nicotine current

(expressed as ratio of the response in mecamylamine solution over the control one) was plotted versus membrane potential.

3.3 Rapid rescue of nicotine currents from mecamylamine block despite continuous antagonist presence.

Could the strong voltage dependence of mecamylamine block confer special blocking properties to this antagonist? This issue was tested in experiments like the one shown in Fig. 26 A: in the continuous presence of 1 μM mecamylamine, after achieving 89% block of nicotine current amplitude, the membrane potential was shifted to +30 mV for 15 s during which a single nicotine pulse was applied to elicit a very small response only (16 pA). Nevertheless, upon return to standard holding potential (-70 mV), nicotine evoked a substantial current which was only 38 % smaller than initial responses in control solution. The protocol of nicotine pulse application was continued to reveal rapid re-establishment of current block (88%) analogous to the one observed before the transient depolarization test. The inset to Fig. 26 A shows (at faster speed and higher gain) superimposed records of nicotine currents in control solution, in the presence of mecamylamine and immediately after membrane depolarization with associated block relief. Block relief expressed as ratio of currents before and after the combined application of a depolarizing step and nicotine was 406±83 % (n=9). Thus, the relieved current corresponds to 64±7% of the control one.

Using a protocol similar to the one of Fig. 26 A with membrane depolarization to variable levels, it was apparent that relief of mecamylamine block was related to the value of membrane depolarization and that depolarization alone (without concomitant application of nicotine) could not temporarily restore current amplitude (Fig. 26 B). From data like those of Fig. 26 B it was possible to calculate the value of H=22.5 mV, that is the coefficient for e-fold change in block relief intensity. Depolarization duration was less critical than amplitude

to determine relief of block since essentially the same results were obtained when the pulse (100 mV from -70 to +30 mV) was varied from 0.5 s to 15 s.

Fig. 26 C shows the I/V relation for nicotine currents during mecamylamine steady state block (open circles) and for responses (filled circles) immediately after the depolarization sojourn at +30 mV.

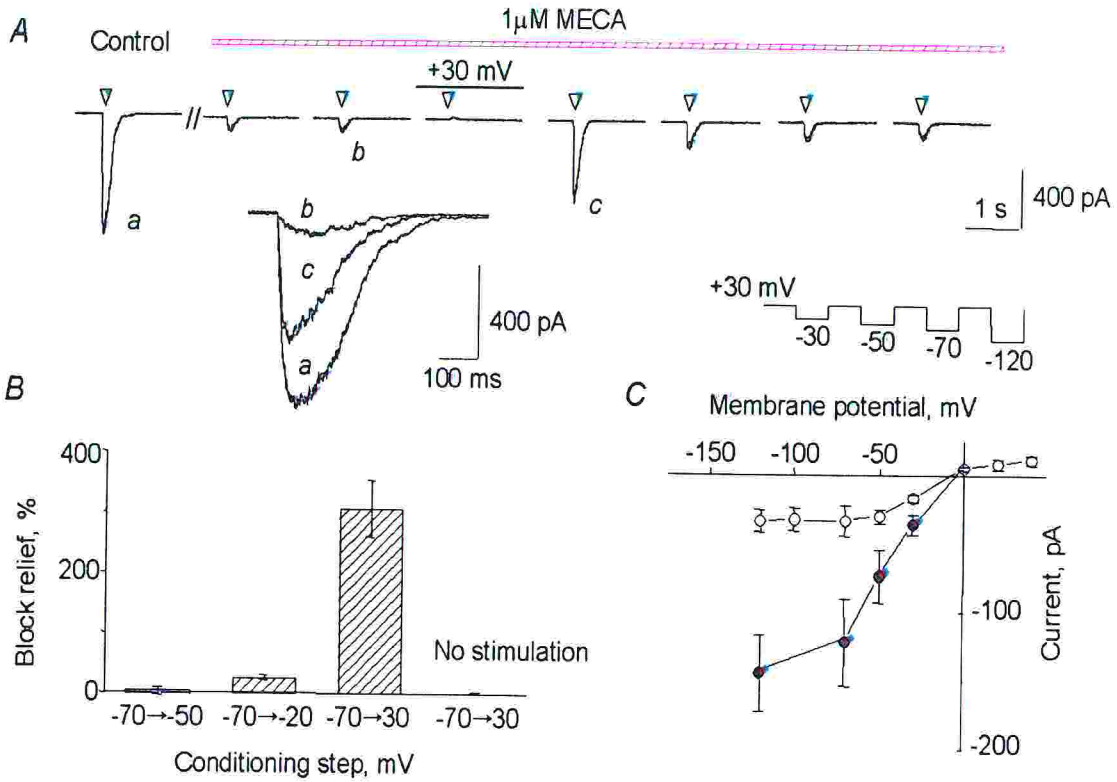

Fig. 26. Rapid relief from 1 μM mecamylamine block. A, control current evoked by nicotine pulses (arrowheads) is reduced at steady state by mecamylamine. After combining depolarization to +30 mV (horizontal line) with nicotine pulse (note slight outward current) the subsequent application of nicotine transiently generated a strong inward current which was then blocked again. Inset shows samples (a-c) of nicotine currents on faster time base and at higher gain taken from likewise labelled traces. B, histograms indicating block relief (as % of the current amplitude before the conditioning protocol) induced by depolarization from -70 mV to -50, -20 or +30 mV in the presence of nicotine or to +30 mV without nicotine (no stimulation). Data are from 6 cells. C, I/V relation for the nicotine current during mecamylamine steady state block (open circles) and for the response (filled circles) immediately after the depolarization sojourn at +30 mV; n=5.

Thus, within at least the -70 to 0 mV range, the characteristics of the nicotine current during block relief were relatively similar to those observed in control solution.

3.4 Prevention of mecamylamine blocking action.

The present experiments were carried out to find out if despite continuous, standard application of mecamylamine it was actually possible to prevent its antagonist effect. For this purpose tests analogous to those performed by (Gurney and Rang, 1984) with methonium compounds were employed. Fig. 27 A shows that, on a cell held at -70 mV, 3 min application of mecamylamine (without applying nicotine) had no effect on the response to nicotine applied 2 min later in control solution. When repeated pulses of nicotine (0.066 Hz) were applied to the same cell held at +30 mV during mecamylamine application, there was no nicotine response in the presence of the antagonist but a full response appeared after 2 min washout (Fig. 27 b). In contrast with this observation, when the same cell was then subjected to the usual protocol of applying mecamylamine at -70 mV during repeated pulses of nicotine, there was strong depression of current amplitude (by 95 % at 3 min) which minimally recovered (20 % of control) after 2 min washout (Fig. 27 c). Similar data were obtained from 5 cells. In accordance with the use-dependent properties of mecamylamine block, these results indicate that the mere presence of this drug was insufficient to block nAChRs unless they were also activated to generate inward currents.

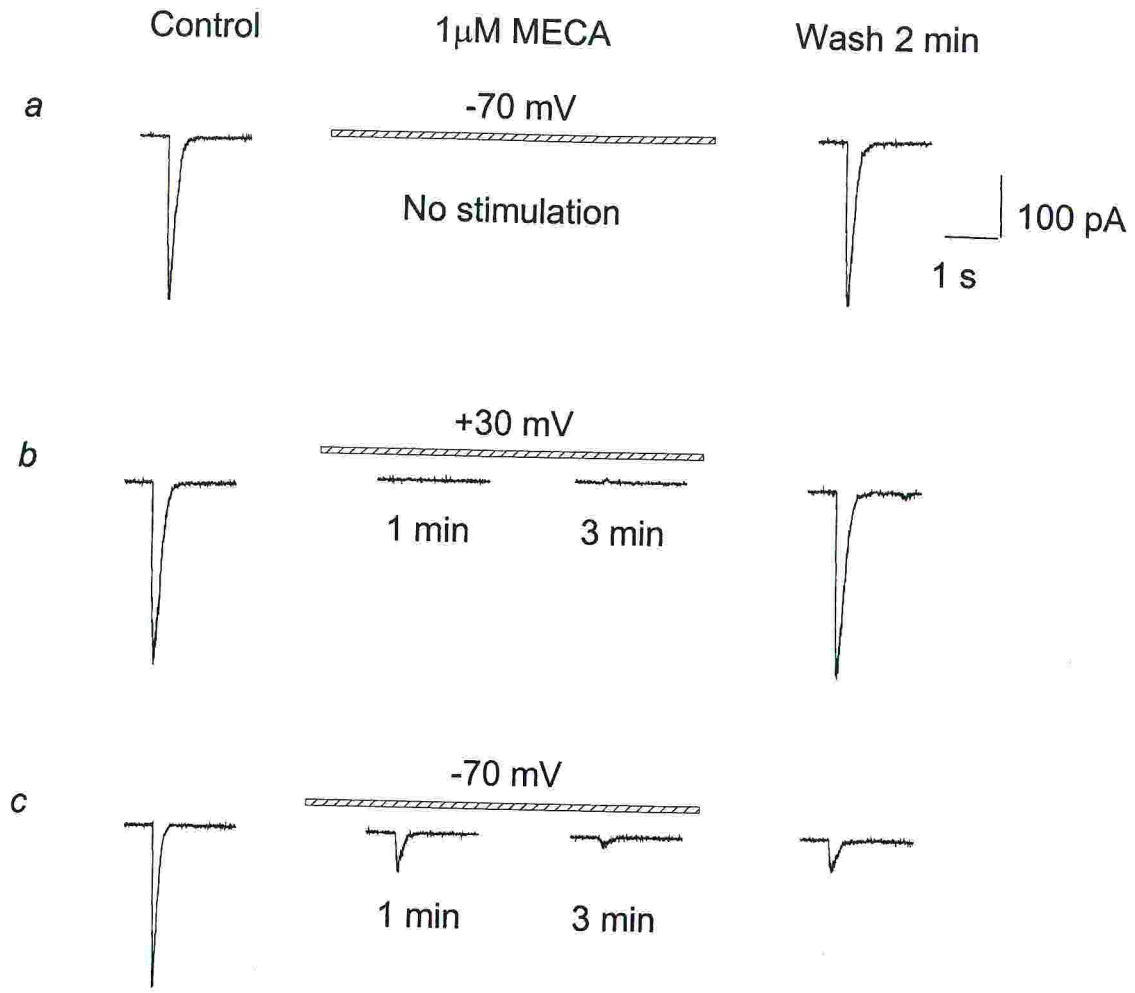

Fig. 27. Prevention of mecamylamine block. A, 3 min application of mecamylamine (hatched bar) to a cell held at -70 mV without pulse application of nicotine fails to affect responses to nicotine after mecamylamine wash; B, if the cell is depolarized to +30 mV and nicotine pulses are applied (0.066 Hz) throughout the 3 min mecamylamine application, subsequent response to nicotine after mecamylamine wash is unaffected; C, nicotine response is readily and strongly blocked when applied in the presence of mecamylamine at -70 mV and, despite 2 min wash of mecamylamine, the nicotine current remains largely reduced. All records are from the same cell.

3.5 Protocols for rescuing AChRs from mecamylamine block remain effective over an extended period.

As the combined depolarization and single agonist application were so effective in producing block relief, one interesting question was for how long after this test the block reversal could still be observed despite the

continuous presence of mecamylamine. To explore this aspect nicotine currents were blocked by 1 μM mecamylamine (87 % at steady state at -70 mV; see Fig. 28 A). The relief protocol consisted in the standard depolarization to +30 mV associated with a pulse of nicotine, which elicited a small outward current (30 pA). Fifteen s later at -70 mV and still in the presence of mecamylamine, the inward current was very large (Fig. 28 Aa; 330% of the response before depolarization).

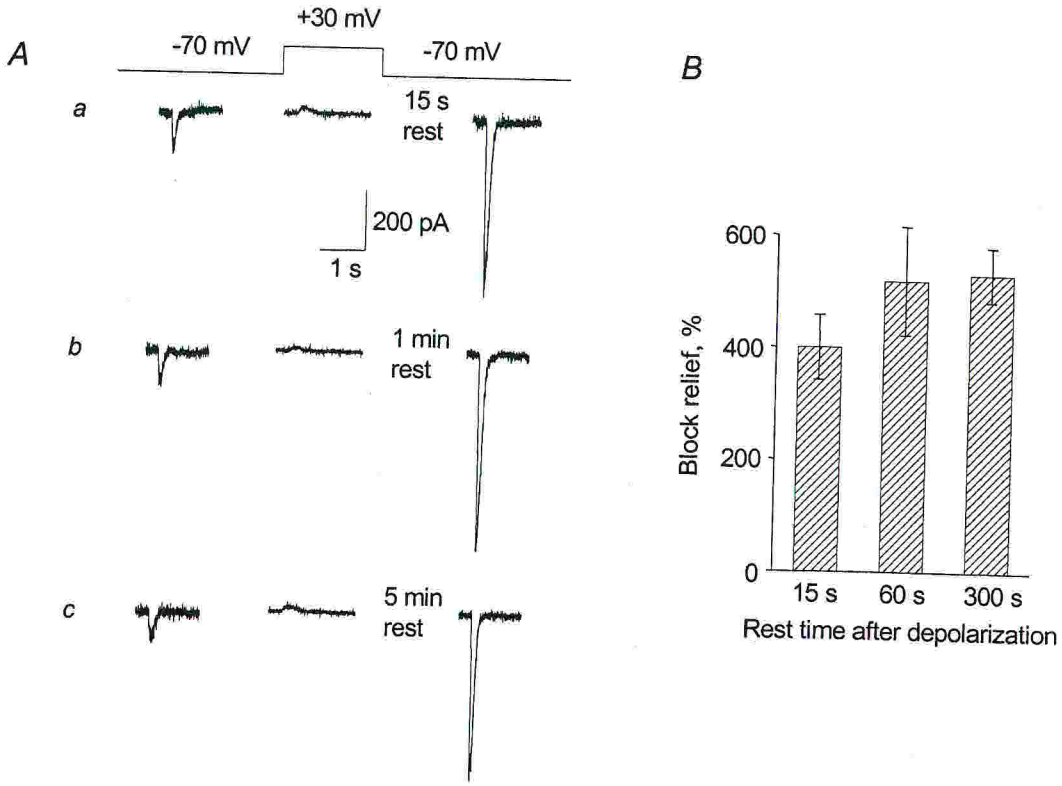

Fig. 28. Relief from mecamylamine block can still be observed after long rest. A, after achieving steady state block of nicotine current, membrane depolarization to +30 mV plus application of nicotine pulse generates substantial block relief observed after 15 s (a), 1 min (b) or 5 min (c) rest. All records are from the same cell held at -70 mV. B, bar chart showing equivalent degree of block relief (expressed as % of steady state blocked current before test protocol) after 15-300 s of rest; n=5.

Interestingly, an equally strong current rescue was observed when the nicotine pulse was applied after 1 min rest (Fig. 28 Ab; 391%). Even a longer resting period (5 min) in the presence of mecamylamine preserved the block relief (Fig. 28 Ac) as the current amplitude was 378%

of the one before depolarization. On average, for 5 cells tested at 15 s or 5 min, block relief was essentially the same (Fig. 28 B).

As the association of nicotine application plus strong membrane depolarization relieved nAChR block, we explored if this combination could speed up recovery from this block during mecamylamine washout.

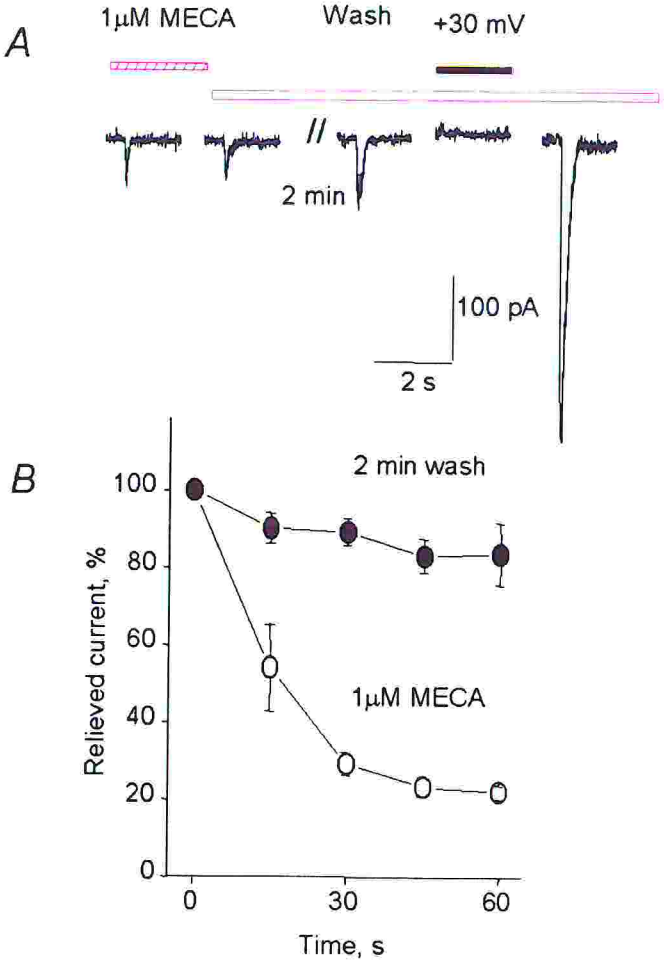

Fig. 29. Accelerated recovery from mecamylamine block by depolarization plus nicotine application. A, after attaining steady state block by mecamylamine of nicotine current (see horizontal hatched bar), responses to nicotine pulses (0.066 Hz) are monitored in standard Krebs solution (horizontal open bar). Recovery is slight after 2 min but it greatly enhanced after +30 mV depolarization (filled bar) plus nicotine pulse. B, time course of nicotine current amplitude (as % of amplitude of relieved current) either in the continuous presence of mecamylamine (open circles; n=6) or during washout of mecamylamine (filled circles; n=6). Note lack of return of mecamylamine block once the current had been restored during washout.

Fig. 29 A shows that, after establishing strong block of nicotine currents by mecamylamine, 150 s washout was accompanied by weak recovery in current amplitude (20%) to test pulses; nevertheless, depolarization to +30 mV plus a single nicotine pulse were able to elicit a very large recovery (249% with respect to amplitude before depolarization). Fig 29 B shows that on a sample of 6 cells the restored current amplitude remained relatively stable in control solution after the depolarizing pulse (filled circles), unlike the rapid block return observed in the continuous presence of mecamylamine (open circles).

3.6 Comparison between mecamylamine and other nicotinic receptor antagonists.

The complex properties of nAChR block by (and recovery from) mecamylamine raised the issue of whether other cholinergic blockers also shared similar properties on rat chromaffin cells *in vitro*. Fig. 30 A shows that dihydro-β-erythroidine (DHβE; 400 μM) rapidly, extensively (by 91±1%; n=4) and reversibly blocked responses to nicotine.

The introduction of the protocol of strong depolarization plus nicotine application made no difference to the DHβE evoked block. Similar data were observed with *d*-tubocurarine (10 μM; block by 46±10 %; n=3), or the oxystilbene derivative F3 (100 nM; block by 44±3 %; n=30). Proadifen (10 μM) blocked nicotine currents by 83±1 % (n=5), a phenomenon partly relieved by membrane depolarization as indicated in Fig. 30 B. Data summarizing observations based on depolarization plus nicotine application are shown in Fig. 30B.

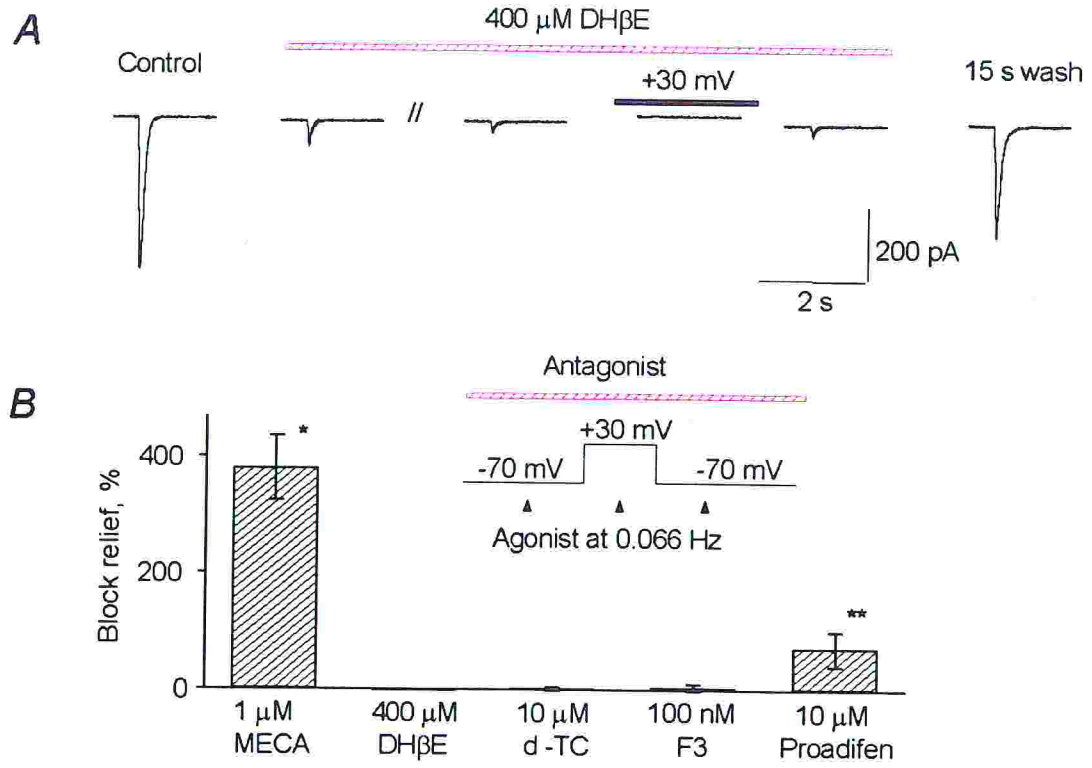

Fig. 30. Lack or minimal relief of nAChR block by various cholinergic antagonists. A, nicotine current (0.066 Hz pulses) is rapidly (<5 s) blocked by DHβE. Apparent steady state antagonism is obtained in 30 s. Combined depolarization to +30 mV (filled bar) plus nicotine pulse does not evoke block relief. Prompt current recovery (15 s) is observed after washout of antagonist. B, bar chart showing block relief (as % of blocked current before test protocol; see scheme in inset) in the presence of mecamylamine (MECA; n=9), DHβE (n=4), *d*-tubocurarine (d-TC; n=3), F3 (n=4) or proadifen (n=5). *=P<0.01, **=P<0.05.

4. Modulation of neuronal nicotinic receptor function by the endogenous neuropeptide CGRP (calcitonin gene-related peptide).

Several neuropeptides can act as neurotransmitters per se as well as neuromodulators of receptors for other transmitters (Hokfelt, 1991; Otsuka and Yoshioka, 1993). In general, it appears that the modulatory role of neuropeptides on fast transmitter-gated channels may comprise at least two distinct processes: an indirect mechanism mediated by the peptide G-protein coupled receptors which through changes in $[Ca^{2+}]_i$ and intracellular second messengers control the phosphorylation state of the fast transmitter receptor (Huganir and Greengard, 1990; Levitan, 1994; Smart, 1997), and an incompletely understood effect which involves direct interaction of the neuropeptide with certain subunits of the fast transmitter receptor (Clapham and Neher, 1984; Stafford et al., 1994). It is however uncertain if these two phenomena can coexist for the same receptors on a single cell although it has recently been shown that Cl^- channels can be regulated in essentially identical manner both ionotropically and metabotropically (Ali et al., 1998; Magoski and Kaczmarek, 1998).

An important insight into the phenomenon of peptide-induced receptor modulation has been provided by studies on muscle type nicotinic acetylcholine receptors (nAChR). In particular, the endogenously occurring calcitonin gene-related peptide (CGRP) facilitates nAChR desensitization by phosphorylating certain receptor subunits (Mulle et al., 1988; Miles et al., 1989; but see Lu et al., 1993) and increases AChR biosynthesis (Changeux et al., 1992). Another endogenous neuropeptide, namely substance P, which is frequently co-localized with CGRP (Bell and McDermott, 1996), inhibits the activity of muscle AChRs (Akasu et al., 1983; Simasko et al., 1985) as well as of neuronal-type AChRs of autonomic ganglia (Simmons et al., 1990; Valenta et al., 1993) or adrenal chromaffin cells (Livett et al., 1979; Clapham and Neher, 1984). Unlike

the case of substance P, the analysis of the modulatory role of CGRP has however been limited to muscle type of nAChR only (Eusebi et al., 1988); (Mulle et al., 1988; Miles et al., 1989; Lu et al., 1993). Since in the adrenal medulla CGRP is present in nerve fibres (Costa et al., 1994; Heym et al., 1995) and in the chromaffin cells themselves (Kuramoto et al., 1987), this tissue appeared to be a suitable model to investigate any potential modulatory action of CGRP on neuronal nAChRs.

We then analyzed the action of CGRP on neuronal nAChRs from rat chromaffin cells using an approach based on combined recording of $[Ca^{2+}]_i$ transients and membrane currents elicited by nicotine (Khiroug et al., 1997; Khiroug et al., 1998).

4.1 Effects of CGRP or nicotine on $[Ca^{2+}]_i$ and membrane current

Fig. 31 shows an example of the contrasting action of nicotine and CGRP on membrane current (B) and $[Ca^{2+}]_i$ changes (A) of a chromaffin cell (note different time scale in A and B). A large and rapid $[Ca^{2+}]_i$ rise was first evoked by a 20 ms puffer pulse of nicotine (0.1 mM; applied at the arrowheads) which also induced a fast inward current (-1156 pA). After the cell recovered from nicotine, subsequent application of CGRP (applied for 1 min by a 1 μM CGRP containing pipette; horizontal bar) did not change the holding current (Fig. 1 B) but slowly increased $[Ca^{2+}]_i$ (Fig. 31 A) which required over 10 s to reach 20 % of its peak amplitude. The $[Ca^{2+}]_i$ rise attained a plateau by the end of the application and was smaller than the one observed with nicotine. Nicotine, applied during recovery from CGRP, induced current and $[Ca^{2+}]_i$ responses of lower amplitude (depressed by 67 and 76 %, respectively, 30 s after stopping CGRP) than in control even when the $[Ca^{2+}]_i$ level had returned to baseline. Full recovery of nicotine responses occurred 2 min later (not shown).

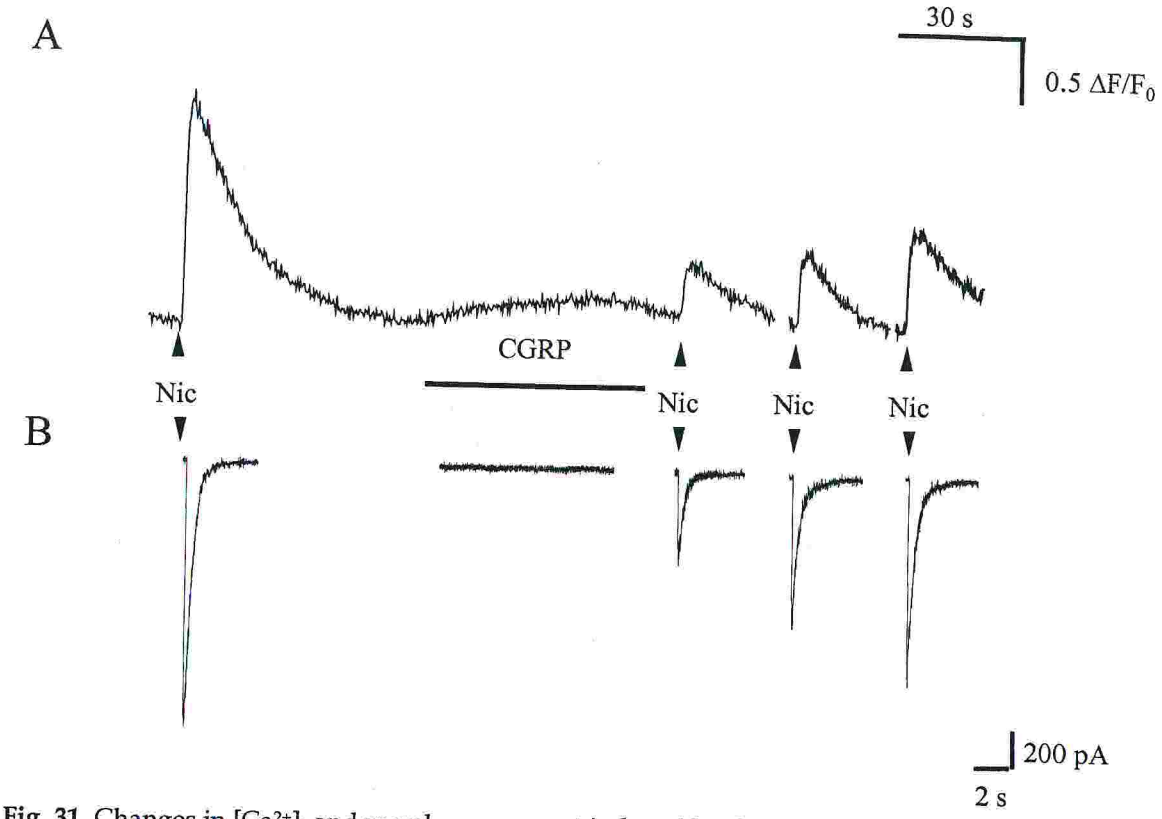

Fig. 31. Changes in $[Ca^{2+}]_i$ and membrane current induced by CGRP or nicotine. A, $[Ca^{2+}]_i$ fluorescence signals induced by pressure application of nicotine (Nic; 20 ms; 0.1 mM pipette concentration; see arrowheads) or CGRP (1 min; 1 μM pipette concentration; horizontal filled bar). Note that the $[Ca^{2+}]_i$ rise evoked by CGRP is smaller and slower than the one evoked by nicotine but that it induces a lasting depression of nicotine responses evoked at 30 s interval. B, Membrane currents induced by the same application of nicotine. CGRP did not change baseline current but depressed subsequent responses to nicotine. Note different time scale for A and B. All traces are from the same cell.

On a sample of 11 cells the $[Ca^{2+}]_i$ rise evoked by 0.1 mM nicotine (20 ms pulse) was significantly higher ($P<0.05$) than the one generated by 1 μM CGRP (1 min) as shown by the histograms in Fig. 32. These observations demonstrated not only that CGRP had a slower action than nicotine on $[Ca^{2+}]_i$ but also that, after application of CGRP, responses to nicotine were depressed.

Any difference in the action by nicotine or CGRP after changing external Ca^{2+} was next examined. An example is shown in Fig. 32 (top) in which on the same cell $[Ca^{2+}]_i$ increases were evoked by 0.1 mM nicotine (20

ms) or 1 μM CGRP (1 min), the latter without any associated variation in holding current (bottom traces). After replacing external Ca^{2+} with equimolar Mg^{2+}, the same test pulse of nicotine elicited an inward current without any $[Ca^{2+}]_i$ rise while CGPR retained its ability to elevate $[Ca^{2+}]_i$. The histograms of Fig. 32 show that on average in Ca^{2+} free medium 0.1 mM nicotine (20 ms) was unable to raise $[Ca^{2+}]_i$ while 1 μM CGRP (1 min) maintained its effect essentially unchanged.

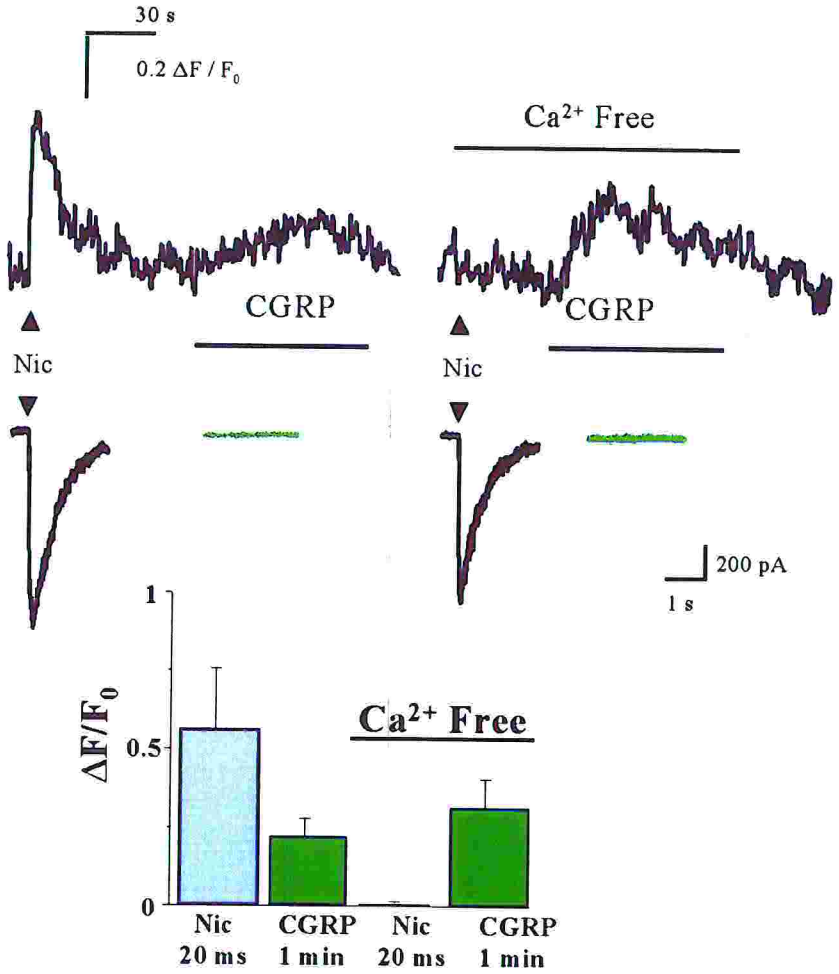

Fig. 32. The action of CGRP does not depend on extracellular Ca^{2+}. Top: combined $[Ca^{2+}]_i$ and current records obtained with pressure application of nicotine (20 ms; arrowheads) or CGRP (1 min; horizontal) in control solution (left) or in Ca^{2+} free medium (right). Note that in the latter condition the effect of nicotine on $[Ca^{2+}]_i$ is suppressed while the one of CGRP persists. For further details see Fig 14 legend. Bottom: histograms of fluorescence signal changes (expressed as fractional increase over baseline) induced by 20 ms nicotine or 1 min CGRP in control solution (n=7) or in Ca^{2+} free medium (n=3).

These results indicate that, while the $[Ca^{2+}]_i$ rise elicited by nicotine was mainly due to influx of this cation via activated nicotinic receptors (Mulle et al., 1992; Vernino et al., 1994; Khiroug et al., 1997, 1998), the $[Ca^{2+}]_i$ rise induced by CGRP was presumably caused by release from internal stores, confirming that not only the time course but also the source of the $[Ca^{2+}]_i$ transients differed when nicotine or CGRP were applied.

4.2 Modulation of nicotine responses by CGRP

The depression of nicotine induced responses observed after applying CGRP (see Fig. 31) raised the question of how the peptide might modulate nicotinic receptors especially as CGRP raised $[Ca^{2+}]_i$ which is thought to control nicotinic receptor activity (Lena and Changeux, 1993; Amador and Dani, 1995). Thus, it was interesting to examine issues such as how quickly this phenomenon could take place, its dependence on $[Ca^{2+}]_i$ and the receptor mechanisms involved. The first two issues were studied by applying nicotine in the presence of CGRP (coapplied via a second puffer pipette) and by buffering $[Ca^{2+}]_i$ with 10 mM BAPTA (which strongly chelated $[Ca^{2+}]_i$ as previously shown by the lack of any change in $[Ca^{2+}]_i$ fluorescence; (Khiroug et al., 1997; Khiroug et al., 1998). Fig. 33 A shows an example of the early depression of nicotine responses by CGRP. The test response to 20 ms nicotine (-1144 pA) was readily depressed (by 56 %) when CGRP was applied for 15 s before nicotine, indicating a relatively rapid onset of this block, with partial return of the response appearing already 45 s after stopping the CGRP application. The down regulation of nicotine responses by CGRP did not depend on the low $[Ca^{2+}]_i$ as analogous results ($P>0.05$; see histograms in Fig. 33 B) were obtained when 25 μM Fluo-3 (which per se does not interfere with endogenous $[Ca^{2+}]_i$ buffering; (Khiroug et al., 1997; Khiroug et al., 1998)) was used instead of 10 mM BAPTA. The use of Fluo-3 also allowed us to investigate the reduction in nicotine-elicited $[Ca^{2+}]_i$ rises during CGRP

application: in this case the increase in $[Ca^{2+}]_i$ (after subtracting any slight increment induced by CGRP itself) was 7±3 % of control (n=6). Comparable reductions in nicotine-induced currents were observed when 1 μM CGRP was continuously applied via the bathing solution as shown by the examples of Fig. 33 C (in which control traces or those in the presence of CGRP are superimposed) suggesting that the blocking action of CGRP was not an artefact due to the pressure pulse application. Note that in this experiment we also wished to explore if CGRP had any significant chemical interaction with nicotine itself which might have reduced the dose of applied agonist. For this purpose we activated approximately equivalent numbers of nAChRs, as judged from equi-amplitude inward currents, by applying presumably the same dose of nicotine from a pipette containing either 0.1 mM concentration (50 ms pulse duration; left panel) or a ten fold higher concentration (1 mM) for a shorter time (10 ms; right panel). On five cells on which these two applications were tested, the 0.1 mM nicotine response was equally sensitive (48±8 % depression) as the 1 mM nicotine response (50±12 % depression) to CGRP ($P>0.05$). These observations thus indicate that the depression of nicotine currents by CGRP was not caused by some interaction between these two substances. The onset of such nicotine currents (measured as rise time from baseline to peak) did not apparently change in the presence of CGRP as it was 142±26 ms and 130±28 ms, respectively ($P>0.05$). Furthermore, the time constant of monoexponential current decay (to 10% of peak amplitude) was not significantly affected, being 736±108 in control and 552±89 ms in the presence of CGRP, respectively ($P>0.05$), making unlikely major underlying changes in activation and deactivation of nAChRs.

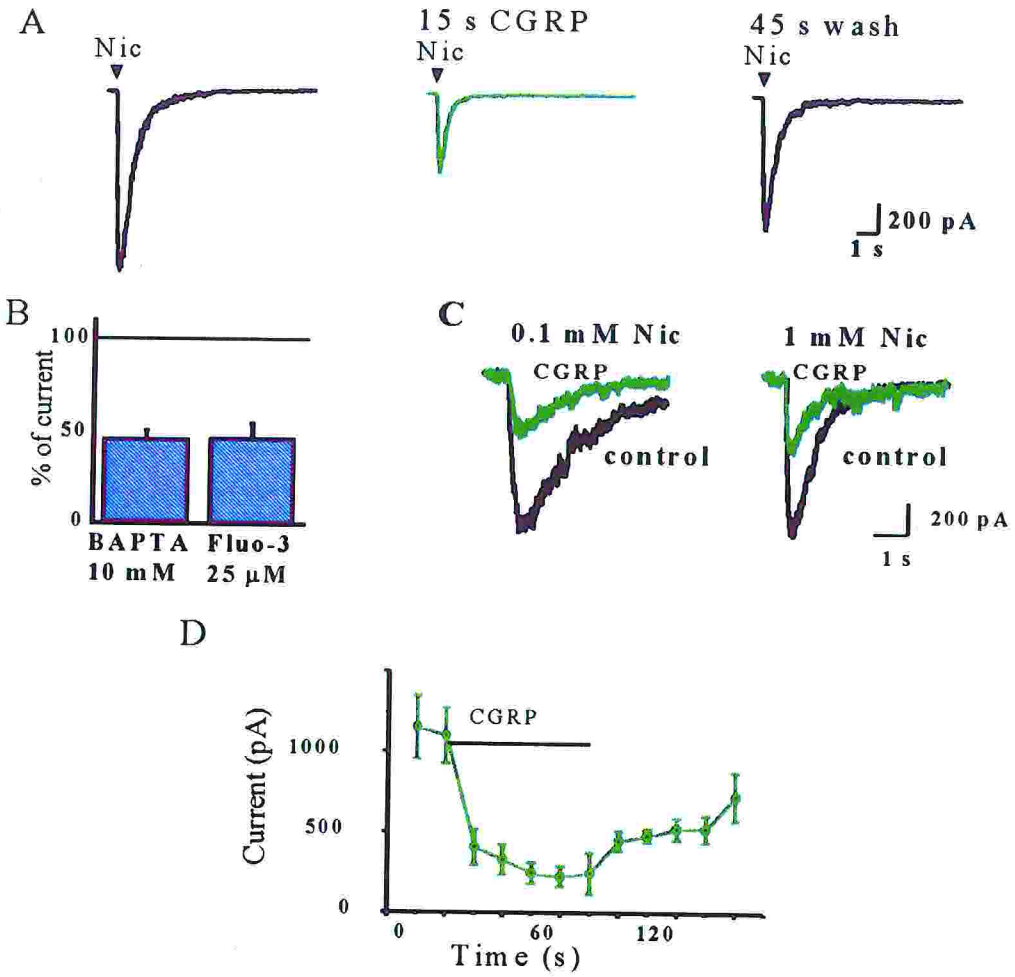

Fig. 33. Rapid downregulation of nicotine-induced responses by CGRP. A, Current records (recorded with a 10 mM BAPTA containing pipette) obtained with 20 ms nicotine (0.1 mM pipette concentration; left), 15 s after starting pressure application of CGRP (1 µM pipette concentration; middle) and 45 s after washout of CGRP. Note reduction in nicotine current amplitude. B, Histograms of 20 ms nicotine current responses (as % of control ones) following 30 s application of CGRP. The same depression ($P>0.05$) was observed regardless of the presence of 10 mM BAPTA (n=20) or 25 µM Fluo-3 (n=11) in the recording pipette. Other details as in A. C, Similar amplitude currents induced by 50 ms nicotine (0.1 mM pipette concentration; left) or 10 ms nicotine (1 mM pipette concentration; right) before and during bath application of CGRP (1 µM; 5 min). Note analogous depression of either response. Control and CGRP data are superimposed for sake of comparison. Records are obtained with Fluo-3 containing pipettes. D, Timecourse of CGRP depression of nicotine currents (20 ms applications; 0.1 mM pipette concentration) following pressure application of CGRP (1 µM pipette concentration) to 8 cells. Other details as in C.

4. 3 Dynamics of nicotine current block by CGRP

Fig. 33 D shows the time course of CGRP depression for 8 cells recorded with a BAPTA containing pipette. It is noteworthy that the extent of depression did not progressively increase during CGRP application and that recovery was achieved 3 min later. Similar data were also obtained when the recording pipette contained Fluo-3 (not shown). Since the protocol used in the experiments of Fig. 33 D relied on low frequency applications of nicotine pulses, it might have caused underestimation of more rapid processes underlying the action of CGRP such as desensitization or channel block which are manifested as fast, use dependent depression. This issue was explored with paired pulse (20 ms) delivery of nicotine (interpulse interval=2 s): in this case in control solution the nicotine current evoked by the second pulse was 84±10 % (n=5) of the first one, and in the presence of 10 μM CGRP the second current amplitude was 102±23 % of the first current ($P>0.05$), indicating that the extent of CGRP block was not augmented by prior activation of nAChRs. The relatively fast onset of the blocking effect of CGRP prompted further tests to see if this phenomenon could also occur on a more rapid time scale. For these experiments we used one puffer pipette filled with 0.1 mM nicotine and a second puffer pipette (filled with 0.1 mM nicotine plus 1 μM CGRP) immediately adjacent to the first one. For 20 ms applications CGRP decreased the nicotine current to 50±10 % of control (n=7; $P<0.01$). This drug delivery protocol therefore suggested that the onset of such a phenomenon was particularly fast. In summary then, these experiments revealed that CGRP induced a $[Ca^{2+}]_i$ independent, strong and rapid depression of nicotinic receptors of chromaffin cells apparently unrelated to the slow action of CGRP on $[Ca^{2+}]_i$.

4.4 CGRP blocking action depended on nicotine dose but not on membrane potential

Further tests were performed to characterize the mechanism underlying the depression by the peptide of nicotinic receptors. Fig. 34 A shows that, on 9 cells recorded with a BAPTA-filled electrode, increasing the duration (5-100 ms) of 0.1 mM nicotine pulses yielded progressively larger current amplitude with apparent saturation at 50 ms pulses. When comparable applications were repeated in the presence of 1 μM CGRP (15 s puffer pipette pre-application) currents induced by 5-30 ms nicotine pulses were blocked while responses induced by 50-100 ms pulses were not affected. Thus, the plot was shifted to the right while retaining analogous maximum response. Taking average responses at approximately mid-point of the curve (20 ms) before and after the peptide application gave a 55±5 % depression with the 1 μM CGRP dose (n=20), a value not different from the one observed with 10 μM CGRP (60±5 %, n=8) while the 0.1 μM dose elicited a smaller depression (19±6 %, n=5). These data suggest that the reduction in nicotine-induced currents was already maximal by focally-applied 1 μM CGRP and that smaller amplitude currents were more sensitive than larger ones to this action of the peptide.

This pattern of antagonism outlined the possibility of a competitive interaction by CGRP with the nicotine binding site of the receptor. Direct comparison of CGRP with F3 seemed to be a possible way to explore the nature of CGRP antagonism. F3 pre-applied for at least 15 s from 30 nM pipette solution induced a parallel, rightward shift of the dose response curve as previously shown (Fig. 34 B). The dose of F3 was selected to induce a degree of antagonism comparable in entity to the one evoked by pressure-applied 1 μM CGRP (Fig. 34 A). The blocking action of F3 had rapid onset with full recovery of nicotine responses after 15-30 s from the end of the F3 application (not shown). These data thus indicate

that F3 and CGRP had analogous blocking effect on nAChRs of rat chromaffin cells.

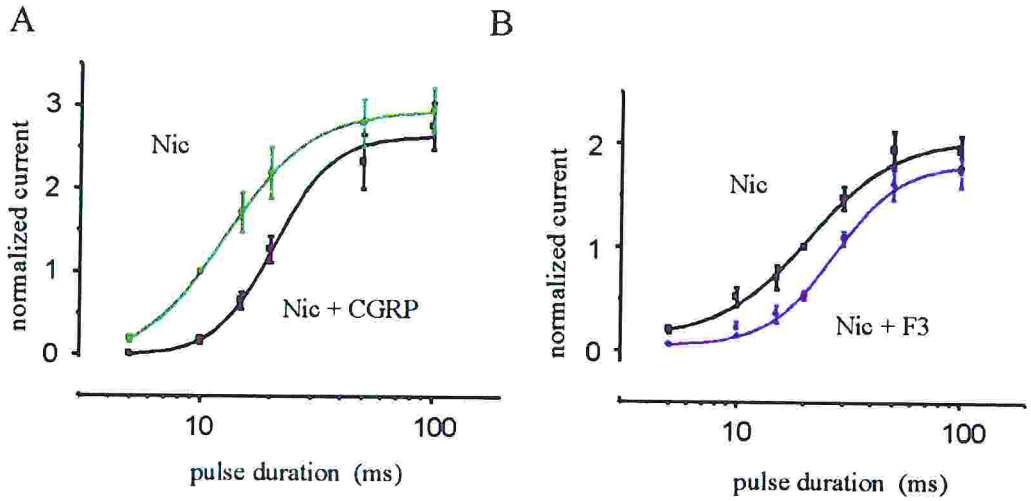

Fig. 34. Plot of nicotine current amplitudes versus increasing duration of nicotine pressure pulses in control solution, in the presence of CGRP or F3.

Ordinate: current amplitude normalized with respect to the response evoked by 10 ms nicotine in control solution for each cell. Abscissa: pulse duration of nicotine (0.1 mM) applications. A: CGRP (1 μM pipette concentration) was applied for about 15 s before each nicotine response (n=9 cells). B: F3 (30 nM pipette concentration) was applied for about 15 s before each nicotine response (n=8-19 cells). Note rightward shift of either plot without decrease in maximal response. All records were obtained with BAPTA containing patch pipettes.

To test whether these substances shared a common site of action, we applied them in low concentrations either alone or in combination. Fig. 35 shows an example of this approach. Application of F3 (30 nM pipette solution for 15 s) caused a 34 % reduction in the peak current induced by 20 ms nicotine (0.1 mM); after washout, bath application of 0.5 μM CGRP reduced the same nicotine current by 26%. Subsequent application of F3 in the continuous presence of CGRP decreased the control nicotine response by 60%, showing additive antagonism.

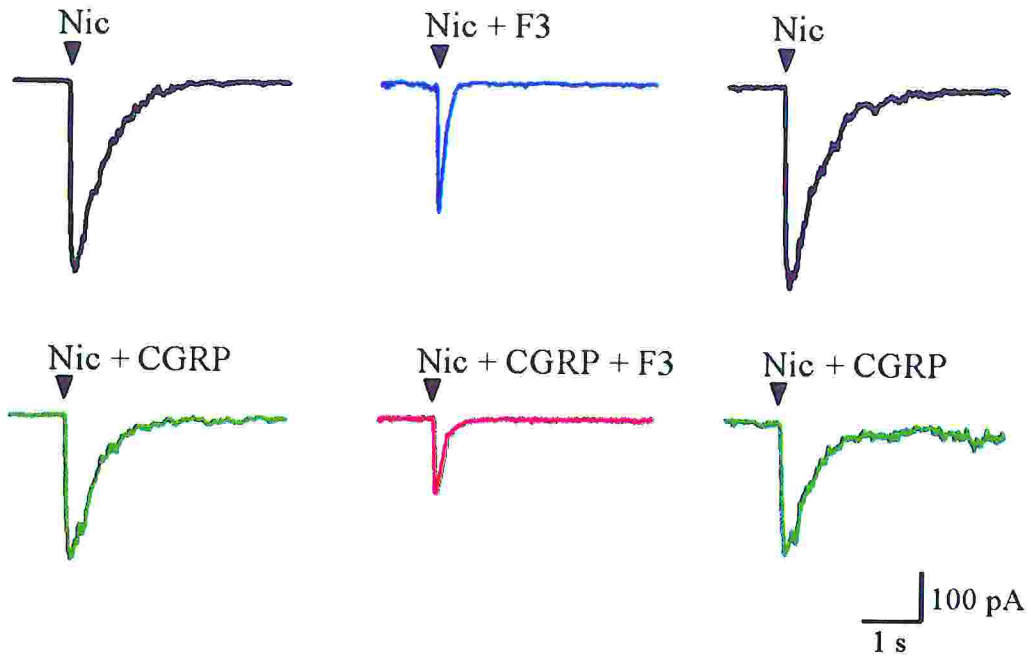

Fig. 35. Depression of nicotine evoked currents by F3, CGRP or a combination of them. Traces are inward currents evoked by nicotine (20 ms pulse; 0.1 mM pipette solution) in control solution, in the presence of F3 (15 s application; 30 nM pipette concentration), or of CGRP (0.5 μM bath application for about 1 min) or during combined application of F3 and CGRP. All records were obtained from the same cell with a BAPTA containing patch pipette.

Table 3 shows that on 6 cells the observed depression of the nicotine current amplitude was very similar to the one calculated by adding the individual antagonism values. According to standard receptor theory (Barlow, 1980), combining two competitive antagonists should produce an agonist dose ratio (DR) value (i.e., the ratio between agonist doses required to reproduce the same amplitude response before and after antagonist application) given by the equation $DR = (DR_1 + DR_2) - 1$ where DR_1 and DR_2 are the DR observed with each one of the antagonists applied separately. This approach has been used in the past to study the site of action of various blockers against, for instance, glutamate (Evans and Smith, 1982; Martin and Lodge, 1985) or GABA (Simmonds, 1982) receptors. In the present experiments precise quantification of DR values was made difficult by the use of pressure

application and non-equilibrium agonist responses; thus, data obtained with this approach only allow an estimate of the antagonist site of action. Notwithstanding this limitation, when taking the nicotine pulse duration as agonist "dose" (20 ms) for 6 cells, CGRP produced a DR_1=1.75±0.12 while F3 induced a DR_2=1.40±0.20. Combining CGRP with F3 gave DR value of 2.50±0.18 which is similar to the calculated one of 2.15±0.32, suggesting that these two blockers were likely to have a similar site of action.

Cell	Observed sum of % depression due to CGRP+F3	Calculated sum of % depression due to CGRP+F3
1	80	80
2	46	55
3	50	58
4	81	98
5	60	60
6	81	90

Table 3 Additive antagonism of nAChRs by low doses of simultaneously applied F3 and CGRP. Data are expressed as % reduction in 20 ms nicotine-induced peak currents observed experimentally (left column) or predicted by simple addition of individual blocking action by each antagonist (right column).

To analyze further the mechanism of action of CGRP on nAChRs we explored if its antagonism was altered when the cell membrane potential is changed, as it would be expected in the case of channel block. Fig. 36 A shows that on the same cell recorded with a BAPTA containing electrode and held at -120 or -70 mV CGRP elicited a similar reduction in nicotine current amplitude (49 and 41 %, respectively). On average the depression at -120 mV was 61±8 % (n=6), a value thus not significantly different (P>0.05) from the 55±5 % observed at -70 mV. Application of a

rapid membrane potential ramp (from -120 to 0 mV) at the peak of the nicotine current allowed us to obtain an I/V plot (after leak subtraction; see Fig. 36 B) with apparent reversal near 0 mV. CGRP (1 μM) reduced the nicotine response uniformly throughout this potential range with no detectable change in extrapolated current reversal potential. This was also apparent by scaling the plot obtained in the presence of CGRP to the one in control and superimposing them as shown in the inset to Fig. 36B.

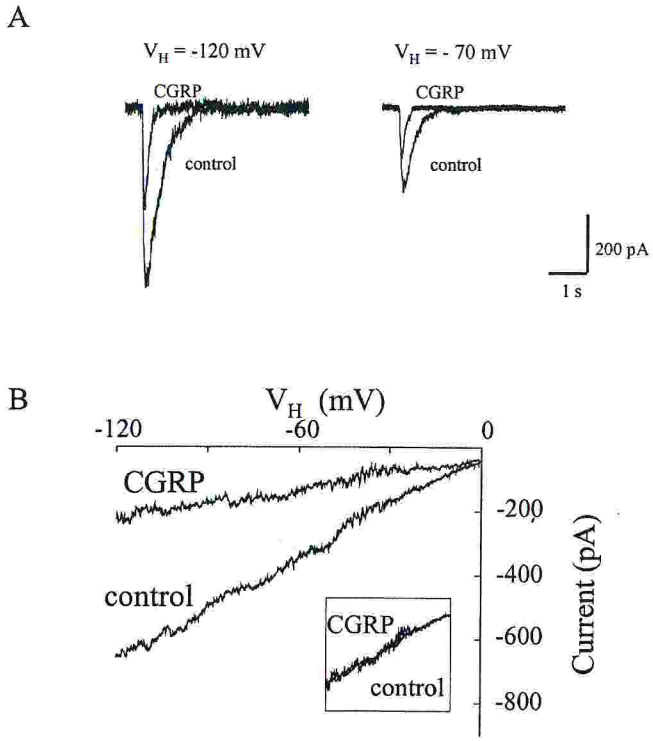

Fig. 36. CGRP induced depression of nicotine currents is voltage independent. A, Comparison of currents induced by 20 ms nicotine (0.1 mM pipette concentration) in control solution or during pressure application of CGRP (1 μM pipette concentration) at -120 mV (left) or -70 mV (right) holding potential. Data are superimposed for comparison. Note that the extent of peak current depression was similar for either holding potential. Traces are from the same cell recorded with a BAPTA containing pipette. B, I/V plot obtained at the peak of 50 ms nicotine induced current in control solution or in the presence of CGRP (1 μM pipette concentration). All data are leak subtracted. Note lack of apparent change in current reversal and that in the presence of CGRP the plot was uniformly reduced. Scaling the latter graph and superimposing it on the control one (see inset) show similar I/V properties. Ramp voltage was from -120 to 0 mV at 0.5 mV/ms.

These data therefore confirm that the block by CGRP of nicotinic receptor mediated responses was voltage independent and not caused by a negative shift in current reversal. Thus, the action of CGRP was unlikely to involve channel block of activated nicotinic receptors.

4.5 Specificity of CGRP blocking action

This issue was addressed by examining if CGRP could modify responses to another fast acting neurotransmitter such as GABA (Peters et al., 1989) or if other neuropeptides could affect nicotine mediated responses. Fig 37 depicts the first case in which bath-applied CGRP (1 μM) depressed peak currents elicited by nicotine (0.1 mM; 20 ms pulse, left) by 46±9 % whereas it left unchanged (96±5 %) the similar amplitude currents evoked by GABA (1 mM; 50 ms pulse, right) on the same cells (n=5).

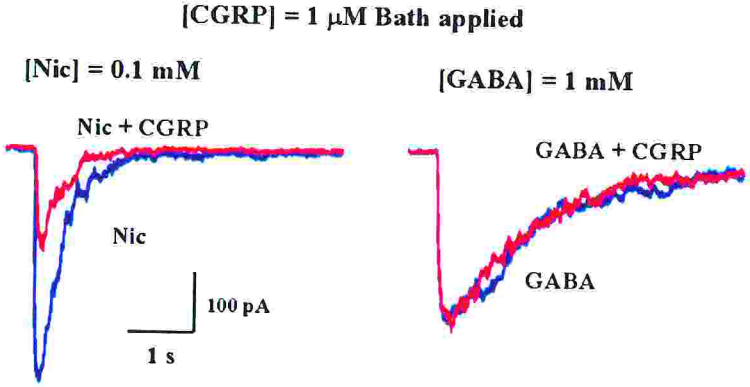

Fig. 37. GABA mediated current were left unchanged by CGRP. Similar amplitude currents induced by 20 ms nicotine (0.1 mM pipette concentration; left) or 50 ms GABA (1 mM pipette concentration; right) before and during bath application of CGRP (1 μM; 5 min). Note that GABA mediated current were not affected by CGRP application. Control and CGRP data are superimposed for sake of comparison.

Fig. 38 A demonstrates as Thyrotropin Releasing Hormone (TRH; 1 μM by pressure application for 1 min) did not change (98±2 %; n=6) nicotine evoked currents.

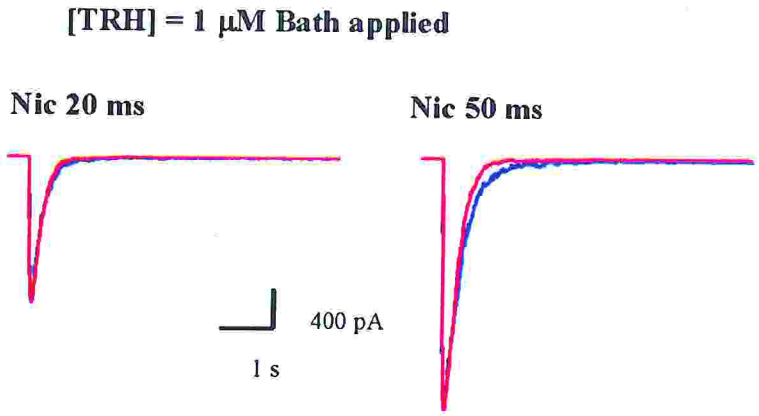

Fig. 38. Nicotine mediated current were left unchanged by TRH. Submaximal currents evoked 20 ms nicotine (0.1 mM pipette concentration; left) or saturating currents evoked by 50 ms nicotine (1 mM pipette concentration; right) were both left unchanged by bath application of CGRP (1 µM; 5 min). Control and CGRP data are superimposed for sake of comparison.

Similarly, dynorphin A (1 µM; pressure applied for 1 min) left the nicotine currents unchanged (95 ± 2 %; n=17, Fig 39 B).

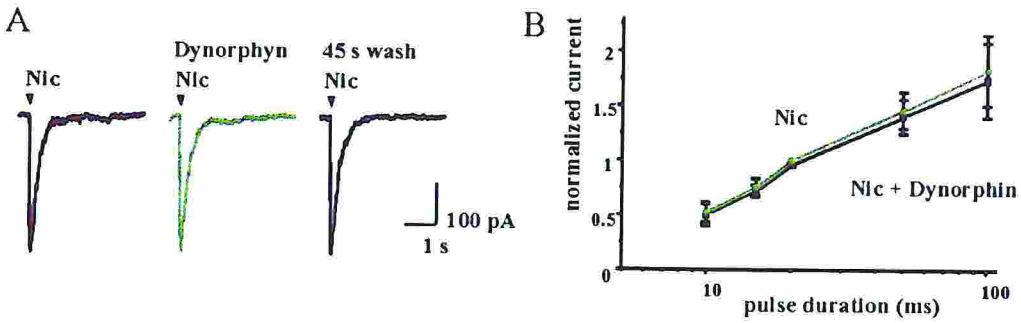

Fig. 39. Dynorphyn does not affect nicotine mediated responses. A: Example of submaximal currents evoked 20 ms nicotine (0.1 mM pipette concentration) in control and during 1 µM Dynorphyn application. B: Plot of nicotine current amplitudes versus increasing duration of nicotine pressure pulses in control solution and in the presence of Dynorphyn. Ordinate: current amplitude normalized with respect to the response evoked by 20 ms nicotine in control solution for each cell. Abscissa: pulse duration of nicotine (0.1 mM) applications. Dynorphyn (1 µM pipette concentration) was applied for about 15 s before each nicotine response (n=7 cells). Note that the plot remains the same as in control.

4.6 Effect of a CGRP receptor antagonist

If CGRP acted directly on nicotinic receptors, this effect would presumably have not been mediated by conventional G-protein coupled CGRP receptors which are known to exist on chromaffin cells (Mazzocchi et al., 1996a, Mazzocchi et al., 1996b) and trigger synthesis of cAMP to activate PKA (Bell and McDermott, 1996). This issue was tested by using human $CGRP_{8-37}$ ($hCGRP_{8-37}$), a pharmacological antagonist selective against G-protein coupled CGRP receptors (Bell and McDermott, 1996) or the selective PKA inhibitor Rp-cAMPS (de Wit et al., 1984; see also Khiroug et al., 1998). Fig. 40 A shows that on the same cell in which pressure-applied CGRP (1 μM) depressed the inward current induced by 20 ms nicotine (0.1 mM), bath-application of 1 μM $hCGRP_{8-37}$ for approximately 5 min failed to change the nicotine current or the baseline current and did not prevent the depressant effect of CGRP. On three cells the CGRP depression observed in the presence of $hCGRP_{8-37}$ was 94±6 % of the one found before superfusion with $hCGRP_{8-37}$ ($P>0.05$), indicating insensitivity of this phenomenon to $hCGRP_{8-37}$. Nevertheless, $hCGRP_{8-37}$ fully prevented the slow $[Ca^{2+}]_i$ rise (measured after transmembrane loading of the cells with Fluo-3 AM) induced by 2 min pressure application of CGRP (as exemplified in Fig. 40 B). Pooling data from 24 cells showed that CGRP (1 μM) increased $[Ca^{2+}]_i$ by 41±11% while in the presence of $hCGRP_{8-37}$ (1 μM) this action of CGRP was suppressed (11±5 %; $P<0.01$ versus control). On 12 cells pre-treated with 10 μM Rp-cAMPS for 20 min, the $[Ca^{2+}]_i$ rise evoked by CGRP was also suppressed (18±10; $P<0.05$ versus control). These results indicate that the slow $[Ca^{2+}]_i$ rise induced by CGRP was mediated by CGRP receptors and involved PKA activity.

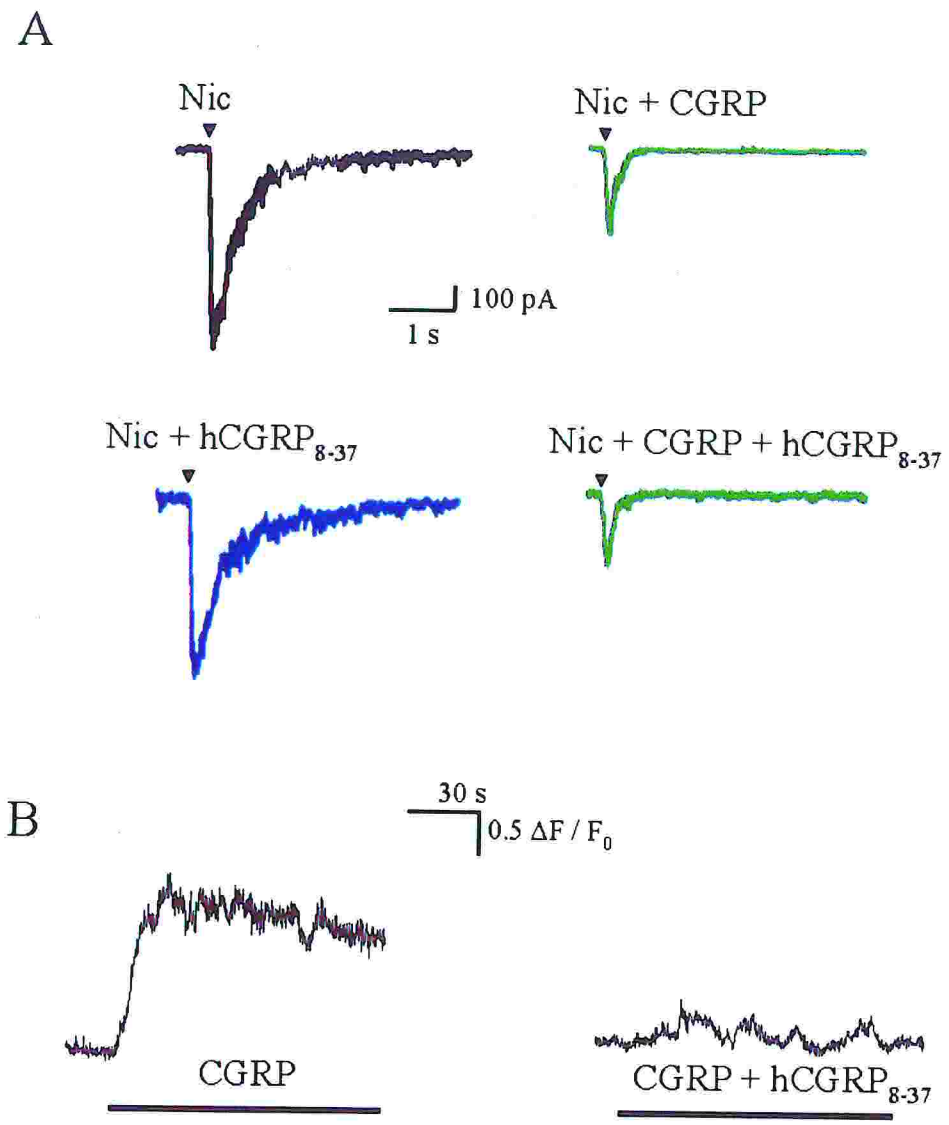

Fig. 40. Effect of the CGRP receptor antagonist $hCGRP_{8-37}$ on nicotine or CGRP responses. A, inward current evoked by 20 ms nicotine (0.1 mM pipette concentration; top left) is depressed by CGRP (1 μM pipette concentration; top right). Subsequent bath application of $hCGRP_{8-37}$ (1 μM; 5 min) does not change nicotine response (bottom left) or the depressant action of CGRP on the nicotine current. All data from the same cell recorded with Fluo-3 containing pipette. B, $[Ca^{2+}]_i$ increase induced by 2 min application of CGRP (1 μM pipette concentration; left) is suppressed in the presence of bath-applied $hCGRP_{8-37}$ (1 μM; right). Data are from a cell loaded with Fluo-3 AM.

4.7 $CGRP_{1-7}$ blocks nicotine mediated currents without changing $[Ca^{2+}]_i$

Since $hCGRP_{8-37}$ had no effect on nicotine currents it seemed likely that the nicotine receptor blocking action was mediated by the 1-7 terminal region of CGRP. For this purpose we used rat $CGRP_{1-7}$ (custom-

synthetized by American Peptides Co., Sunnyvale, CA) to test its action on nicotine-mediated response. Fig. 41 A shows representative records of nicotine (0.1 mM; 20 ms) induced currents before and during the pressure application of $CGRP_{1-7}$ (1 μM) which depressed by 48 % the nAChR-mediated inward current with rapid recovery after washout. Fig. 41 B depicts the time course of $CGRP_{1-7}$ blocking action which was already fully developed at the first pulse of nicotine in the continuous presence of this antagonist, thus showing lack of use dependent block. Prompt recovery of nicotine responses was attained at the end of $CGRP_{1-7}$ application. The profile of pharmacological antagonism by $CGRP_{1-7}$ was characterized by a rightward shift of the nicotine plot with unchanged maximum (Fig. 41 C), a phenomenon thus similar to the one reported above for native CGRP (see Fig. 34 A). In particular, for a 20 ms test pulse of nicotine the depression by $CGRP_{1-7}$ (1 μM intrapipette solution) amounted to 46±5 % (n=15; $P<0.01$). Conversely, $CGRP_{1-7}$ did not significantly increase $[Ca^{2+}]_i$ ($\Delta F/F_0=0.2\pm0.1$, n=9; $P>0.05$) while application of 20 ms nicotine (0.1 mM) raised $[Ca^{2+}]_i$ ($\Delta F/F_0=3.1\pm1.1$; $P<0.01$) in the same group of cells (n=9). These observations suggest that $CGRP_{1-7}$ interacted with nAChRs but did not activate the G-protein coupled CGRP receptors responsible for the $[Ca^{2+}]_i$, thus indicating that distinct regions of the peptide sequence were responsible for fast nicotine current modulation and slow metabotropic changes on chromaffin cells.

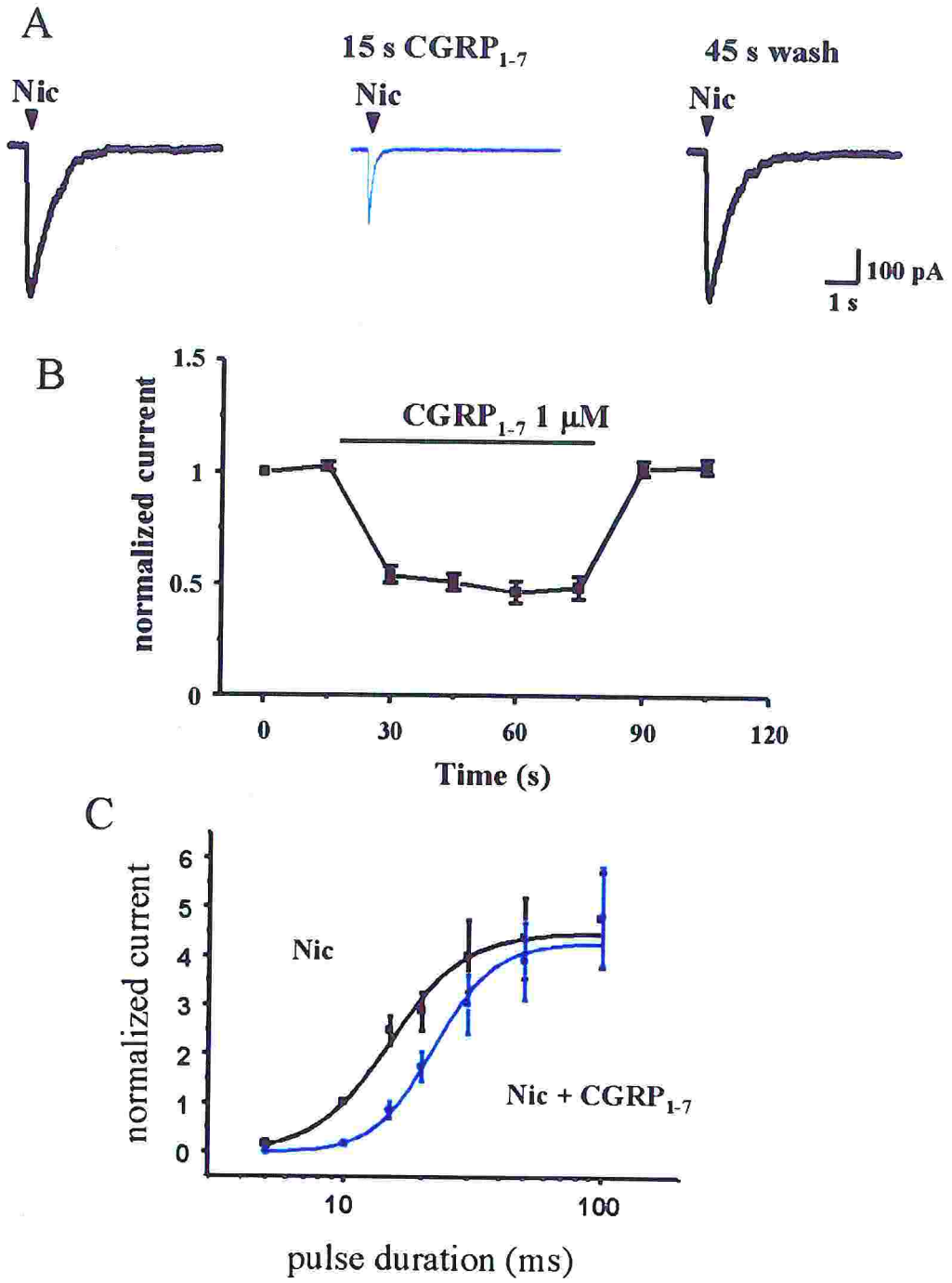

Fig. 41. Depression of nicotine currents by the $CGRP_{1-7}$ fragment. A: inward current induced by nicotine (20 ms; 0.1 mM pipette concentration) is largely and reversibly depressed by $CGRP_{1-7}$ (15 s pulse; 1 µM). B: time course of depression of nicotine currents by pressure applied $CGRP_{1-7}$. Data are from 8-17 cells. Note rapid onset and offset of current depression and absence of use dependent block. C: plots of normalized nicotine current amplitude versus increasing duration of nicotine pressure pulses in control solution or in the presence of CGRP1-7 (1 µM; pressure applied; n=4-18 cells). For further details see legend to Fig. 34.

5. Modulation of neuronal nicotinic receptors by short CGRP N-terminal fragments.

What emerged from the last results was that the 1-7 N-terminal fragment of calcitonin gene related peptide ($CGRP_{1-7}$) behaves as a potent antagonist of nAChRs as efficiently as the entire peptide (Giniatullin et al., 1999). In the attempt to identify the minimal amino acid sequence retaining this antagonist action, we decided to investigate the effects of shorter fragments of this peptide, namely $CGRP_{1-6}$, $CGRP_{1-5}$, $CGRP_{1-4}$ and $CGRP_{1-3}$. Fig. 42 lists their amino acid sequences.

CGRP1-7: Ser-Cys-Asn-Thr-Ala-Thr-Cys

CGRP1-7A: Ser-Cys-Asn-Thr-Ala-Thr-Ala

CGRP1-6: Ser-Cys-Asn-Thr-Ala-Thr

CGRP2-7: Cys-Asn-Thr-Ala-Thr-Cys

CGRP1-5: Ser-Cys-Asn-Thr-Ala

CGRP1-4: Ser-Cys-Asn-Thr

CGRP1-3: Ser-Cys-Asn

Fig. 42. Linear amino-acid structure of the peptides $CGRP_{1-7}$ (note disulfide bond), $CGRP_{1-7A}$, $CGRP_{2-7}$, $CGRP_{1-6}$, $CGRP_{1-5}$, $CGRP_{1-4}$ and $CGRP_{1-3}$.

5.1 Potentiation of nicotine evoked responses by $CGRP_{1-6}$

Fig. 43 A shows inward currents generated by nicotine (applied via brief pressure pulses from a 0.1 mM pipette concentration to minimize rapid

desensitization; Khiroug et al., 1997) from a chromaffin cell in culture. When a 20 ms pulse was delivered in the presence of $CGRP_{1-6}$ (1 μM; applied by rapid superfusion), the inward current was unexpectedly potentiated (53%; Fig. 43 A, top). This phenomenon was not associated with any direct action of $CGRP_{1-6}$ on resting conductance or baseline current, indicating that this substance did not have agonist activity on nAChRs or non-specific actions on membrane leak channels. On the same cell, $CGRP_{1-6}$ (1 μM) was ineffective on 200 ms pulse nicotine currents (Fig. 43 A, bottom) which were large enough to reach response plateau (Giniatullin et al., 1999). Fig. 43 B shows effects observed when nicotine or nicotine plus $CGRP_{1-6}$ were both applied via the fast superfusion system. Again, the inward current induced by 20 μM nicotine was potentiated by co-applied $CGRP_{1-6}$ (1 μM; 39 % potentiation) while the maximal current elicited by 200 μM nicotine was unaffected by the peptide. On average, $CGRP_{1-6}$ enhanced currents to 20 μM nicotine by 33±8 % (n=5; $P<0.05$). Calibration experiments (see Methods section) have indicated that semilog plots of pressure pulse/current responses were linear within the 10-50 ms application range and corresponded very closely to those produced by superfusing 20-100 μM nicotine (Di Angelantonio, 2001), suggesting the upper and lower concentration limits reached with puffer application.

The $CGRP_{1-6}$ effect was manifested already with the first nicotine response elicited just 5 s after starting peptide superfusion, and was reversible after 1 min washout (Fig. 43 C; n=11). The rapid action of $CGRP_{1-6}$ was also confirmed by the fact that, when coapplied with nicotine, it immediately increased nicotine currents as long as the responses were submaximal (Fig. 43 B).

Further tests were performed to characterize the action of $CGRP_{1-6}$ (1 μM).

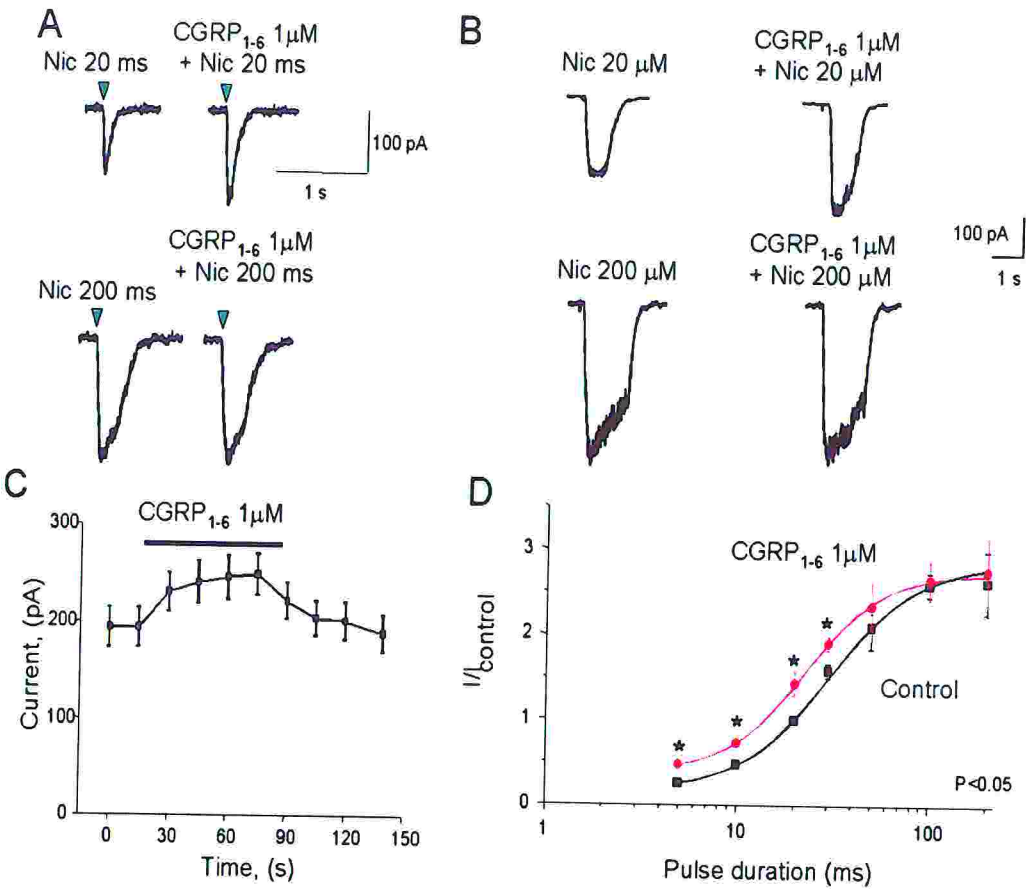

Fig. 43. Effect of $CGRP_{1-6}$ on nicotine evoked currents. A, top: submaximal currents induced by a short, non-saturating nicotine pulse (20 ms) are potentiated by this peptide fragment whereas maximal currents (200 ms nicotine pulse) are not affected (bottom). B, current response to superfusion of 20 μM nicotine together with $CGRP_{1-6}$ (1 μM) is enhanced with respect to control (top) whereas maximum response to 200 μM nicotine is unaffected by 1 μM $CGRP_{1-6}$ (bottom). C, Time course of the $CGRP_{1-6}$ action on nAChR: currents elicited by nicotine are rapidly potentiated and this effect is reversible after 45-60 s washout. D, Dose-response curve (expressed as pulse duration versus response) for nicotine in control and in the presence of $CGRP_{1-6}$ (1μM); the plot in the presence of the peptide is shifted to the left in a parallel fashion without altering maximal responses (n=5-12). Currents are normalized with respect to response to 20 ms pulse in control solution and fitted with the logistic equation. *=P<0.05.

Fig. 43 D shows that the plot relating inward current amplitude to the amount of nicotine (expressed as ms application; Giniatullin et al., 1999) with plateau value at 100 ms pulse (n=5-12 cells). When comparable applications were repeated in the presence of 1 μM $CGRP_{1-6}$ (15 s pre-

application), inward currents induced by 5-30 ms nicotine pulses were significantly ($P<0.05$) potentiated while responses induced by 50-200 ms pulses were unaffected. Thus, the plot was shifted to the left in an apparently parallel fashion while retaining analogous maximum response. $CGRP_{1-6}$ (1 μM) enhanced nicotine responses at approximately mid-point of the curve (20 ms) by 31±7 % (n= 30). These data therefore demonstrate that the potentiating action of $CGRP_{1-6}$ was dependent on the amount of agonist delivered to the cell.

Fig. 44 A shows the concentration dependence (0.05-100 μM range) of $CGRP_{1-6}$ effects on nAChRs activated by a fixed dose of nicotine (20 ms; 0.1 mM): potentiation had threshold at 0.1 μM (5±7%, n=7; $P<0.05$) and reached an apparent maximum at 50 μM (56±6%, n=5; $P<0.05$). Note that, as indicated by Fig 43 D, this "dose" of puffer-applied nicotine induced membrane current amplitudes approximately half of the apparent maximum. The $CGRP_{1-6}$ potentiating action was also present when cytisine rather than nicotine was the test agonist (20 ms; 0.1 mM; Fig. 44 B), as also indicated by the superimposed plots for the potentiation by $CGRP_{1-6}$ towards nicotine or cytisine evoked currents (Fig. 44 B, inset). The slope values for the nicotine or cytisine plots of Fig. 44 A,B were 1.1±0.02 and 1.02±0.02.

These results thus demonstrate that nAChR facilitation by $CGRP_{1-6}$ was agonist independent.

The $CGRP_{1-6}$ potentiating action was independent also from membrane potential as shown in Fig. 44 C in which average current responses from 6 cells held at -40, -70 or -100 mV are compared.

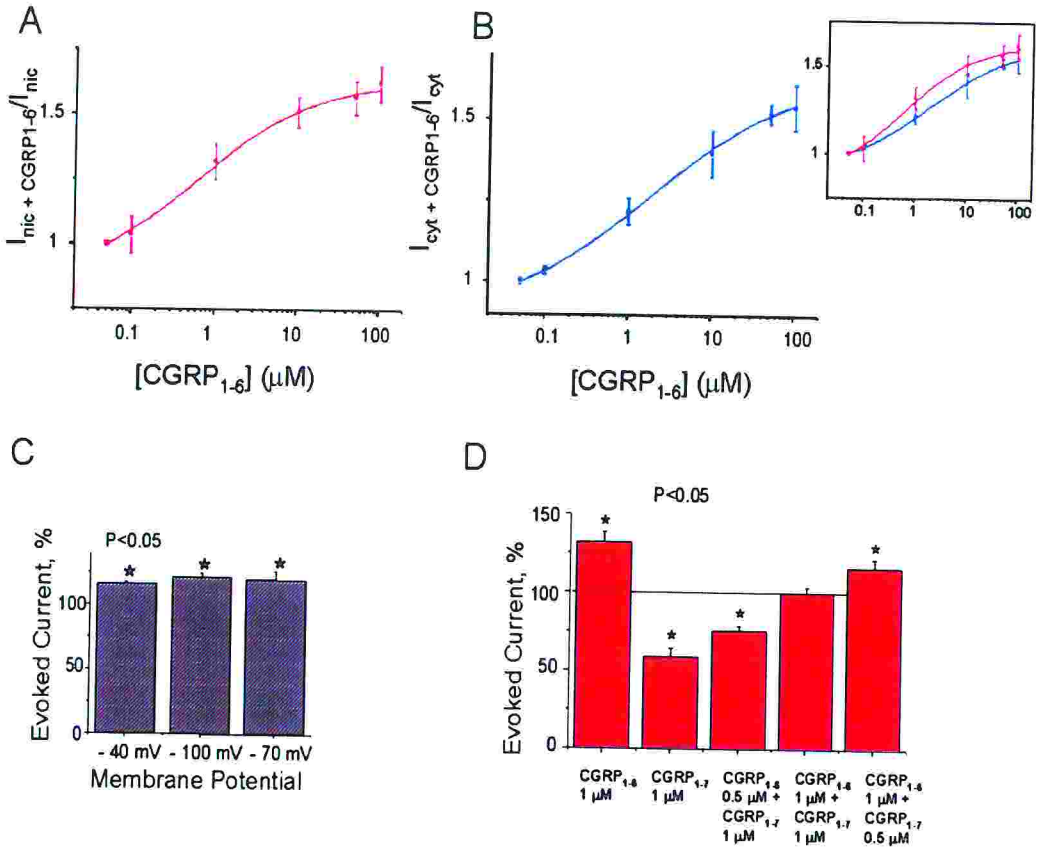

Fig. 44. Analysis of the mechanism of action of $CGRP_{1-6}$. A, The plot shows nicotine currents potentiation (0.1 mM, 20 ms) at different $CGRP_{1-6}$ concentrations; the threshold for potentiation is 0.1 μM; the same behaviour is shown in B with cytisine as test agonist (0.1mM, 20 ms). Abscissa: $CGRP_{1-6}$ concentrations (log units); ordinate: current ratio in $CGRP_{1-6}$ ($I_{nic+CGRP}$ or $I_{cyt+CGRP}$) over the one in control solution (I_{nic} or I_{cyt}). Inset shows superimposed plots for nicotine and cytisine responses, indicating similar shape. C, Histograms demonstrating the equiamplitude increase in 20 ms nicotine-evoked currents (expressed as % of control) at the three holding membrane potentials indicated below bars. Each bar is significantly different from control (*=P<0.05; n=7). D, Comparison of the action of $CGRP_{1-6}$ or $CGRP_{1-7}$ or a mixture of the two on 20 ms nicotine currents. Note that the potentiation due to $CGRP_{1-6}$ is cancelled out by the competitive antagonism exerted by $CGRP_{1-7}$ when the two peptides are applied together. All responses are expressed as ratio of nicotine evoked currents in the presence of the peptides with respect to control (n=6).

While these experiments showed an interesting potentiating action of $CGRP_{1-6}$, they did not clarify if this was specific for nAChRs. To this end we studied if this peptide possessed similar effects also on muscle-type

nicotinic receptors of I28 cells in culture (these are primary myoblasts; Irintchev et al., 1997; Wernig et al., 2000). On these cells (clamped at -60 mV holding potential) superfusion of nicotine (0.1 mM which was the EC_{50} concentration) evoked average responses of 1.06±0.22 nA peak (n=7), readily reversible after washout. When nicotine was applied in the continuous presence of 1 μM $CGRP_{1-6}$ (pre-applied for 2 min), evoked currents did not change in amplitude (1.09±0.24 nA, that corresponded to 101±2 % of controls; n=7, data not shown). Further tests were carried out to find out if distinct ionotropic receptors gated by other transmitters, for instance GABA, could also be affected by $CGRP_{1-6}$ (1 μM). For this purpose, we recorded inward currents generated by 3 ms application of 1 mM GABA to HEK 293 cells (n=6) expressing α1β2γ2 $GABA_A$ receptors (Granja et al., 1998). $CGRP_{1-6}$ did not change (101±1 %) responses to GABA, indicating that its action was not present on muscle type AChRs and was not generalized to ionotropic neuronal receptors.

5.2 Interaction between $CGRP_{1-6}$ and $CGRP_{1-7}$

The potentiation by $CGRP_{1-6}$ is in sharp contrast with the depression of nicotine evoked currents induced by $CGRP_{1-7}$ (Giniatullin et al., 1999). Loss of a single amino acid thus transformed the biological activity of the peptide fragment. Which of the two effects on nAChRs would prevail if these compounds were applied simultaneously? This issue was tested in experiments like those reported in Fig. 44 D. The average potentiation due to $CGRP_{1-6}$ was 31±7% (n=30) and the mean depression due to $CGRP_{1-7}$ was 42±11 % (n=17). Co-application of 0.5 μM $CGRP_{1-6}$ plus 1 μM $CGRP_{1-7}$ depressed (by 34±3 %; n=5) the 20 ms nicotine-induced submaximal currents whereas co-application of the same peptides at equimolar concentration (1 μM) left nicotine responses unchanged (99±4 %, n=9). When 1 μM $CGRP_{1-6}$ plus 0.5 μM $CGRP_{1-7}$ were applied, the nicotine currents were significantly enhanced by 16±6 % (n=5). These results suggest that these peptide fragments were

apparently equipotent in exerting their modulatory action although of diametrically opposite direction.

5.3 Effect of $CGRP_{1-5}$, $CGRP_{1-4}$ or $CGRP_{1-3}$ fragments

How conserved is the enhancing action of $CGRP_{1-6}$? This question was addressed by studying the effects of the shorter fragments $CGRP_{1-5}$, $CGRP_{1-4}$ or $CGRP_{1-3}$. Fig. 45A shows that $CGRP_{1-5}$ significantly potentiated 20 ms nicotine-induced currents in a concentration dependent fashion. However, this facilitation was less pronounced with respect to the one exerted by $CGRP_{1-6}$. In fact, while $CGRP_{1-6}$ (1 μM) potentiated by 31±7% (n=30), $CGRP_{1-5}$ (1 μM) potentiated by 20±4 % only (n=8). To obtain a comparable degree of potentiation (26±4%) it was necessary to use a 10 fold higher concentration of $CGRP_{1-5}$ (10 μM, n=5). Further increases in $CGRP_{1-5}$ concentrations (50-100 μM) did not augment the extent of potentiation (see Fig. 45 A).

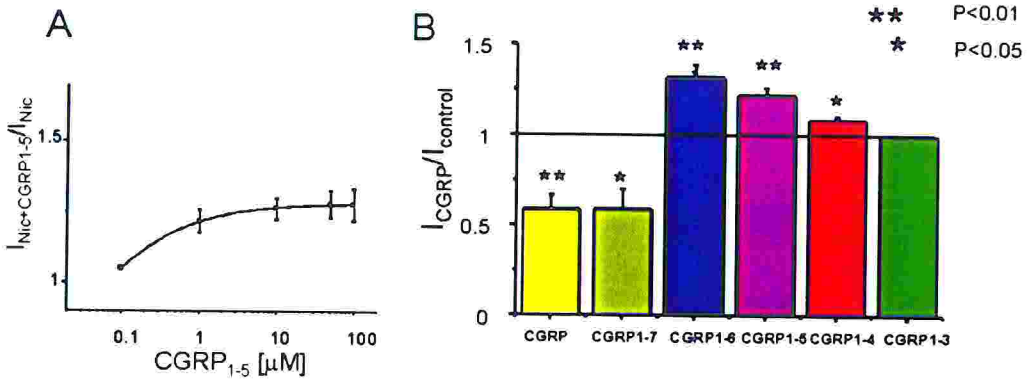

Fig. 45. Effect of $CGRP_{1-5}$, $CGRP_{1-4}$ and $CGRP_{1-3}$ fragments on nAChRs. A, plot showing the concentration dependence of potentiation of nicotine currents by $CGRP_{1-5}$. B, Histograms summarizing the action of different fragments of CGRP (all compounds applied at 1 μM concentration) on nicotine mediated responses. The efficacy of $CGRP_{1-5}$ is less than the one observed with the 1-6 fragment. $CGRP_{1-4}$ maintains a slight potentiating effect, while $CGRP_{1-3}$ is inactive. For comparison, data corresponding to the antagonism exerted by CGRP and $CGRP_{1-7}$ are reported. Responses are expressed as ratios of currents in the presence of CGRP or its fragment (I_{CGRP}) with respect to controls.

The fragment $CGRP_{1-4}$ (1 μM) also displayed a slight, yet significant, potentiating effect (8±1%; n=14) while at 10 μM concentration it significantly potentiated by 18±3 % (n=6). $CGRP_{1-3}$ (1 or 10 μM) did not alter nicotine induced currents (0±1%, n=7). These data are summarized in Fig. 45 B, in which the action of the various CGRP fragments is compared with the one of the native peptide (all compounds tested at 1 μM concentration).

5.4 Comparison between $CGRP_{1-6}$ and a typical allosterically potentiating ligand

The unusual action by $CGRP_{1-6}$ on nAChRs raised the possibility that this substance might belong to the category of APLs. These drugs bind to a discrete site of nAChRs from which they allosterically up or downregulate the action of nicotinic agonists (Maelicke et al., 1997; Changeux and Edelstein, 1998; Maelicke and Albuquerque, 2000). APLs often produce a biphasic action such that, in low doses, they facilitate agonist responses whereas, in higher doses, they depress them. One example of an APL is physostigmine which at the concentration of 0.5 μM maximally enhances nAChRs via allosteric modulation while at higher concentrations it actually inhibits them (Maelicke et al., 1993). In the present investigation we first tested if this action of physostigmine was also present on native nAChRs of chromaffin cells. To this end, nicotine (20 ms pulse) was applied in the presence of either a small (0.5 μM) or a high (5 μM) concentration of physostigmine. Fig. 46A shows sample traces demonstrating that 0.5 μM physostigmine potentiated nicotine induced responses (on average 28±5 %, n=14) while 5 μM depressed them (on average 48±2%, n=4). Fig. 46B shows the nicotine dose-response curve in control solution or in the presence of 0.5 μM physostigmine (n=4-14 cells). Physostigmine shifted the plot to the left which attained a larger (85±5%) maximal response ($P<0.01$). These data confirm that physostigmine acted on nAChRs of chromaffin cells with a

pharmacological profile typical of an APL and quite distinct from that of $CGRP_{1-6}$ (see Fig. 43).

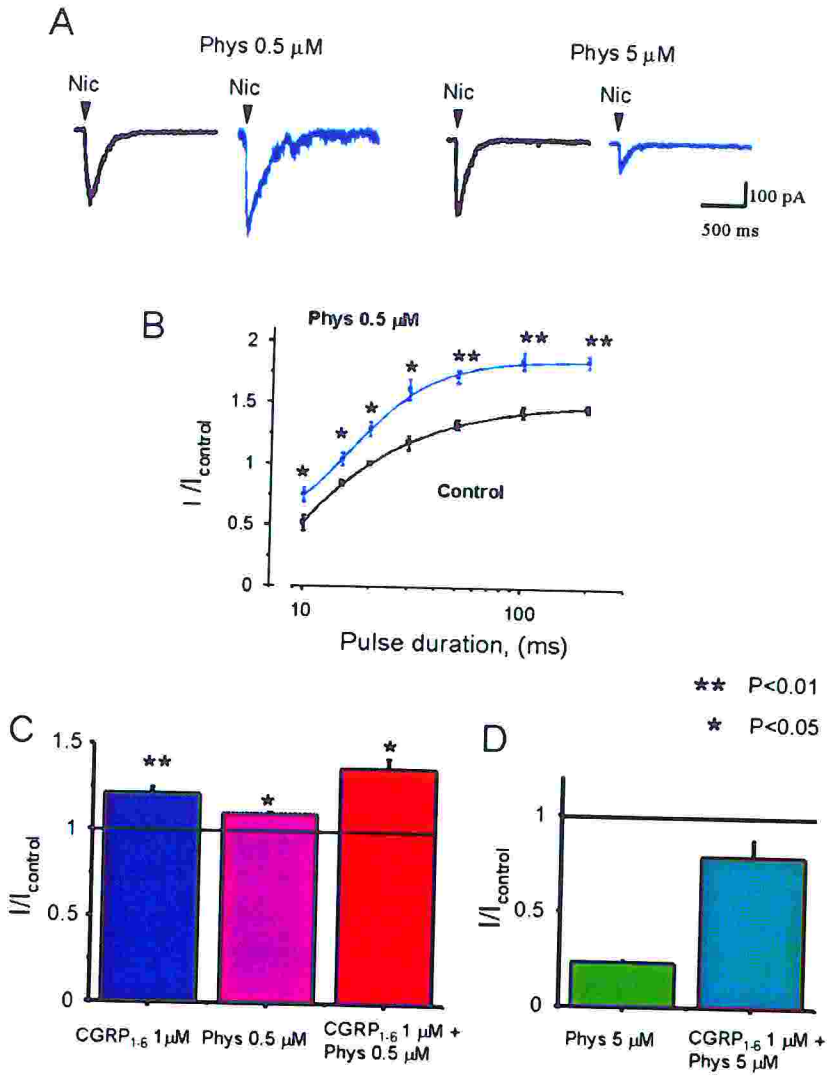

Fig. 46. Interaction between $CGRP_{1-6}$ and physostigmine (Phys). A, on the same cell a small concentration (0.5 μM) of physostigmine potentiates nicotine induced currents (0.1 mM, 20 ms), while a higher one depresses them (5 μM). B, Nicotine dose response curve (0.1 mM) in control and in the presence of physostigmine (0.5 μM; n=4-14). Physostigmine potentiates all nicotine mediated responses, including the maximal one. C, Histograms summarizing the action on nicotine (20 ms) induced currents by $CGRP_{1-6}$ (1 μM) or physostigmine (0.5 μM) applied either separately or simultaneously. Asterisks indicate level of significance (n=5). D, Histograms showing the depressant action of physostigmine (5 μM) on nicotine evoked responses and the opposing action by subsequent application of $CGRP_{1-6}$ (1 μM; n=4). Responses to nicotine are expressed as ratio between the current in the presence of the drug (I) and in control solution ($I_{control}$).

On the basis of these observations we then decided to study if $CGRP_{1-6}$ and physostigmine had distinct action on nAChRs. For this purpose, on a sample of 5 cells, standard responses induced by 20 ms nicotine were first potentiated, by the same degree, by $CGRP_{1-6}$ (1 μM) or physostigmine (0.5 μM) applied separately (21±4 or 20±6 % potentiation, respectively; Fig. 46C). We then co-administered these two substances while testing currents produced by 20 ms nicotine puffs. In the latter case the potentiation was 37±6 % which is a value close to the sum of the two individual effects (Fig. 46C).

Conversely, when the physostigmine concentration was higher (5 μM), nicotine induced currents became 23±1 % of the control amplitude (Fig. 46D). In this case, adding $CGRP_{1-6}$ (1 μM) could partly counteract the inhibition caused by physostigmine as the nicotine evoked responses were 79±1 % of the control amplitude (Fig. 46D; n=4). These results indicate that the action of $CGRP_{1-6}$ on nAChRs took place regardless of whether these were enhanced or inhibited by physostigmine.

5.5 Effect of $CGRP_{1-7A}$ or $CGRP_{2-7}$ fragments

Why did deletion of a single amino acid from $CGRP_{1-7}$ convert a depressant action into a potentiating one? Inspection of the primary amino acid sequences in Fig. 42 shows that absence of Cys from position 7 removed the disulfide bridge linking two cysteines in position 2 and 7. Assuming that removal of the disulfide bridge by deleting Cys_7 mediated switching of $CGRP_{1-7}$ from receptor antagonist to receptor enhancer, we predicted that a seven amino acid chain similar to the one of $CGRP_{1-7}$ but lacking a cyclic structure should yield an AChR potentiating peptide. This hypothesis was tested by replacing Cys_7 with Ala, thus yielding a new fragment termed $CGRP_{1-7A}$ (Fig. 42). Fig. 47A shows that the $CGRP_{1-7A}$ potentiated (+18 %) the nicotine (20 ms) evoked current, and that this effect was reversible after 1 min washout. The time course of the $CGRP_{1-7A}$ action on nicotine induced responses is depicted

in Fig. 47B: this potentiation was rapid in onset, reached apparent steady-state conditions (maximum potentiation =17±4 %; n=8) and was readily reversible during washout.

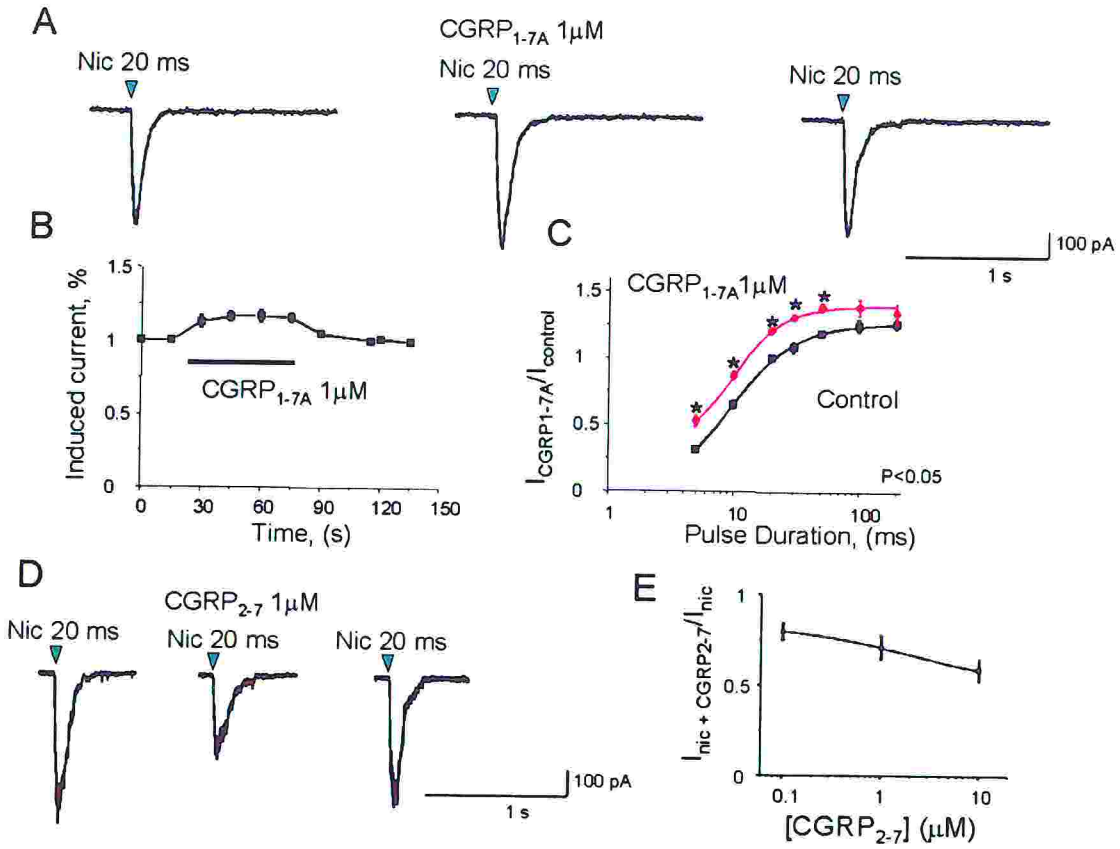

Fig. 47. Effect of the $CGRP_{1-7A}$ fragment on nicotine evoked responses. A, examples of current induced by 20 ms nicotine that is potentiated by 1 μM $CGRP_{1-7A}$ (pre-applied for 15 s). This effect is reversible after peptide washout (right panel). B, Time course of $CGRP_{1-7A}$ potentiation of 20 ms nicotine induced responses. Note rapid onset of the potentiation that reaches 18 % and is rapidly washed out. C, nicotine dose response curve (doses expressed as pulse duration, ms) in control solution and in the presence of 1 μM $CGRP_{1-7A}$ (n=4-8 cells). The plot is shifted to the left in an apparently parallel fashion without significantly changing maximal response. Asterisks indicate P<0.05. D: example of reversible depression by $CGRP_{2-7}$ (1 μM) of inward currents induced by 20 ms nicotine. E: log plot of $CGRP_{2-7}$ concentration versus response ratio of currents observed in $CGRP_{2-7}$ solution over control ones. Data are from 6 cells.

Fig. 47C shows the nicotine dose-response curve in control solution and in the presence of 1 μM $CGRP_{1-7A}$ (15 s pre-application; n=4-8 cells). In the presence of this peptide inward currents induced by 5-50 ms nicotine pulses were significantly ($P<0.05$) potentiated while responses induced by 100-200 ms pulses were unaffected. Thus, the plot was shifted to the left in an apparently parallel fashion while retaining analogous maximum response.

Further insight into the structure-activity relation of these peptides was sought by deleting Ser_1 from $CGRP_{1-7}$, thus converting this peptide into a shorter fragment which, nevertheless, retained the disulfide bridge (Fig. 42). Fig. 47D shows that 1 μM $CGRP_{2-7}$ reversibly depressed (by 43 %) the current response to 20 ms nicotine. The plot of Fig. 47E indicates that the depressant action by $CGRP_{2-7}$ toward 20 ms nicotine currents was concentration-dependent (within the 0.1-10 μM range). Hence, the $CGRP_{2-7}$ retained (albeit weakly) the depressant action of the longer compound $CGRP_{1-7}$ because, at 1 μM concentration, $CGRP_{1-7}$ and $CGRP_{2-7}$ inhibited nicotine currents by 45±5 % (see also Fig. 28B) and 32±8 % (n=6; Fig. 47E), respectively.

DISCUSSION

Neuronal nicotinic acetylcholine receptors (nAChRs) are a family of ACh-gated cationic channels consisting of different subtypes with distinct anatomical distribution in the vertebrate central and peripheral nervous systems (for reviews see Role and Berg, 1996; Gotti et al., 1997; Lindstrom, 1997). The role and function of most of these subtypes are difficult to establish because they may be coexpressed in individual neurons.

Studies about the structure, functions and pharmacology of neuronal receptors are very important because it was recently shown that these receptors are involved in a large number of cerebral functions and pathological mechanisms of nervous system diseases (for recent reviews see Special Issue on "*nicotinic neuronal receptors*" Clementi and Adlkofer, 2000).

Thus, it follows that agonists, antagonists and modulators of these receptors have stimulated widespread therapeutic or diagnostic interest in relation to different neuropathological conditions.

Some of the pathologies resulting from dysfunction of neuronal nicotinic receptors are, for example, Alzheimer's disease, Parkinson's disease, epilepsy, other mental diseases such as schizophrenia, Tourette's syndrome, anxiety and depression.

In view of above considerations, it is therefore apparent the need to identify and provide chemical substances for dissection of different subtypes and for the therapy of diseases resulting from nAChR dysfunction.

Up to date there are problems to study nAChRs in native systems because nAChRs are widely localized at post-synaptic as well at pre-synaptic level, within the main cholinergic pathways of central and peripheral nervous systems (Lindstrom, 1997).

Many studies have been carried out on heterologous expression systems, consisting of cells constitutively lacking nicotinic receptors and made to

express nAChRs with various sub-unit combination. Different biophysical and pharmacological properties of numerous subunit aggregates can then be investigated.

Often, the first step is the use of Xenopus oocytes or mammalian cells, e.g. HEK cells as expression system. This approach presents some limitation, in fact it has been shown (Lewis et al., 1997; Sivilotti et al., 1997) that these heterologously expressed receptors have different kinetics properties respect to the native ones, and also that some compounds, for example atropine and ivermectine, which modulate oocyte-expressed nAChRs, do not have a similar effect on native receptors (Krause et al., 1998).

However the use of oocyte as expression system is useful to investigate the molecular properties of nAChRs, because it allows to use a reporter mutation strategy (Groot-Kormelink et al., 2001).

Thus, native receptor-expressing cells remain indispensable for biophysical and pharmacological studies of nAChRs, particularly for the development of drugs active on central and peripheral neurons for the diagnosis and treatment of various neuropsychiatric disorders.

Our model is represented by rat chromaffin cells which constitute the medullary portion of adrenal glands.

Composition of nAChRs of rat chromaffin cells

Chromaffin cells are exposed to acetylcholine released by the splanchnic nerve and possess high nAChR density. Due to their properties, these cells have been widely used for pharmacological and physiological studies aiming at characterizing nAChRs (Giniatullin et al., 1999; Khiroug et al., 1998; Khiroug et al., 1997). However since the subunit composition of nAChRs natively expressed in these cells was unknown, our first goal was to characterize the multiple subtypes of heteromeric nAChRs. Bovine chromaffin cells are reported to express both

homomeric α7 receptors and heteromeric α3β4 (probably together with a α5) receptors (Campos-Caro et al., 1997), in this study we demonstrated that in rat chromaffin cells the α7 receptor is not expressed, while the multiple classes of heteromeric receptors are possible.

RT-PCR analysis of mRNA expression in cultured chromaffin cells indicated the presence of nearly every known nAChR subunit (α2, α3, α4, α5, α7,β2, β4). Only the transcripts for α6 and β6 subunits were never detected.

To detect the protein expression immunofluorescence staining of nAChRs subunits and western blot detection of protein bands were performed immunofluorescence staining and immunoblotting analysis with the available antibodies.

Western blots of adrenal glands tissue extracts demonstrated the presence of protein bands recognized by the rabbit anti-α3 and the anti-β2 antibodies. In these extracts, the antibodies recognized a protein band of the molecular mass expected for the α3 subunit, and also a band the molecular mass expected for β2. All goat polyclonal antibodies did not work properly in western blot experiments.

Immunofluorescence staining of cultured chromaffin cells revealed that the α7 protein was not expressed and this was confirmed also pharmacologically: the selective blocker α-bungarotoxin did not change nicotine evoked currents and did not competed in binding assays. Also MLA failed to block nicotine induced current when used ad submicromolar concentrations.

The presence of a large amount of α3 was revealed by immunofluorescence staining of this protein. α3 is known to coassembly both with β2 and β4 (for review see Gotti et al., 1997), the β2 antibody stained most of the cells indicating the presence of this subunit, unfortunately at this time the anti-β4 antibody is still unavailable. A combined pharmacological and immunocytochemical approach was then chosen to detect and characterize the nAChRs functionally

expressed on our cells. The block exerted by the two α- conotoxins MII and AuIB when used at nanomolar concentrations demonstrated that the two subunit combination α3β4 and α3β2 were plausible. However, the very limited availability of these toxins prevented experiments with their combined application to characterize the residual nicotinic receptor mediated response.

It should be noted that other nAChR subunits are likely to be included in each of the receptor categorizations above. α5, α2 and α4 subunits mRNA and protein were also detected in these cells by our RT-PCR analysis and immunofluorescence staining. α5 has been shown to co-assemble with other nAChRs to create more diverse receptor profiles. For example, α5 in addition to α3β4 or α3β2 receptors expressed in *Xenopus* oocytes enhances receptor desensitization (Groot-Kormelink et al., 2001; Gerzanich et al., 1998)and increases Ca2+ permeability (Gerzanich et al., 1998). α4 and β2 subunits are largely colocalized in the CNS (Le Novere et al., 1996).

On the basis of these considerations and the current results it is possible to suggest the following potential combination of receptor subunits: α3β4, α3α5β4, α3β2 and α4β2. These data are only the minimum number of receptor subunit assemblies and does not intend to be exclusive of other subunit combinations which will have to be examined in future studies.

It is however noteworthy that rat chromaffin cells did not express functional α7 receptors.

Antagonism of nAChRs mediated current by F3

While searching for new compounds active on nAChRs, we started from F3 compound; F3 is one oxystilbene derivatives (synthesized by the group of F.Clementi and C. Gotti) that have been shown to bind to the chick αBgtx sensitive nAChRs (Gotti et al., 1998).

Oxystilbene derivatives have been originally developed as a ganglioplegic drug and found to produce potent ganglion blocking activity measured as strong hypotension (Cavallini et al., 1953; Mantegazza and Tommasini, 1955). Rat chromaffin cells that form the inner part of the adrenal gland seemed a suitable model to test the activity of F3 onto the nicotinic receptor subclass expressed in the autonomic nervous system.

The finding of this study is that the oxystilbene derivative F3 acted as an apparently competitive antagonist on native nAChRs of rat chromaffin cells. This action was manifested as a rapid onset and agonist surmountable block of inward currents evoked by pulse application of nicotine.

Characteristics of the fast action of F3 on nicotine induced currents

When F3 was rapidly superfused onto a single chromaffin cell for up to 15 s before nicotine application, it evoked no change in baseline current (indicating lack of partial agonist activity or of non-selective effects on membrane permeability) but it strongly depressed inward currents induced by nicotine. The extent of this block did not intensify during continuous application of F3 and was readily reversible on washout.

The electrophysiological protocol which relied on pulse applications of nicotine was used to minimize rapid-onset receptor desensitization (developing with a time constant of about 100 ms; see Khiroug et al., 1997, 1998). Nevertheless, the use of non-equilibrium responses to nicotine and the puffer application protocol precluded obtaining strictly quantitative pharmacological data to analyze in detail the nature of the F3 antagonism. Even with these constraints it was apparent that F3 preferentially blocked small (and short) responses to nicotine and that increasing the amount of nicotine delivered to the cell counteracted the inhibitory effect of F3. In fact, the graph plotting the fractional response amplitude *vs* the amount of nicotine delivered by pressure pulse showed

a rightward shift in the presence of F3. This observation is consistent with an apparently competitive antagonism of F3 on nicotinic receptors. Another possibility is that F3 acted as a channel blocker (Neher and Steinbach, 1978) on nAChRs of chromaffin cells in analogy with the results obtained with other cholinergic antagonists like for example mecamylamine (Nooney et al., 1992). Two observations clearly stand against this interpretation, namely the absence of any use dependence of the block and its voltage independence through a wide range of membrane potentials.

Although the present experimental conditions did not allow performing Schild analysis, it is worth noting that this method remains an extremely valuable approach to give important information on the nature of antagonism. Furthemore, the Schild plot is a powerful tool for the classification of drugs because it indicates whether or not a drug is a simple competitive antagonist when measured at equilibrium. However, since the present experiments relied on brief pressure pulses of agonist, these non equilibrium conditions were unsuitable for Schild analysis. Future experiments with different agonist delivery protocols will have to be performed in order to use Schild regression analysis.

It is worth noting that also the present experiments could not detect any nAChR activity with pharmacological properties typical of α7 receptors since αBgtx was inactive in electrophysiological and binding tests. Even if the bovine α7 receptors may display rapid desensitization capable of making them insensitive over a period of nearly one s (Lopez et al., 1998), as described before all our electrophysiological tests based on very short pulse application of nicotine (10 to 50 ms) should have been able to demonstrate their functional presence. We therefore suggest that on rat chromaffin cells any homomeric α7 receptors present were not functional and their density was below threshold for detection with binding and immunodetection methods.

Stereo-selectivity of the antagonism

When the two optical isomers were tested on nicotine evoked responses, the *R* form resulted as the most potent one. The antagonism profile by *R*-F3 was the same as the one found with the racemic compound. In fact, we observed apparently competitive antagonism, no voltage dependence of the block and similar time course of action. The fact that we observed stereo-selectivity in the action of F3 suggests that ganglion-type nAChRs preferentially recognize one stereo-isomer of the antagonist. Steroeselectivity has also been shown for the antagonist methyl-epibatidine on recombinant α3β4 receptors (Bertrand et al., 1999), which are one of the subtype expressed by chromaffin cells (Garcia-Guzman et al., 1995). In the present experiments the difference in stereoselectivity potency was approximately five-fold.

Epibatidine and nicotine are similarly antagonized

When epibatidine was applied to chromaffin cells, it generated inward currents of different shape (slower onset and offset) from those observed with nicotine. The most glaring difference between epibatidine and nicotine induced currents was the slow off-rate of the epibatidine one. Epibatidine behaved as an extremely potent agonist on native nAChRs expressed in chromaffin cells. Nevertheless, pipette doses of epibatidine higher than 1 μM elicited inward currents smaller than those evoked by 100 nM (see also Gerzanich et al., 1995; Zhang et al., 1999) presumably because these receptors are prone to desensitization (Khiroug et al., 1998; Khiroug et al., 1997) and epibatidine is very effective in promoting desensitization (Zhang et al., 1999). When epibatidine was 1,000 fold less concentrated than nicotine, the peaks of the current evoked by either agonist were virtually the same, so the number of activated nAChRs was presumably equivalent. In this case the extent of the block exerted by of *R*-F3 was the same indicating that the antagonism by F3 was not peculiar

to the action of nicotine but it was equipotently exerted also against another nicotinic agonist.

Binding of F3 to adrenal receptors

Binding studies of adrenal gland homogenates demonstrated the presence of a single class of ^{125}I -epibatidine high affinity receptors. The K_d value for ^{125}I-epibatidine binding to this receptor subtype is in the range of those previously reported for the α3β4 subtype expressed in oocytes (Parker et al., 1998) or in a transfected cell line (Xiao et al., 1998). In agreement with the data already reported by (Davila-Garcia et al., 1997), we found that the number of adrenal nAChRs was quite low, whereas rat SCG membranes, taken as control, expressed approximately 30-40 times more receptor sites per mg of protein.

To further characterize the nAChRs expressed by adrenal tissue, binding studies were also carried out with agonists such as ACh or cytisine (K_i=348 or 68 nM, respectively) which displayed receptor affinity close to the ones (K_i=560 or 56 nM, respectively) previously observed for binding to oocytes expressing the rat α3β4 subtype (Parker et al., 1998). Nevertheless, the present experiments indicated that the K_i value for the antagonist F3 was much larger than the IC_{50} value obtained with patch clamp recording. It is interesting that, when the activity of the agonist was considered, a mirror-like situation emerged whereby the agonist affinity in binding experiments was much higher (pM range) than in electrophysiological experiments which, although not strictly quantitative, used nM doses to elicit responses.

The fact that the "apparent affinity" of the agonist in the binding assay was much higher than the functional EC_{50} value can be explained by the fact that nAChRs coexist in a minimum of three interconvertible states. Among these states the desensitized one (receptors refractory to activation) has high affinity for the agonist (reviewed in Galzi and

Changeux, 1995). Since binding assay values were obtained under equilibrium conditions, that required long incubation, it seem likely that receptors were in the desensitised high affinity state preferential for agonist binding.

Species-specificity of the F3 action

It has previously demonstrated that, in the chick, oxystilbene derivatives are selective antagonists for the α7 receptor subtype and possess a low activity against brain-type nAChRs (Gotti et al., 1998; Maggi et al., 1999). Conversely, in the present study we showed that F3 had strong antagonist activity (with high affinity) for ganglion-type nAChRs of rat chromaffin cells which lacked α7 receptors. It has been also shown that F3 display nM affinity and antagonist activity against human and rat α7 receptors expressed in Xenopus oocytes (C. Gotti and R. Zwart, unpublished). Thus, we can conclude that in mammals oxystilbene derivatives are very active but do not retain subtype selectivity.

Since the precise identification of the agonist/antagonist binding sites on nAChRs is not yet available, any hypothesis on the identity of the aminoacids responsible for conferring species-specificity is currently unwarranted. Nonetheless, the present results suggest that caution is required in assuming that pharmacological data obtained from receptors in one animal species can be applied to similar receptors in another species, especially when dealing with drugs potentially targeted for future clinical development.

Block by mecamylamine of nAChRs.

Mecamylamine is a secondary amine acting as an antagonist on nAChRs (Ascher et al., 1979; Fieber and Adams, 1991; Nooney et al., 1992). The blocking action of mecamylamine is exerted on all native subtypes of

nAChRs despite their different subunit composition (Connolly et al., 1992).

On autonomic nAChRs the action of mecamylamine can be either competitive (Ascher et al., 1979; Gurney and Rang, 1984) or non-competitive (Fieber and Adams, 1991; Nooney et al., 1992), a difference which perhaps due to different subunit composition of these receptors. In fact, even within the same tissue, namely the superior cervical ganglion, mecamylamine can produce distinct types of receptor block depending on the cells examined (Shen and Horn, 1998).

We demonstrated that on rat chromaffin cells the blocking action of mecamylamine is relatively slow in onset (compare it with DHβE, or with F3; Giniatullin et al., 1999), potent (IC_{50}=0.34 μM), and persistent on washout. Such a block could be rapidly relieved by combining a large membrane depolarization with nicotine application, suggesting that mecamylamine was trapped inside nAChRs from which it could be subsequently released upon channel re-opening. Activation of nAChRs in the presence of mecamylamine was therefore possible as long as there was coincidence of agonist binding with strong membrane depolarization.

The reduction in current decay during mecamylamine block is similar to that found on recombinant $\alpha_3\beta_4$ receptors (Zhang et al., 1999). The use and voltage dependence of mecamylamine block accords with the notion that this substance antagonizes nAChRs of chromaffin cells non competitively (Xiao et al., 1998) as confirmed by single channel recordings of recombinant $\alpha_3\beta_4$ receptors (Nelson and Lindstrom, 1999) which are the one of the receptor subclasses natively present on chromaffin cells (Campos-Caro et al., 1997). These characteristics, however, indicate that the effect of mecamylamine can be classified as "un-competitive" antagonism. This type of receptor block, which has recently been investigated in relation to glutamate receptors (Blanpied et al., 1997; Chen and Lipton, 1997), implies that the blocker can only acts

once the receptor has been activated (for a recent review see Dingledine et al., 1999).

Mechanism of mecamylamine action.

Mecamylamine has a pK_a value of 11.2 which means that at pH 7.4 more than 99% of this compound will be ionized (Goldstein et al., 1979), making possible its interaction with the strong negative charges inside the nicotinic channel (Pascual and Karlin, 1998). This property suggests that, at negative membrane potentials, mecamylamine can deeply penetrate into open nAChRs as indicated by our calculations based on the Woodhull's (Woodhull, 1973) method.

The ability of membrane depolarization to reverse the mecamylamine block was a striking property of the action of this antagonist. Intracellular processes played little, if any, role in this rapid recovery. Thus, potential involvement of Ca^{2+}-dependent second messengers due to depolarization-evoked Ca^{2+} influx was made unlikely by the fact that cells had been dialyzed with a solution containing the fast Ca^{2+} chelator BAPTA. In addition, simple depolarization (which should have opened voltage dependent Ca^{2+} channels) without activation of nAChRs was ineffective on mecamylamine block. The special voltage dependence of the mecamylamine block and unblock should therefore be sought to reside in some intrinsic characteristics of nAChR operation.

In this sense we might envisage at least two distinct mechanisms underlying un-competitive antagonism: i) mecamylamine bound to (and came off from) a site deep inside the channel with strong voltage dependence which was also manifested as depolarization-dependent block relief (similar to positively charged channel blockers; (Adams and Feltz, 1980; Chen and Lipton, 1997); ii) mecamylamine entered open nAChR channels in which it remained trapped after receptor closure; in this case voltage dependence resided in the processes which control opening and closure of mecamylamine-bound channels, and agonist

sensitivity. The present experimental data based on whole cell currents could not resolve which steps were voltage dependent. However, even single channel recordings may not help to separate a voltage dependent, open channel block from a voltage dependent, trapping mechanism particularly if the latter is manifested as non-specific decrease in macroscopic charge transfer or reduction in opening frequency (Neher, 1983; Nelson and Lindstrom, 1999). Indeed, using mecamylamine at relatively high (5-50 μM) concentrations on recombinant nAChRs of excised patches, Nelson and Lindstrom (Nelson and Lindstrom, 1999) observed that the persistent, strong reduction in channel open frequency (which might be related to trapping mechanisms) precluded estimation of the channel closed state.

How general is the phenomenon of block relief?

A trapping block mechanism has first been proposed for tetraethylammonium acting on potassium channels (Armstrong, 1971). The first suggestion of an analogous process for cholinergic receptors originated from a report on lobster muscle receptors activated by slowly applied cholinergic agonists (Lingle, 1983). On submandibular ganglia Gurney and Rang (1984) observed substantial relief of the hexametonium block but not of the mecamylamine one. On bovine chromaffin cell nAChRs (Nooney et al., 1992) briefly reported mecamylamine block relief by depolarization plus ACh application without further quantitative data. In our study the characteristics of block analogous to that by mecamylamine were not found with the competitive antagonists DHβE (Xiao et al., 1998) or F3 (Giniatullin et al., 1999). Tubocurarine, a voltage-dependent blocker of submandibular ganglion nAChRs (Ascher et al., 1979), also did not demonstrate sensitivity to voltage steps combined with nicotine application. Weak block relief was observed in the case of proadifen, an agent which facilitates receptor desensitization (SKF-525A; Giniatullin et al., 1999). In

general, one may conclude that the rapid reversal of the action of mecamylamine on chromaffin cells remains an outstanding, although not unique, case. This agent could thus be a tool to identify the molecular structure inside the nAChR channel so sensitive to trapping block.

Functional implications.

One interesting aspect was the requirement for the coincidence of two factors to achieve rapid block relief. One was a selective signal, namely activation of nAChRs, while the other was non-specific cell depolarization. This situation is reminiscent of the Mg^{2+} block (and relief) of NMDA receptors by combining membrane depolarization with glutamate application (reviewed by Dingledine et al., 1999). In the case of chromaffin cells (and perhaps even of brain nicotinic receptors sensitive to mecamylamine which can cross the blood brain barrier) this antagonist might generate a system detecting the coincidence of pre- and postsynaptic activity, *i.e.* an Hebbian synapse. In other words, application of a drug like mecamylamine might simply unveil a phenomenon generated in standard conditions by endogenous substances acting together with ACh. Physiological compounds which might possess a mecamylamine like-action are 5-hydroxytryptamine (Grassi, 1999), or substance P (Clapham and Neher, 1984; Boyd and Leeman, 1987), that depress nAChR function by voltage-dependent but incompletely understood mechanisms. Depolarization of the postsynaptic membrane necessary for block relief might be achieved via a distinct synaptic input, which together with endogenous ACh, might quickly restore cholinergic transmission. ATP (Ralevic and Burnstock, 1998) is one potential candidate for such interplay with blocked nAChRs.

Modulation of native nAChRs by the endogenous neuropeptide CGRP and its N-terminal fragments

Several neuropeptides can act as neurotransmitters per se as well as neuromodulators of receptors for other transmitters (Hokfelt, 1991; Otsuka and Yoshioka, 1993). An important insight into the phenomenon of peptide-induced receptor modulation has been provided by studies on muscle type nicotinic acetylcholine receptors (nAChR). In particular, the endogenously occurring calcitonin gene-related peptide (CGRP) facilitates nAChR desensitization by phosphorylating certain receptor subunits (Mulle et al., 1988; Miles et al., 1989; but see Lu et al., 1993) and increases AChR biosynthesis (Changeux et al., 1992). While CGRP modulates muscle type nicotinic acetylcholine receptors (nAChRs) via intracellular second messenger mediated phosphorylation, the action of this peptide on neuronal type nAChRs remains unknown.

We then studied CGRP modulation of neuronal nAChRs on rat chromaffin cells. CGRP modulation of nAChRs was manifested as a rapid onset and agonist-surmountable block of inward currents (and associated $[Ca^{2+}]_i$ transients) evoked by pulse applications of nicotine. Such a phenomenon was distinct from the slow rise in $[Ca^{2+}]_i$ induced by CGRP via its G-protein coupled receptors in view of its sensitivity to $hCGRP_{8-37}$ antagonism or intracellular BAPTA. Because of the endogenous occurrence of CGRP in the adrenals (Kuramoto et al., 1987); (Costa et al., 1994); (Heym et al., 1995), such a quick and reversible down regulation of nicotinic receptors suggests that CGRP may play an important modulatory role in fast signalling of these cells, before any Ca^{2+} dependent modulation of nAChRs could develop.

Characteristics of the fast action of CGRP on nicotine-mediated responses

When CGRP was focally applied to a chromaffin cell for up to 15 s prior to nicotine application it evoked no change in baseline current but strongly depressed the inward currents and $[Ca^{2+}]_i$ rises induced by nicotine. The extent of the block did not intensify during continuous application of CGRP and was unrelated to $[Ca^{2+}]_i$ buffering by BAPTA. In fact, we often used BAPTA in the recording pipette to eliminate the slow $[Ca^{2+}]_i$ rise elicited by CGRP so as to avoid a possible contamination of the early CGRP action. The similarity of blocking action with puffer or bath applied CGRP excluded the possibility of drug delivery artefact or large underestimation of the peptide potency. When CGRP and nicotine were co-applied from the same pipette the ensuing current response was decreased even if the application time was only 20 ms long. This finding shows that CGPR could act on a very rapid time-scale, as fast in fact as nicotine itself, raising the possibility that CGRP interacted directly with the nicotinic receptors. This effect of CGRP did not extend to the ionotropic receptors opened by GABA nor was it mimicked by other neuropeptides such as dynorphin A (which modulates NMDA receptors of central neurons; (Bauer et al., 1997), (Zhang et al., 1997) or TRH. These observations concur to assign specificity to the blocking action of CGRP on nAChRs. The recent description of a discrete, direct blocking action by substance P against certain subunits of nAChRs suggests that a similar phenomenon is not a peculiarity of CGRP action (Stafford et al., 1994).

One obvious possibility is that CGRP blocked receptor channels opened by nicotine in analogy with the results obtained with other substances like local anaesthetics (Neher and Steinbach, 1978) especially as this process has been shown to occur with substance P (Clapham and Neher, 1984). This mechanism seems however unlikely under the present conditions because the block was not use-dependent either during

continuous application of CGRP or with the paired pulse protocol. Furthermore, there was no voltage dependence of the block which appeared to be uniform throughout a wide range of membrane potential.

The use of non-equilibrium responses to nicotine and the puffer application protocol precluded strictly quantitative pharmacological data to analyze in detail the nature of the CGRP antagonism. Even with these constraints it was apparent that CGRP preferentially blocked small (and short) responses to nicotine and that increasing the amount of nicotine delivered to the cell counteracted the inhibitory effect of CGRP. In fact, the graph plotting the fractional response amplitude versus the amount of nicotine delivered by pressure pulse showed a rightward shift in the presence of CGRP. This observation is consistent with an apparently competitive antagonism of CGRP on nicotinic receptors especially because the competitive antagonist F3 elicited a very similar type of antagonism. Coapplication of rather low doses of CGRP and F3 produced antagonism summation. When the extent of the rightward shift of the nicotine plot was analyzed in terms of agonist DR values to reproduce equivalent responses, it was apparent that the DR value in the combined presence of CGRP and F3 was the sum of the individual values for each blocker alone. This is regarded as indicative of competitive antagonism on the basis of the standard receptor theory (Barlow 1980) although the present experiments cannot identify the discrete receptor structure to which CGRP would bind to exert its effect.

The residual nicotine currents (left despite the wide range of CGRP concentrations tested) might have reflected heterogeneity in nAChR sensitivity to CGRP antagonism. As we demonstrated that nAChRs of rat chromaffin cells comprise various subunit assemblies it seems conceivable that CGRP preferentially blocked some of them only.

Several other processes appeared unable to account for the blocking effect of CGRP. For example, facilitation of desensitization (as proposed

for substance P (Clapham and Neher, 1984; Simmons et al., 1990; Valenta et al., 1993); appeared also improbable because responses induced by large doses of nicotine which are more prone to desensitization (Valenta et al., 1993; Khiroug et al., 1998; Khiroug et al., 1997) were relatively spared by CGRP. Allosteric modulation of nAChRs by binding to a discrete region of the nicotinic receptor distinct from the agonist site would also depress nicotinic responses as amply investigated in the case of substance P (Livett et al., 1979; Stafford et al., 1994): while a similar action by CGRP is not excluded, this should be accompanied by a downward shift of the agonist dose-response curve (Akasu et al., 1983; Stafford et al., 1994), a prediction not borne out by the present findings. A more direct examination of these possibilities will however require future studies based on single channel recording and site-directed mutagenesis of recombinant receptors in expression systems.

Characteristics of the slow action of CGRP

CGRP is known to be present in adrenal tissue (Kuramoto et al., 1987; Costa et al., 1994; Heym et al., 1995) where it binds predominantly to the $CGRP_1$ receptor subclass (Mazzocchi et al., 1996b) preferentially antagonized by the peptide fragment $hCGRP_{8-37}$ (Bell and McDermott, 1996). CGRP receptors are G protein coupled units which trigger slow metabolic reactions typically mediated by a rise in intracellular cAMP and PKA activity (Bell and McDermott, 1996). In keeping with this general property we also observed that CGRP elicited a delayed increment in $[Ca^{2+}]_i$ blocked by $hCGRP_{8-37}$ or the PKA inhibitor Rp-cAMPS. The CGRP-induced slow $[Ca^{2+}]_i$ rise presumably involved release of this divalent cation from internal stores since it persisted in Ca^{2+} free solution whereas the nicotine-induced $[Ca^{2+}]_i$ transients, which are mainly due to transmembrane influx (Mulle et al., 1992; Vernino et al., 1994; Khiroug et al., 1998; Khiroug et al., 1997), were abolished. It is interesting that $hCGRP_{8-37}$ per se had no effect on $[Ca^{2+}]_i$ suggesting that

this substance was not a partial agonist on these cells (Bell and McDermott, 1996).

Structural determinants for the action of CGRP

$hCGRP_{8-37}$ did not affect nicotine-induced currents, yet this compound differs from CGRP for missing only a terminal sequence series of amino acids. This consideration suggests that CGRP actually interacted with nicotinic receptors through the amino acid sequence missing from the antagonist molecule. This possibility was supported by the direct demonstration that $CGRP_{1-7}$ acted like full length CGRP to rapidly block nAChRs with comparable effectiveness. At the same time, even sustained applications of $CGRP_{1-7}$ failed to raise $[Ca^{2+}]_i$ significantly, indicating that one terminal sequence of the peptide was responsible for rapid block of nAChRs while the full length molecule was necessary for the slow $[Ca^{2+}]_i$ increase presumably mediated by metabotropic CGRP receptor activation. This secondary, albeit small, increase in $[Ca^{2+}]_i$ induced by CGRP might be expected to control the phosphorylation state of the nAChRs as it has been shown to occur in the case of CGRP on muscle type nAChRs (Mulle et al., 1988; Miles et al., 1989; Lu et al., 1993) or of substance P on neuronal type nAChRs (for review see Huganir and Greengard, 1990). Thus, on chromaffin cells a slow rise in $[Ca^{2+}]_i$ might have important functional consequences as it regulates the rate of recovery of nAChRs from desensitization by controlling the balance between their phosphorylation/dephosphorylation (Khiroug et al., 1998; Khiroug et al., 1997), or it would directly enable tonic catecholamine release (Rosenfeld et al., 1992). In summary then, on chromaffin cells CGRP may regulate nAChRs via a dual action consisting of fast, direct receptor interaction and a slow, indirect receptor modulation mediated by $[Ca^{2+}]_i$ rise.

A novel and unexpected discovery, that arised when during some experiments we were looking for the minimal structure of the CGRP fragments capable to depress nicotine evoked currents, is that some fragments of the CGRP peptide rapidly and reversibly enhance responses mediated by the activation of native neuronal nicotinic receptors.

This phenomenon was manifested as a rapid onset and agonist-surmountable potentiation of inward currents evoked by pulse applications of nicotine. Such a potentiation of nicotinic receptors suggests $CGRP_{1-6}$ and its derivatives to be prototypes of a new class of molecules capable of enhancing responses mediated by nAChRs.

Characteristics of the action of $CGRP_{1-6}$ on nicotine-mediated responses

When $CGRP_{1-6}$ was superfused onto a chromaffin cell, it evoked no direct change in baseline current or input conductance but it strongly potentiated inward currents induced by nicotine. Potentiation was not use-dependent and was present even with the first response to nicotine in $CGRP_{1-6}$ solution, suggesting that this peptide fragment could have bound nAChRs in the absence of their agonist. The action of $CGRP_{1-6}$ was voltage and agonist independent, as responses to cytisine or nicotine were equally increased at various membrane potentials. Note that the slope value for the facilitating action by $CGRP_{1-6}$ was very close to 1, suggesting that, within the sensitivity limits of the present technique, there was no apparent heterogeneity of nAChR potentiation or uneven distribution of the peptide. When $CGRP_{1-6}$ was tested on I28 cells, it did not modify responses mediated by muscle nicotinic receptors, indicating specificity of action towards nAChRs present on chromaffin cells. Future work will be necessary to explore the sensitivity of other classes of nAChRs present in the central nervous system to this peptide. It is however clear that $CGRP_{1-6}$ was not a non-specific modulator of ionotropic neuronal receptors as $GABA_A$ receptors were

insensitive to it. It is also possible to rule out that the observed enhancing effects of CGRP fragments were due to their interaction with voltage-gated Ca^{2+} or Na^{+} because cells were routinely voltage clamped at -70 mV, a value very far from the voltage threshold for activating those conductances.

Discrete changes in amino acid composition of the N-terminal sequence of CGRP induced different effects on nAChRs.

It was interesting to observe that equimolar concentrations of $CGRP_{1-6}$ and $CGRP_{1-7}$ (Giniatullin et al., 1999), co-applied to the same cell, left nicotine-induced submaximal currents unchanged. This observation suggests that a discrete change in the amino acid sequence, consisting of a single amino acid deletion, could transform an antagonist into a potentiating substance. It seemed thus useful to test if further reduction in the amino acid sequence length might influence the type of effect on nAChRs. This approach should also help to identify the minimal structure for receptor modulation and to outline some structural characteristics of the peptide molecules which could be exploited with molecular dynamics studies to unveil analogies or differences in spatial conformation.

Deleting one amino acid from the COO^{-} end of the $CGRP_{1-6}$ sequence clearly yields a compound ($CGRP_{1-5}$) still endowed with potentiating activity on nAChRs (although with reduced potency). Even the $CGRP_{1-4}$ fragment retained a slight, yet significant potentiation which was lost with $CGRP_{1-3}$. This realization was further examined by analyzing the tri-dimensional structure of these peptides.

Structure/function studies of CGRP fragments.

Inspection of the linear sequence of the CGRP fragments revealed one major difference between $CGRP_{1-7}$ and $CGRP_{1-6}$, namely the presence of a disulfide bridge between Cys_2 and Cys_7 which determined the closed

ring structure of $CGRP_{1-7}$. The presence of the disulfide bridge was probably responsible for producing the depressant effect because the shorter fragment $CGRP_{2-7}$ (retaining Cys_2 and Cys_7) induced antagonism of nicotine responses.

$CGRP_{1-6}$, which was obtained by deleting Cys_7, was a more flexible molecule with more freedom to assume various spatial conformations. This realization prompted us to implement the synthesis of a seven amino acid peptide analogous to $CGRP_{1-7}$ except that the terminal Cys_7 was replaced by Ala and was thus devoid of the disulfide bridge. This new compound, termed $CGRP_{1-7A}$, was observed to behave like its shorter length counterpart $CGRP_{1-6}$ in potentiating nAChRs although with somewhat reduced potency.

Insights into the mechanism of action of $CGRP_{1-6}$.

While these data suggested some properties that may account for the receptor modulating activity of these peptides, the precise mechanisms responsible for these effects remain unclear. This is partly due to methodological considerations as the use of non-equilibrium responses to nicotine and the puffer application protocol (to minimize receptor desensitization) precluded strictly quantitative pharmacological data to analyze in detail the nature of the $CGRP_{1-6}$ potentiating action. Recent work has, however, indicated that the amount of agonist delivered by 10-50 ms puffer application closely corresponds to superfusing 20-100 μM nicotine (Di Angelantonio, 2001), thus providing a relatively narrow range of agonist concentrations eliciting responses sensitive to $CGRP_{1-6}$.

Even with the interpretation constraints imposed by using non-equilibrium responses to brief pulses of nicotine, it was apparent that $CGRP_{1-6}$ preferentially potentiated small over large responses to nicotine. In fact, the graph plotting the fractional response amplitude versus the amount of nicotine showed a leftward shift (with unchanged maximum response) in the presence of $CGRP_{1-6}$. Thus, this peptide

increased the sensitivity of nAChRs to their agonist nicotine without changing the agonist efficacy on them.

On muscle-type nicotinic receptors two ligand binding sites, formed at α-γ and α-δ interfaces, differ in their affinities for agonists and competitive antagonists Sine et al., 1995. On nAChRs distinct binding sites can bind certain neurotoxins which, nevertheless, share a similar mechanism of competitive antagonism (Harvey et al., 1997). It is currently unknown if, on nAChRs, different agonists can bind to discrete sites of the receptor and activate it. It might be possible that $CGRP_{1-6}$ operated by binding to one of these sites and thus facilitated the action of the agonist nicotine. This hypothetical mode of action should however be considered in the light of inactivity of $CGRP_{1-6}$ alone on native nAChRs, indicating that the CGRP1-6 sensitive site could not activate nicotinic channels in the absence of nicotine (or cytisine). This possibility will therefore require future experiments based on recombinant receptors with identified subunit binding sites.

Another possibility is that $CGRP_{1-6}$ might have acted as an APL on nAChRs (Changeux and Edelstein, 1998). When used at submicromolar concentration APLs facilitate nicotine induced responses even if generated by desensitized receptors, while a ten times higher dose depresses nAChR mediated responses (Maelicke et al., 1997; Maelicke and Albuquerque, 2000). This property was confirmed in the present study with physostigmine which enhanced nicotine currents at 0.5 μM and depressed them at 5 μM concentration. Note also that, for either potentiation or depression, the maximum of the nicotine dose-response curve was significantly changed, unlike the observations with CGRP derivatives which could not increase the maximum responses and, therefore, could not reverse receptor desensitization associated with large membrane currents. Co-application of enhancing concentrations of physostigmine and $CGRP_{1-6}$ led to linear summation of the individual effects while $CGRP_{1-6}$ could partly reverse the depression by a large

concentration of physostigmine. All together, these data indicate pharmacologically different effects by $CGRP_{1-6}$ and physostigmine on nicotine-induced currents and suggest functionally distinct sites of action for $CGRP_{1-6}$ and physostigmine.

CONCLUSIONS

The main conclusions of the present study are as follows:

1.Rat chromaffin cells express nAChRs comprising at least the following combinations of subunits: α3β4, α3α5β4, α3β2 and α4β2.

2. The oxystilbene derivative F3 can be used as a powerful and reversible blocker of such nAChRs with an apparent competitive mode of antagonism.

3. Functional α7 receptors could not be detected on rat chromaffin cells.

4. Mecamylamine was a potent blocker apparently trapped by channels opened by nicotine. Block relief could be readily obtained by combining membrane depolarization with agonist application.

5. CGRP produced two kinds of modulation of nAChRs a slow downregulation due to delayed rise in intracellular calcium plus a very fast block due to a direst interaction with the nAChRs.

6. N-terminal fragments of CGRP like CGRP1-7 retained rapid blocking activity, while the CGRP1-6, 1-5 and 1-4 fragments produced rapid enhancement of nAChR function.

7. The ability to increase responses by nAChRs was due to removal of the disulphide bridge linking Cys2 and 7 in these peptide structures.

8. Short fragments of CGRP can be prototypes of a novel class of drugs which can facilitate nAChRs function, a properties which deserves further investigations using nAChRs of brain neurons.

ACKNOWLEDGMENTS

First I wish to express my gratitude to Professor Andrea Nistri for his careful and stimulating supervision, invaluable help in filling my gap in neurobiology, and human support during my PhD program.
I also wish to thank Drs Cristina Marchetti, Elena Sokolova and Cosetta Matteoni with whom I shared set-up and some experiments, and Prof. Rashid Giniatullin for helpful discussions about some of the experiments presented in this thesis.
Many thanks to Dr. Massimo Righi for his help in cell preparation and his patience in teaching immunocytochemistry. Tanks to Dr. Luigi Corvetti and Dr. Elisa Margotti for helpful discussion about the importance of negative controls in immunocytochemical experiments and for their help in learning the western blot technique.
I wish to thank all friends which have been sharing with me these years in Trieste; they contributed to make this experience a special one.
Finally, my love goes to Giovanni and Andrea (the small one) for these joyful years spent together.

Reference List

Adams DJ, Nutter TJ (1992) Calcium permeability and modulation of nicotinic acetylcholine receptor-channels in rat parasympathetic neurons. J Physiol Paris 86: 67-76.

Akasu T, Kojima M, Koketsu K (1983) Substance P modulates the sensitivity of the nicotinic receptor in amphibian cholinergic transmission. Br J Pharmacol 80: 123-131.

Albuquerque EX, Alkondon M, Pereira EF, Castro NG, Schrattenholz A, Barbosa CT, Bonfante-Cabarcas R, Aracava Y, Eisenberg HM, Maelicke A (1997) Properties of neuronal nicotinic acetylcholine receptors: pharmacological characterization and modulation of synaptic function. J Pharmacol Exp Ther 280: 1117-1136.

Ali DW, Catarsi S, Drapeau P (1998) Ionotropic and metabotropic activation of a neuronal chloride channel by serotonin and dopamine in the leech Hirudo medicinalis. J Physiol 509: 211-219.

Alkondon M, Pereira EF, Albuquerque EX (1998) alpha-bungarotoxin- and methyllycaconitine-sensitive nicotinic receptors mediate fast synaptic transmission in interneurons of rat hippocampal slices. Brain Res 810: 257-263.

Alkondon M, Pereira EF, Barbosa CT, Albuquerque EX (1997b) Neuronal nicotinic acetylcholine receptor activation modulates gamma-aminobutyric acid release from CA1 neurons of rat hippocampal slices. J Pharmacol Exp Ther 283: 1396-1411.

Alkondon M, Pereira EF, Cortes WS, Maelicke A, Albuquerque EX (1997a) Choline is a selective agonist of alpha7 nicotinic acetylcholine receptors in the rat brain neurons. Eur J Neurosci 9: 2734-2742.

Alkondon M, Pereira EF, Eisenberg HM, Albuquerque EX (1999) Choline and selective antagonists identify two subtypes of nicotinic acetylcholine receptors that modulate GABA release from CA1 interneurons in rat hippocampal slices. J Neurosci 19: 2693-2705.

Amador M, Dani JA (1995) Mechanism for modulation of nicotinic acetylcholine receptors that can influence synaptic transmission. J Neurosci 15: 4525-4532.

Amberla K, Nordberg A, Viitanen M, Winblad B (1993) Long-term treatment with tacrine (THA) in Alzheimer's disease--evaluation of neuropsychological data. Acta Neurol Scand Suppl 149:55-7.: 55-57.

Anderson DJ (1993) Cell fate determination in the peripheral nervous system: the sympathoadrenal progenitor. J Neurobiol 24: 185-198.

Aramakis VB, Metherate R (1998) Nicotine selectively enhances NMDA receptor-mediated synaptic transmission during postnatal development in sensory neocortex. J Neurosci 18: 8485-8495.

Ascher P, Large WA, Rang HP (1979) Studies on the mechanism of action of acetylcholine antagonists on rat parasympathetic ganglion cells. J Physiol 295:139-70.: 139-170.

Balestra B, Vailati S, Moretti M, Hanke W, Clementi F, Gotti C (2000) Chick optic lobe contains a developmentally regulated alpha2alpha5beta2 nicotinic receptor subtype. Molecular Pharmacology 58: 300-311.

Barlow RB (1980) Quantitative aspects of chemical pharmacology. University Park Press, Baltimore, Maryland.

Bartus RT, Dean RL, III, Beer B, Lippa AS (1982) The cholinergic hypothesis of geriatric memory dysfunction. Science 217: 408-414.

Bauer SH, Zhang XY, Liang F, De Potter WP, Claeys M, Przybylski M (1997) Isolation and identification of intact chromogranin A and two N-terminal processing products, vasostatin I and II, from bovine adrenal medulla chromaffin granules by chromatographic and mass spectrometric methods. Neuropeptides 31: 273-280.

Bell D, McDermott BJ (1996) Calcitonin gene-related peptide in the cardiovascular system: characterization of receptor populations and their (patho)physiological significance. Pharmacol Rev 48: 253-288.

Benowitz NL, Jacob P, III, Yu L (1989) Daily use of smokeless tobacco: systemic effects. Ann Intern Med 111: 112-116.

Benwell ME, Balfour DJ, Birrell CE (1995) Desensitization of the nicotine-induced mesolimbic dopamine responses during constant infusion with nicotine. Br J Pharmacol 114: 454-460.

Bertrand S, Patt JT, Spang JE, Westera G, Schubiger PA, Bertrand D (1999) Neuronal nAChR stereoselectivity to non-natural epibatidine derivatives. FEBS Lett 450: 273-279.

Bertrand S, Weiland S, Berkovic SF, Steinlein OK, Bertrand D (1998) Properties of neuronal nicotinic acetylcholine receptor mutants from humans suffering from autosomal dominant nocturnal frontal lobe epilepsy. Br J Pharmacol 125: 751-760.

Bianchi MT, Macdonald RL (2001) Agonist Trapping by GABAA Receptor Channels. J Neurosci 21: 9083-9091.

Blanpied TA, Boeckman FA, Aizenman E, Johnson JW (1997) Trapping channel block of NMDA-activated responses by amantadine and memantine. J Neurophysiol 77: 309-323.

Boyd ND, Leeman SE (1987) Multiple actions of substance P that regulate the functional properties of acetylcholine receptors of clonal rat PC12 cells. J Physiol 389:69-97.: 69-97.

Broide RS, Leslie FM (1999) The alpha7 nicotinic acetylcholine receptor in neuronal plasticity. Mol Neurobiol 20: 1-16.

Buisson B, Bertrand D (1998) Open-channel blockers at the human alpha4beta2 neuronal nicotinic acetylcholine receptor. Mol Pharmacol 53: 555-563.

Campos-Caro A, Smillie FI, Dominguez dT, Rovira JC, Vicente-Agullo F, Chapuli J, Juiz JM, Sala S, Sala F, Ballesta JJ, Criado M (1997) Neuronal nicotinic acetylcholine receptors on bovine chromaffin cells: cloning, expression, and genomic organization of receptor subunits. J Neurochem 68: 488-497.

Cartier GE, Yoshikami D, Gray WR, Luo S, Olivera BM, McIntosh JM (1996) A new alpha-conotoxin which targets alpha3beta2 nicotinic acetylcholine receptors. J Biol Chem 271: 7522-7528.

Castro NG, Albuquerque EX (1995) alpha-Bungarotoxin-sensitive hippocampal nicotinic receptor channel has a high calcium permeability. Biophys J 68: 516-524.

Caulfield MP (1993) Muscarinic receptors--characterization, coupling and function. Pharmacol Ther 58: 319-379.

Cavallini G, Mantegazza P, Massarini E, Tommasini R (1953) Sull'attivita' ganglioplegica di alcuni derivati alchilaminici dello stilbene e del difenile. Il Farmaco 6, 317-331.

Changeux JP (1990) The TiPS lecture. The nicotinic acetylcholine receptor: an allosteric protein prototype of ligand-gated ion channels. Trends Pharmacol Sci 11: 485-492.

Changeux JP, Duclert A, Sekine S (1992) Calcitonin gene-related peptides and neuromuscular interactions. Ann N Y Acad Sci 657:361-78.: 361-378.

Changeux JP, Edelstein SJ (1998) Allosteric receptors after 30 years. Neuron 21: 959-980.

Changeux JP, Rubin MM (1968) Allosteric interactions in aspartate transcarbamylase. 3. Interpretation of experimental data in terms of the model of Monod, Wyman, and Changeux. Biochemistry 7: 553-561.

Chen HS, Lipton SA (1997) Mechanism of memantine block of NMDA-activated channels in rat retinal ganglion cells: uncompetitive antagonism. J Physiol 499: 27-46.

Clapham DE, Neher E (1984) Substance P reduces acetylcholine-induced currents in isolated bovine chromaffin cells. J Physiol 347:255-77.: 255-277.

Clementi F, Adlkofer F (2000) Special issue "nicotinic neuronal receptors". Eur J Pharmacol 393: 1.

Colquhoun D, Sakmann B (1985) Fast events in single-channel currents activated by acetylcholine and its analogues at the frog muscle end-plate. J Physiol 369:501-57.: 501-557.

Colquhoun D, Sakmann B (1998) From muscle endplate to brain synapses: a short history of synapses and agonist-activated ion channels. Neuron 20: 381-387.

Connolly J, Boulter J, Heinemann SF (1992) Alpha 4-2 beta 2 and other nicotinic acetylcholine receptor subtypes as targets of psychoactive and addictive drugs. Br J Pharmacol 105: 657-666.

Costa JJ, Averill S, Ching YP, Priestley JV (1994) Immunocytochemical localization of a growth-associated protein (GAP-43) in rat adrenal gland. Cell Tissue Res 275: 555-566.

Couturier S, Bertrand D, Matter JM, Hernandez MC, Bertrand S, Millar N, Valera S, Barkas T, Ballivet M (1990) A neuronal nicotinic acetylcholine receptor subunit (alpha 7) is developmentally regulated and forms a homo-oligomeric channel blocked by alpha-BTX. Neuron 5: 847-856.

Covernton PJ, Kojima H, Sivilotti LG, Gibb AJ, Colquhoun D (1994) Comparison of neuronal nicotinic receptors in rat sympathetic neurones with subunit pairs expressed in Xenopus oocytes. J Physiol 481: 27-34.

Coyle JT, Price DL, DeLong MR (1983) Alzheimer's disease: a disorder of cortical cholinergic innervation. Science 219: 1184-1190.

Criado M, Alamo L, Navarro A (1992) Primary structure of an agonist binding subunit of the nicotinic acetylcholine receptor from bovine adrenal chromaffin cells. Neurochem Res 17: 281-287.

Dani JA (2001a) Overview of nicotinic receptors and their roles in the central nervous system. Biol Psychiatry 49: 166-174.

Dani JA (2001b) Overview of nicotinic receptors and their roles in the central nervous system. [Review] [95 refs]. Biological Psychiatry 49: 166-174.

Dani JA, Heinemann S (1996) Molecular and cellular aspects of nicotine abuse. Neuron 16: 905-908.

Dani JA, Mayer ML (1995) Structure and function of glutamate and nicotinic acetylcholine receptors. Curr Opin Neurobiol 5: 310-317.

Dani JA, Radcliffe KA, Pidoplichko VI (2000) Variations in desensitization of nicotinic acetylcholine receptors from hippocampus and midbrain dopamine areas. Eur J Pharmacol 393: 31-38.

Davila-Garcia MI, Musachio JL, Perry DC, Xiao Y, Horti A, London ED, Dannals RF, Kellar KJ (1997) [125I]IPH, an epibatidine analog, binds with high affinity to neuronal nicotinic cholinergic receptors. J Pharmacol Exp Ther 282: 445-451.

de Wit RJ, Hekstra D, Jastorff B, Stec WJ, Baraniak J, Van Driel R, Van Haastert PJ (1984) Inhibitory action of certain cyclophosphate derivatives of cAMP on cAMP-dependent protein kinases. Eur J Biochem 142: 255-260.

Decker ER, Dani JA (1990) Calcium permeability of the nicotinic acetylcholine receptor: the single-channel calcium influx is significant. J Neurosci 10: 3413-3420.

Decker MW, Brioni JD, Sullivan JP, Buckley MJ, Radek RJ, Raszkiewicz JL, Kang CH, Kim DJ, Giardina WJ, Wasicak JT, . (1994) (S)-3-methyl-5-(1-methyl-2-pyrrolidinyl)isoxazole (ABT 418): a novel cholinergic ligand with cognition-enhancing and anxiolytic activities: II. In vivo characterization. J Pharmacol Exp Ther 270: 319-328.

Di Angelantonio S, Nistri A, Moretti M, Clementi F, Gotti C (2000) Antagonism of nicotinic receptors of rat chromaffin cells by N,N, N-trimethyl-1-(4-trans-stilbenoxy)-2-propylammonium iodide: a patch clamp and ligand binding study. Br J Pharmacol 129: 1771-1779.

Di Angelantonio SN (2001) Calibration of agonist concentrations applied by pressure pulses or via rapid solution exchanger. Journal of Neuroscience Methods 110: 155-161.

Dilger JP, Liu Y (1992) Desensitization of acetylcholine receptors in BC3H-1 cells. Pflugers Arch 420: 479-485.

Dingledine R, Borges K, Bowie D, Traynelis SF (1999) The glutamate receptor ion channels. Pharmacol Rev 51: 7-61.

Eusebi F, Farini D, Grassi F, Monaco L, Ruzzier F (1988) Effects of calcitonin gene-related peptide on synaptic acetylcholine receptor-channels in rat muscle fibres. Proc R Soc Lond B Biol Sci 234: 333-342.

Evans RH, Smith DA (1982) Effect of urethane on synaptic and amino acid-induced excitation in isolated spinal cord preparations. Neuropharmacology 21: 857-860.

Everitt BJ, Robbins TW (1997) Central cholinergic systems and cognition. Annu Rev Psychol 48:649-84.: 649-684.

Feltz A, Trautmann A (1982) Desensitization at the frog neuromuscular junction: a biphasic process. J Physiol 322:257-72.: 257-272.

Fenster CP, Beckman ML, Parker JC, Sheffield EB, Whitworth TL, Quick MW, Lester RA (1999b) Regulation of alpha4beta2 nicotinic receptor desensitization by calcium and protein kinase C. Mol Pharmacol 55: 432-443.

Fenster CP, Hicks JH, Beckman ML, Covernton PJ, Quick MW, Lester RA (1999a) Desensitization of nicotinic receptors in the central nervous system. Ann N Y Acad Sci 868:620-3.: 620-623.

Fieber LA, Adams DJ (1991) Acetylcholine-evoked currents in cultured neurones dissociated from rat parasympathetic cardiac ganglia. J Physiol 434:215-37.: 215-237.

Frazier CJ, Buhler AV, Weiner JL, Dunwiddie TV (1998) Synaptic potentials mediated via alpha-bungarotoxin-sensitive nicotinic acetylcholine receptors in rat hippocampal interneurons. J Neurosci 18: 8228-8235.

Freedman R, Adams CE, Leonard S (2000) The alpha7-nicotinic acetylcholine receptor and the pathology of hippocampal interneurons in schizophrenia. J Chem Neuroanat 20: 299-306.

Freedman R, Coon H, Myles-Worsley M, Orr-Urtreger A, Olincy A, Davis A, Polymeropoulos M, Holik J, Hopkins J, Hoff M, Rosenthal J, Waldo MC, Reimherr F, Wender P, Yaw J, Young DA, Breese CR, Adams

C, Patterson D, Adler LE, Kruglyak L, Leonard S, Byerley W (1997) Linkage of a neurophysiological deficit in schizophrenia to a chromosome 15 locus. Proc Natl Acad Sci U S A 94: 587-592.

Galzi JL, Revah F, Bessis A, Changeux JP (1991) Functional architecture of the nicotinic acetylcholine receptor: from electric organ to brain. Annu Rev Pharmacol Toxicol 31:37-72.: 37-72.

Garcia-Guzman M, Sala F, Sala S, Campos-Caro A, Stuhmer W, Gutierrez LM, Criado M (1995) alpha-Bungarotoxin-sensitive nicotinic receptors on bovine chromaffin cells: molecular cloning, functional expression and alternative splicing of the alpha 7 subunit. Eur J Neurosci 7: 647-655.

Gerzanich V, Peng X, Wang F, Wells G, Anand R, Fletcher S, Lindstrom J (1995) Comparative pharmacology of epibatidine: a potent agonist for neuronal nicotinic acetylcholine receptors. Mol Pharmacol 48: 774-782.

Gerzanich V, Wang F, Kuryatov A, Lindstrom J (1998) alpha 5 Subunit alters desensitization, pharmacology, Ca++ permeability and Ca++ modulation of human neuronal alpha 3 nicotinic receptors. J Pharmacol Exp Ther 286: 311-320.

Giniatullin R, Di Angelantonio S, Marchetti C, Sokolova E, Khiroug L, Nistri A (1999) Calcitonin gene-related peptide rapidly downregulates nicotinic receptor function and slowly raises intracellular Ca2+ in rat chromaffin cells in vitro. J Neurosci 19: 2945-2953.

Giniatullin RA, Sokolova EM, Di Angelantonio S, Skorinkin A, Talantova MV, Nistri A (2000) Rapid relief of block by mecamylamine of neuronal nicotinic acetylcholine receptors of rat chromaffin cells in vitro: an electrophysiological and modeling study. Molecular Pharmacology 58: 778-787.

Goldstein A, Aronov L, Kalman SM (1979) Principles of drug action: the basis of pharmacology. p. 194. John Wiley, New-York.

Gotti C, Balestra B, Moretti M, Rovati GE, Maggi L, Rossoni G, Berti F, Villa L, Pallavicini M, Clementi F (1998) 4-Oxystilbene compounds are selective ligands for neuronal nicotinic alphaBungarotoxin receptors. Br J Pharmacol 124: 1197-1206.

Gotti C, Fornasari D, Clementi F (1997) Human neuronal nicotinic receptors. Prog Neurobiol 53: 199-237.

Granja R, Strakhova M, Knauer CS, Skolnick P (1998) Anomalous rectifying properties of 'diazepam-insensitive' GABA(A) receptors. Eur J Pharmacol 345: 315-321.

Grassi F (1999) 5-hydroxytryptamine blocks the fetal more potently than the adult mouse muscle acetylcholine receptor. Pflugers Arch 437: 903-909.

Gray R, Rajan AS, Radcliffe KA, Yakehiro M, Dani JA (1996) Hippocampal synaptic transmission enhanced by low concentrations of nicotine. Nature 383: 713-716.

Groot-Kormelink PJ, Boorman JP, Sivilotti LG (2001) Formation of functional alpha3beta4alpha5 human neuronal nicotinic receptors in Xenopus oocytes: a reporter mutation approach. Br J Pharmacol 134: 789-796.

Groot-Kormelink PJ, Luyten WH, Colquhoun D, Sivilotti LG (1998) A reporter mutation approach shows incorporation of the "orphan" subunit beta3 into a functional nicotinic receptor. J Biol Chem %19;273: 15317-15320.

Grosman C, Auerbach A (2001) The dissociation of acetylcholine from open nicotinic receptor channels. Proc Natl Acad Sci U S A %20;98: 14102-14107.

Gurney AM, Rang HP (1984) The channel-blocking action of methonium compounds on rat submandibular ganglion cells. Br J Pharmacol 82: 623-642.

Harvey SC, McIntosh JM, Cartier GE, Maddox FN, Luetje CW (1997) Determinants of specificity for alpha-conotoxin MII on alpha3beta2 neuronal nicotinic receptors. Mol Pharmacol 51: 336-342.

Hefft S, Hulo S, Bertrand D, Muller D (1999) Synaptic transmission at nicotinic acetylcholine receptors in rat hippocampal organotypic cultures and slices. Journal of Physiology 515: 769-776.

Heinemann U, Stabel J, Rausche G (1990) Activity-dependent ionic changes and neuronal plasticity in rat hippocampus. Prog Brain Res 83:197-214.: 197-214.

Hellstrom-Lindahl E, Gorbounova O, Seiger A, Mousavi M, Nordberg A (1998) Regional distribution of nicotinic receptors during prenatal development of human brain and spinal cord. Brain Res Dev Brain Res 108: 147-160.

Heym C, Braun B, Shuyi Y, Klimaschewski L, Colombo-Benkmann M (1995) Immunohistochemical correlation of human adrenal nerve fibres and thoracic dorsal root neurons with special reference to substance P. Histochem Cell Biol 104: 233-243.

Hokfelt T (1991) Neuropeptides in perspective: the last ten years. Neuron 7: 867-879.

Huganir RL, Greengard P (1990) Regulation of neurotransmitter receptor desensitization by protein phosphorylation. Neuron 5: 555-567.

Irintchev A, Langer M, Zweyer M, Theisen R, Wernig A (1997) Functional improvement of damaged adult mouse muscle by implantation of primary myoblasts. J Physiol 500: 775-785.

Itier V, Bertrand D (2001) Neuronal nicotinic receptors: from protein structure to function. [Review] [102 refs]. FEBS Letters 504: 118-125.

Jaeger C (1965) Diffusion from constrictions. In Curtis DR, McIntyre AK, editors. Studies in Physiology. Springer: Berlin 06-17.

Janson AM, Moller A (1993) Chronic nicotine treatment counteracts nigral cell loss induced by a partial mesodiencephalic hemitransection: an analysis of the total number and mean volume of neurons and glia in substantia nigra of the male rat. Neuroscience 57: 931-941.
Ji D, Dani JA (2000) Inhibition and disinhibition of pyramidal neurons by activation of nicotinic receptors on hippocampal interneurons. J Neurophysiol 83: 2682-2690.

Jones GM, Sahakian BJ, Levy R, Warburton DM, Gray JA (1992) Effects of acute subcutaneous nicotine on attention, information processing and short-term memory in Alzheimer's disease. Psychopharmacology (Berl) 108: 485-494.

Kaiser SA, Soliakov L, Harvey SC, Luetje CW, Wonnacott S (1998) Differential inhibition by alpha-conotoxin-MII of the nicotinic stimulation of [3H]dopamine release from rat striatal synaptosomes and slices. J Neurochem 70: 1069-1076.

Karlin A (1967) On the application of "a plausible model" of allosteric proteins to the receptor for acetylcholine. J Theor Biol 16: 306-320.

Kasa P (1986) The cholinergic systems in brain and spinal cord. Prog Neurobiol 26: 211-272.

Katz B, Miledi R (1977) Suppression of transmitter release at the neuromuscular junction. Proc R Soc Lond B Biol Sci 196: 465-469.

Khiroug L, Giniatullin R, Sokolova E, Talantova M, Nistri A (1997) Imaging of intracellular calcium during desensitization of nicotinic acetylcholine receptors of rat chromaffin cells. Br J Pharmacol 122: 1323-1332.

Khiroug L, Sokolova E, Giniatullin R, Afzalov R, Nistri A (1998) Recovery from desensitization of neuronal nicotinic acetylcholine receptors of rat chromaffin cells is modulated by intracellular calcium through distinct second messengers. J Neurosci 18: 2458-2466.

Kihara T, Shimohama S, Urushitani M, Sawada H, Kimura J, Kume T, Maeda T, Akaike A (1998) Stimulation of alpha4beta2 nicotinic acetylcholine receptors inhibits beta-amyloid toxicity. Brain Res 792: 331-334.

Krause RM, Buisson B, Bertrand S, Corringer PJ, Galzi JL, Changeux JP, Bertrand D (1998) Ivermectin: a positive allosteric effector of the alpha7 neuronal nicotinic acetylcholine receptor. Mol Pharmacol 53: 283-294.

Kuramoto H, Kondo H, Fujita T (1987) Calcitonin gene-related peptide (CGRP)-like immunoreactivity in scattered chromaffin cells and nerve fibers in the adrenal gland of rats. Cell Tissue Res 247: 309-315.

Lange KW, Wells FR, Jenner P, Marsden CD (1993) Altered muscarinic and nicotinic receptor densities in cortical and subcortical brain regions in Parkinson's disease. J Neurochem 60: 197-203.

Lazareno S, Birdsall NJ (1993) Estimation of antagonist Kb from inhibition curves in functional experiments: alternatives to the Cheng-Prusoff equation. Trends Pharmacol Sci 14: 237-239.

Le Novere N, Corringer PJ, Changeux JP (1999) Improved secondary structure predictions for a nicotinic receptor subunit: incorporation of solvent accessibility and experimental data into a two-dimensional representation. Biophys J 76: 2329-2345.

Le Novere N, Zoli M, Changeux JP (1996) Neuronal nicotinic receptor alpha 6 subunit mRNA is selectively concentrated in catecholaminergic nuclei of the rat brain. Eur J Neurosci 8: 2428-2439.

Lena C, Changeux JP (1993) Allosteric modulations of the nicotinic acetylcholine receptor. Trends Neurosci 16: 181-186.

Lena C, Changeux JP (1997) Pathological mutations of nicotinic receptors and nicotine-based therapies for brain disorders. Curr Opin Neurobiol 7: 674-682.

Lena C, Changeux JP (1998) Allosteric nicotinic receptors, human pathologies. J Physiol Paris 92: 63-74.

Lena C, Changeux JP, Mulle C (1993) Evidence for "preterminal" nicotinic receptors on GABAergic axons in the rat interpeduncular nucleus. J Neurosci 13: 2680-2688.

Lester RA, Dani JA (1994) Time-dependent changes in central nicotinic acetylcholine channel kinetics in excised patches. Neuropharmacology 33: 27-34.

Levin ED, Rose JE (1991) Nicotinic and muscarinic interactions and choice accuracy in the radial-arm maze. Brain Res Bull 27: 125-128.

Levin ED, Rose JE, Behm F, Caskey NH (1991) The effects of smoking-related sensory cues on psychological stress. Pharmacol Biochem Behav 39: 265-268.

Levitan IB (1994) Modulation of ion channels by protein phosphorylation and dephosphorylation. Annu Rev Physiol 56:193-212.: 193-212.

Lewis TM, Harkness PC, Sivilotti LG, Colquhoun D, Millar NS (1997) The ion channel properties of a rat recombinant neuronal nicotinic receptor are dependent on the host cell type. J Physiol 505: 299-306.

Lindstrom J (1997) Nicotinic acetylcholine receptors in health and disease. Mol Neurobiol 15: 193-222.

Lingle C (1983) Different types of blockade of crustacean acetylcholine-induced currents. J Physiol 339:419-37.: 419-437.

Livett BG, Kozousek V, Mizobe F, Dean DM (1979) Substance P inhibits nicotinic activation of chromaffin cells. Nature 278: 256-257.

Lopez MG, Montiel C, Herrero CJ, Garcia-Palomero E, Mayorgas I, Hernandez-Guijo JM, Villarroya M, Olivares R, Gandia L, McIntosh JM, Olivera BM, Garcia AG (1998) Unmasking the functions of the chromaffin cell alpha7 nicotinic receptor by using short pulses of acetylcholine and selective blockers. Proc Natl Acad Sci U S A 95: 14184-14189.

Lu B, Fu WM, Greengard P, Poo MM (1993) Calcitonin gene-related peptide potentiates synaptic responses at developing neuromuscular junction. Nature 363: 76-79.

Luo S, Kulak JM, Cartier GE, Jacobsen RB, Yoshikami D, Olivera BM, McIntosh JM (1998) alpha-conotoxin AuIB selectively blocks alpha3 beta4 nicotinic acetylcholine receptors and nicotine-evoked norepinephrine release. J Neurosci 18: 8571-8579.

Maconochie DJ, Knight DE (1992) A study of the bovine adrenal chromaffin nicotinic receptor using patch clamp and concentration-jump techniques. J. Physiol. (Lond) 454:129-153.

Maelicke A, Albuquerque EX (2000) Allosteric modulation of nicotinic acetylcholine receptors as a treatment strategy for Alzheimer's disease. Eur J Pharmacol 393: 165-170.

Maelicke A, Coban T, Schrattenholz A, Schroder B, Reinhardt-Maelicke S, Storch A, Godovac-Zimmermann J, Methfessel C, Pereira EF, Albuquerque EX (1993) Physostigmine and neuromuscular transmission. Ann N Y Acad Sci 681:140-54.: 140-154.

Maelicke A, Coban T, Storch A, Schrattenholz A, Pereira EF, Albuquerque EX (1997) Allosteric modulation of Torpedo nicotinic acetylcholine receptor ion channel activity by noncompetitive agonists. J Recept Signal Transduct Res 17: 11-28.

Maelicke A, Schrattenholz A, Samochocki M, Radina M, Albuquerque EX (2000) Allosterically potentiating ligands of nicotinic receptors as a treatment strategy for Alzheimer's disease. Behav Brain Res 113: 199-206.

Maggi L, Palma E, Eusebi F, Moretti M, Balestra B, Clementi F, Gotti C (1999) Selective effects of a 4-oxystilbene derivative on wild and mutant neuronal chick alpha7 nicotinic receptor. Br J Pharmacol 126: 285-295.

Maggi L, Sher E, Cherubini E (2001) Regulation of GABA release by nicotinic acetylcholine receptors in the neonatal rat hippocampus. J Physiol 536: 89-100.

Maggio R, Riva M, Vaglini F, Fornai F, Molteni R, Armogida M, Racagni G, Corsini GU (1998) Nicotine prevents experimental parkinsonism in rodents and induces striatal increase of neurotrophic factors. J Neurochem 71: 2439-2446.

Magoski NS, Kaczmarek LK (1998) Direct and indirect regulation of a single ion channel. J Physiol 509: 1.

Maltby N, Broe GA, Creasey H, Jorm AF, Christensen H, Brooks WS (1994) Efficacy of tacrine and lecithin in mild to moderate Alzheimer's disease: double blind trial. BMJ 308: 879-883.

Mantegazza P, Tommasini R (1955) Central antinicotinic activity of 4-oxystilbene and 4-oxydiphenylethane derivatives. Arch. Int. Pharmacodyn. 4, 371-403.

Martin D, Lodge D (1985) Ketamine acts as a non-competitive N-methyl-D-aspartate antagonist on frog spinal cord in vitro. Neuropharmacology 24: 999-1003.

Marubio LM, Mar Arroyo-Jimenez M, Cordero-Erausquin M, Lena C, Le Novere N, de Kerchove dA, Huchet M, Damaj MI, Changeux JP (1999)

Munson PJ, Rodbard D (1980) Ligand: a versatile computerized approach for characterization of ligand-binding systems. Anal Biochem 107: 220-239.

Neher E (1983) The charge carried by single-channel currents of rat cultured muscle cells in the presence of local anaesthetics. J Physiol 339:663-78.: 663-678.

Neher E, Steinbach JH (1978) Local anaesthetics transiently block currents through single acetylcholine-receptor channels. J Physiol 277:153-76.: 153-176.

Nelson ME, Lindstrom J (1999) Single channel properties of human alpha3 AChRs: impact of beta2, beta4 and alpha5 subunits. J Physiol 516: 657-678.

Nicoll RA, Malenka RC (1999) Expression mechanisms underlying NMDA receptor-dependent long-term potentiation. Ann N Y Acad Sci 868:515-25.: 515-525.

Nooney JM, Peters JA, Lambert JJ (1992) A patch clamp study of the nicotinic acetylcholine receptor of bovine adrenomedullary chromaffin cells in culture. J Physiol 455:503-27.: 503-527.

Nordberg A (1994) Human nicotinic receptors--their role in aging and dementia. Neurochem Int 25: 93-97.

Nordberg A, Svensson AL (1998) Cholinesterase inhibitors in the treatment of Alzheimer's disease: a comparison of tolerability and pharmacology. Drug Saf 19: 465-480.

Obata K, Takeda K, Shinozaki H (1970) Electrophoretic release of gamma-aminobutyric acid and glutamic acid from micropipettes. Neuropharmacol 9:191-194.

Ogden DC, Colquhoun D (1985) Ion channel block by acetylcholine, carbachol and suberyldicholine at the frog neuromuscular junction. Proc R Soc Lond B Biol Sci 225: 329-355.

Olale F, Gerzanich V, Kuryatov A, Wang F, Lindstrom J (1997) Chronic nicotine exposure differentially affects the function of human alpha3, alpha4, and alpha7 neuronal nicotinic receptor subtypes. J Pharmacol Exp Ther 283: 675-683.

Otsuka M, Yoshioka K (1993) Neurotransmitter functions of mammalian tachykinins. Physiol Rev 73: 229-308.

Papke RL, Bencherif M, Lippiello P (1996) An evaluation of neuronal nicotinic acetylcholine receptor activation by quaternary nitrogen

compounds indicates that choline is selective for the alpha 7 subtype. Neurosci Lett 213: 201-204.

Paradiso K, Brehm P (1998) Long-term desensitization of nicotinic acetylcholine receptors is regulated via protein kinase A-mediated phosphorylation. J Neurosci 18: 9227-9237.

Parker MJ, Beck A, Luetje CW (1998) Neuronal nicotinic receptor beta2 and beta4 subunits confer large differences in agonist binding affinity. Mol Pharmacol 54: 1132-1139.

Pascual JM, Karlin A (1998) Delimiting the binding site for quaternary ammonium lidocaine derivatives in the acetylcholine receptor channel. J Gen Physiol 112: 611-621.

Paterson D, Nordberg A (2000) Neuronal nicotinic receptors in the human brain. [Review] [291 refs]. Progress in Neurobiology 61: 75-111.

Perry E, Martin-Ruiz C, Lee M, Griffiths M, Johnson M, Piggott M, Haroutunian V, Buxbaum JD, Nasland J, Davis K, Gotti C, Clementi F, Tzartos S, Cohen O, Soreq H, Jaros E, Perry R, Ballard C, McKeith I, Court J (2000) Nicotinic receptor subtypes in human brain ageing, Alzheimer and Lewy body diseases. Eur J Pharmacol 393: 215-222.

Perry EK, Morris CM, Court JA, Cheng A, Fairbairn AF, McKeith IG, Irving D, Brown A, Perry RH (1995) Alteration in nicotine binding sites in Parkinson's disease, Lewy body dementia and Alzheimer's disease: possible index of early neuropathology. Neuroscience 64: 385-395.

Perry EK, Perry RH (1995) Acetylcholine and hallucinations: disease-related compared to drug-induced alterations in human consciousness. Brain Cogn 28: 240-258.

Peters JA, Lambert JJ, Cottrell GA (1989) An electrophysiological investigation of the characteristics and function of GABAA receptors on bovine adrenomedullary chromaffin cells. Pflugers Arch 415: 95-103.

Picciotto MR, Zoli M, Lena C, Bessis A, Lallemand Y, LeNovere N, Vincent P, Pich EM, Brulet P, Changeux JP (1995) Abnormal avoidance learning in mice lacking functional high-affinity nicotine receptor in the brain. Nature 374: 65-67.

Picciotto MR, Zoli M, Rimondini R, Lena C, Marubio LM, Pich EM, Fuxe K, Changeux JP (1998) Acetylcholine receptors containing the beta2 subunit are involved in the reinforcing properties of nicotine. Nature 391: 173-177.

Pich EM, Pagliusi SR, Tessari M, Talabot-Ayer D, Hooft vH, Chiamulera C (1997) Common neural substrates for the addictive properties of nicotine and cocaine. Science 275: 83-86.

Pidoplichko VI, DeBiasi M, Williams JT, Dani JA (1997) Nicotine activates and desensitizes midbrain dopamine neurons. Nature 390: 401-404.

Quiram PA, Jones JJ, Sine SM (1999) Pairwise interactions between neuronal alpha7 acetylcholine receptors and alpha-conotoxin ImI. J Biol Chem 274: 19517-19524.

Radcliffe KA, Dani JA (1998) Nicotinic stimulation produces multiple forms of increased glutamatergic synaptic transmission. J Neurosci 18: 7075-7083.

Radcliffe KA, Fisher JL, Gray R, Dani JA (1999) Nicotinic modulation of glutamate and GABA synaptic transmission of hippocampal neurons. Ann N Y Acad Sci 868:591-610.: 591-610.

Ralevic V, Burnstock G (1998) Receptors for purines and pyrimidines. Pharmacol Rev 50: 413-492.

Reitstetter R, Lukas RJ, Gruener R (1999) Dependence of nicotinic acetylcholine receptor recovery from desensitization on the duration of agonist exposure. J Pharmacol Exp Ther 289: 656-660.

Reynolds JA, Karlin A (1978) Molecular weight in detergent solution of acetylcholine receptor from Torpedo californica. Biochemistry 17: 2035-2038.

Roerig B, Nelson DA, Katz LC (1997) Fast synaptic signaling by nicotinic acetylcholine and serotonin 5-HT3 receptors in developing visual cortex. J Neurosci 17: 8353-8362.

Role LW, Berg DK (1996) Nicotinic receptors in the development and modulation of CNS synapses. Neuron 16: 1077-1085.

Rusted J, Graupner L, O'Connell N, Nicholls C (1994) Does nicotine improve cognitive function? Psychopharmacology (Berl) 115: 547-549.

Schneider JS, Pope-Coleman A, Van Velson M, Menzaghi F, Lloyd GK (1998) Effects of SIB-1508Y, a novel neuronal nicotinic acetylcholine receptor agonist, on motor behavior in parkinsonian monkeys. Mov Disord 13: 637-642.

Schneider JS, Tinker JP, Van Velson M, Menzaghi F, Lloyd GK (1999) Nicotinic acetylcholine receptor agonist SIB-1508Y improves cognitive

functioning in chronic low-dose MPTP-treated monkeys. J Pharmacol Exp Ther 290: 731-739.

Seguela P, Wadiche J, Dineley-Miller K, Dani JA, Patrick JW (1993) Molecular cloning, functional properties, and distribution of rat brain alpha 7: a nicotinic cation channel highly permeable to calcium. J Neurosci 13: 596-604.

Sheffield EB, Quick MW, Lester RA (2000) Nicotinic acetylcholine receptor subunit mRNA expression and channel function in medial habenula neurons. Neuropharmacology 39: 2591-2603.

Shen WX, Horn JP (1998) Mecamylamine selectively blocks nicotinic receptors on vasomotor sympathetic C neurons. Brain Res 788: 118-124.

Simasko SM, Soares JR, Weiland GA (1985) Structure-activity relationship for substance P inhibition of carbamylcholine-stimulated 22Na+ flux in neuronal (PC12) and non-neuronal (BC3H1) cell lines. J Pharmacol Exp Ther 235: 601-605.

Simmonds MA (1982) Classification of some GABA antagonists with regard to site of action and potency in slices of rat cuneate nucleus. Eur J Pharmacol 80: 347-358.

Simmons LK, Schuetze SM, Role LW (1990) Substance P modulates single-channel properties of neuronal nicotinic acetylcholine receptors. Neuron 4: 393-403.

Sine SM, Steinbach JH (1984) Agonists block currents through acetylcholine receptor channels. Biophys J 46: 277-283.

Sivilotti LG, McNeil DK, Lewis TM, Nassar MA, Schoepfer R, Colquhoun D (1997) Recombinant nicotinic receptors, expressed in Xenopus oocytes, do not resemble native rat sympathetic ganglion receptors in single-channel behaviour. J Physiol 500: 123-138.

Smart TG (1997) Regulation of excitatory and inhibitory neurotransmitter-gated ion channels by protein phosphorylation. Curr Opin Neurobiol 7: 358-367.

Smit AB, Syed NI, Schaap D, van Minnen J, Klumperman J, Kits KS, Lodder H, van der Schors RC, van Elk R, Sorgedrager B, Brejc K, Sixma TK, Geraerts WP (2001) A glia-derived acetylcholine-binding protein that modulates synaptic transmission. Nature 411: 261-268.

Smith FM, McGuirt AS, Hoover DB, Armour JA, Ardell JL (2001) Chronic decentralization of the heart differentially remodels canine

intrinsic cardiac neuron muscarinic receptors. Am J Physiol Heart Circ Physiol 281: H1919-H1930.

Stafford GA, Oswald RE, Weiland GA (1994) The beta subunit of neuronal nicotinic acetylcholine receptors is a determinant of the affinity for substance P inhibition. Mol Pharmacol 45: 758-762.

Steinlein OK, Mulley JC, Propping P, Wallace RH, Phillips HA, Sutherland GR, Scheffer IE, Berkovic SF (1995) A missense mutation in the neuronal nicotinic acetylcholine receptor alpha 4 subunit is associated with autosomal dominant nocturnal frontal lobe epilepsy. Nat Genet 11: 201-203.

Sudweeks SN, Yakel JL (2000) Functional and molecular characterization of neuronal nicotinic ACh receptors in rat CA1 hippocampal neurons. Journal of Physiology 527 Pt 3: 515-528.

Sullivan JP, Donnelly-Roberts D, Briggs CA, Anderson DJ, Gopalakrishnan M, Xue IC, Piattoni-Kaplan M, Molinari E, Campbell JE, McKenna DG, Gunn DE, Lin NH, Ryther KB, He Y, Holladay MW, Wonnacott S, Williams M, Arneric SP (1997) ABT-089 [2-methyl-3-(2-(S)-pyrrolidinylmethoxy)pyridine]: I. A potent and selective cholinergic channel modulator with neuroprotective properties. J Pharmacol Exp Ther 283: 235-246.

Tachikawa E, Mizuma K, Kudo K, Kashimoto T, Yamato S, Ohta S (2001) Characterization of the functional subunit combination of nicotinic acetylcholine receptors in bovine adrenal chromaffin cells. Neurosci Lett 312: 161-164.

Tsigelny I, Sugiyama N, Sine SM, Taylor P (1997) A model of the nicotinic receptor extracellular domain based on sequence identity and residue location. Biophys J 73: 52-66.

Udgaonkar JB, Hess GP (1987b) Acetylcholine receptor: channel-opening kinetics evaluated by rapid chemical kinetic and single-channel current measurements. Biophys J 52: 873-883.

Udgaonkar JB, Hess GP (1987a) Chemical kinetic measurements of a mammalian acetylcholine receptor by a fast-reaction technique. Proc Natl Acad Sci U S A 84: 8758-8762.

Unwin N (1993) Nicotinic acetylcholine receptor at 9 A resolution. J Mol Biol %20;229: 1101-1124.

Unwin N (1996) Projection structure of the nicotinic acetylcholine receptor: distinct conformations of the alpha subunits. J Mol Biol 257: 586-596.

Valenta DC, Downing JE, Role LW (1993) Peptide modulation of ACh receptor desensitization controls neurotransmitter release from chicken sympathetic neurons. J Neurophysiol 69: 928-942.

Vernino S, Amador M, Luetje CW, Patrick J, Dani JA (1992) Calcium modulation and high calcium permeability of neuronal nicotinic acetylcholine receptors. Neuron 8: 127-134.

Vernino S, Rogers M, Radcliffe KA, Dani JA (1994) Quantitative measurement of calcium flux through muscle and neuronal nicotinic acetylcholine receptors. J Neurosci 14: 5514-5524.

Weiland S, Witzemann V, Villarroel A, Propping P, Steinlein O (1996) An amino acid exchange in the second transmembrane segment of a neuronal nicotinic receptor causes partial epilepsy by altering its desensitization kinetics. FEBS Lett 398: 91-96.

Wernig A, Zweyer M, Irintchev A (2000) Function of skeletal muscle tissue formed after myoblast transplantation into irradiated mouse muscles. J Physiol 522 Pt 2:333-45.: 333-345.

Wesnes K, Warburton DM (1983) Smoking, nicotine and human performance. Pharmacol Ther 21: 189-208.

Whitehouse PJ, Martino AM, Marcus KA, Zweig RM, Singer HS, Price DL, Kellar KJ (1988) Reductions in acetylcholine and nicotine binding in several degenerative diseases. Arch Neurol 45: 722-724.

Wiest MC, Eagleman DM, King RD, Montague PR (2000) Dendritic spikes and their influence on extracellular calcium signaling. J Neurophysiol 83: 1329-1337.

Wonnacott S (1990) The paradox of nicotinic acetylcholine receptor upregulation by nicotine. Trends Pharmacol Sci 11: 216-219.

Wonnacott S, Thorne B (1990) Separation of pre- and post-synaptic receptors on Percoll gradients. Biochem Soc Trans 18: 885-886.

Woodhull AM (1973) Ionic blockage of sodium channels in nerve. J Gen Physiol 61: 687-708.

Woolf NJ (1991) Cholinergic systems in mammalian brain and spinal cord. Prog Neurobiol 37: 475-524.

Xiao Y, Meyer EL, Thompson JM, Surin A, Wroblewski J, Kellar KJ (1998) Rat alpha3/beta4 subtype of neuronal nicotinic acetylcholine receptor stably expressed in a transfected cell line: pharmacology of ligand binding and function. Mol Pharmacol 54: 322-333.

Yu CR, Role LW (1998a) Functional contribution of the alpha5 subunit to neuronal nicotinic channels expressed by chick sympathetic ganglion neurones. J Physiol 509: 667-681.

Yu CR, Role LW (1998b) Functional contribution of the alpha7 subunit to multiple subtypes of nicotinic receptors in embryonic chick sympathetic neurones. J Physiol 509: 651-665.

Zhang J, Xiao Y, Abdrakhmanova G, Wang W, Cleemann L, Kellar KJ, Morad M (1999) Activation and Ca2+ permeation of stably transfected alpha3/beta4 neuronal nicotinic acetylcholine receptor. Mol Pharmacol 55: 970-981.

Zhang L, Peoples RW, Oz M, Harvey-White J, Weight FF, Brauneis U (1997) Potentiation of NMDA receptor-mediated responses by dynorphin at low extracellular glycine concentrations. J Neurophysiol 78: 582-590.

Zoli M, Lena C, Picciotto MR, Changeux JP (1998) Identification of four classes of brain nicotinic receptors using beta2 mutant mice. J Neurosci 18: 4461-4472.